JOURNAL OF ATA-CHEM
(J Ata-Chem)

ATA-KİMYA DERGİSİ
(Ata-Kim Derg)

https://dergipark.org.tr/tr/pub/atakim

EDITORIAL BORD

JOURNAL OF ATA-CHEM / ATA-KİMYA DERGİSİ
(J Ata-Chem /Ata-Kim Derg)

CONTENTS / İÇİNDEKİLER

Production and Characterization of Nanotechnological Wound Dressing Containing Ozone Oil

Erdinc DOGANCI[1a*], Merve DANDAN DOGANCI[1b], Gulseren SAKARYA BULUS[2c], Erdi BULUS[3d]

[1]*Chemistry and Chemical Processing Technologies Department, Kocaeli University, Kocaeli 41140, Turkey*
[2]*Directorate of Health Services, Istanbul Provincial Directorate of Health Istanbul Cad. General Kani Elitez Sok. No:8-1 Yenimahalle, Istanbul 34140, Turkey*
[3]*ArelPOTKAM (Polymer Technologies and Composite Applications and Research Center), Istanbul Arel University, Istanbul 34500, Turkey*

ORCID: [a]0000-0003-2490-0671, [b]0000-0001-5393-6820, [c]0000-0001-6096-8177, [d]0000-0002-2045-2499

Abstract: In this study, polyvinyl alcohol (PVA), which is very useful for the electrospinning method, was used in terms of its properties such as being easily dissolved in water, easy to spin, and forming qualified nanofiber surfaces. A mixture of 10% by mass of pure water and granular PVA was prepared by weighing on a precision scale. The mixture was stirred at 80 $^{\circ}$C for 3 hours in a heated magnetic stirrer and left at room temperature for 24 hours. The resulting 10% PVA solution was mixed with a magnetic stirrer at 30 $^{\circ}$C for 45 minutes by adding 5% ozone oil. 10% PVA, 10% PVA-5% Ozone Oil composites were obtained by electrospinning technique. Morphological characterization of the obtained composites was carried out with Field Emission Gun Scanning Electron Microscopy (FEGSEM). Membranes that we produce for chronic wounds, especially for diabetes patients, will be ideal material candidates with their rapid wound healing properties.

Keywords: Ozone oil, polyvinyl alcohol, electrospinning, wound dressing, diabetes

Ozon Yağı İçeren Nanoteknolojik Yara Örtüsü Üretimi ve Karakterizasyonu

Özet: Bu çalışmada suda kolay çözünebilmesi, kolay spinlenebilmesi, nitelikli nanofiber yüzeyler oluşturabilmesi gibi özellikleri bakımından elektroeğirme yöntemi için oldukça kullanışlı olan polivinil alkol (PVA) kullanılmıştır. Hassas terazide tartılarak granül haldeki PVA ile saf suyun kütlece %10'luk karışımı hazırlanmıştır. Karışım ısıtıcılı manyetik karıştırıcıda 80 $^{\circ}$C sıcaklıkta 3 saat boyunca karıştırılmış ve 24 saat boyunca oda sıcaklığında bekletilmiştir. Oluşan %10'luk PVA çözeltisine %5 oranında ozon yağı maddesi katılarak 45 dakika 30 $^{\circ}$C sıcaklıkta manyetik karıştırıcıda karıştırılmıştır. %10 PVA, %10 PVA-%5 Ozon Yağı kompozitleri elektroeğirme tekniği ile elde edilmiştir. Elde edilen kompozitlerin Alan Emisyon Tabancalı Taramalı Elektron Mikroskobu (FEGSEM) ile morfolojik karakterizasyonları gerçekleştirilmiştir. Diyabet hastaları başta olmak üzere kronik yaralara yönelik ürettiğimiz membranlar hızlı yara iyileştiri özellikleri ile ideal malzeme adayı olabilecektir.

Anahtar Kelimeler: Ozan yağı, polivinil alkol, elektroeğirme, yara örtüsü, diyabet

*Corresponding Author: edoganci@kocaeli.edu.tr (E. Doganci)

1. INTRODUCTION

The deterioration of the integrity and functions of tissues or organs by various factors is called wound healing, and the restoration of this integrity through a series of intertwined processes is called wound healing. Wound healing is a dynamic and complex process consisting of successive periods. The use of appropriate dressings plays an important role in the wound healing process. The duties of wound dressings are to provide protective properties against infection and microorganisms, to absorb blood and wound fluid, to provide wound healing and in some cases to apply drug therapy on the wound. Other tasks of dressings include fluid control, odour removal, microbial control, physical barrier, space-filling effect, and complete cleaning (debridement) of foreign bodies and damaged and infected tissues in the wound [1].

A wide variety of wound care products are used in wound care today. These include composite dressings, transparent film dressings, hydrocolloids, alginate dressings and wound fillers, antibacterial dressings, and hydrogel dressings. There is no ideal wound care product to be used for every wound and at all times. Wound care products are selected according to the wound and are changed according to the need in different periods of the same wound. It is used in wound healing, regeneration, and healing of dermal and epidermal tissue. The materials used

in the preparation of the dressing protect the wound as a physical barrier against microorganisms and are permeable to moisture and oxygen. An ideal dressing should have the following features: It should accelerate wound healing, provide a moist environment for the wound, remove excess exudate and toxic substances from the environment without allowing the wound to dry, prevent odour, protect the temperature of the wound surface, not allow the passage of microorganisms from the air to the wound surface, allow oxygen exchange and gas exchange. It should aid cell migration and division by allowing [2].

Wound dressing is an important method to complete the wound healing process quickly and properly. Wound dressings are materials that act as a barrier to protect the wound. Due to the importance of wound protection, the development of appropriate wound dressings is extremely important. Purpose in the treatment of surgical wounds in the past; the wound was to bring the lips closer together to quickly heal the wound. Nowadays, the dressings are understood that a moist and warm environment created around the wound is more effective in wound healing. This current approach is based on the ideal environment for wound healing and the ability of epithelial cells to move easily [3].

An ideal dressing should have the following properties:
- Providing a moist environment for the wound,
- Removing exudates,
- Preventing microorganisms from entering the wound,
- Allowing gaseous exchange,

- Must be sterile,
- Must not be toxic and allergic,
- Minimal frequency of dressing exchange,
- Thermal insulation,
- Easy of application,
- Comfortable and conformable [4,5].

Biomaterials are defined as materials that can adapt to the human body, perform the functions performed by the human body, support and heal. Biomaterials science is an interdisciplinary branch that studies the physical and biological studies of materials and their interactions in the biological environment [6].

PVA, a biocompatible and water-soluble hydroxy polymer, has very good chemical resistance, flexibility, mechanical strength, and biodegradability. Chemical stability at room temperature with very good physical and mechanical properties, ability to form very good fibrous material alone or mixed with other polymers [7].

The oil known as ozone oil is actually ozone-enriched pure olive oil. Although the ozonisation process is usually done with olive oil, it can also be done with other natural oils such as argan oil, hemp oil. The main feature of ozone molecules is the ability to destroy organic compounds such as bacteria and viruses with a high purification process. One of the most important benefits of ozone oil is that it provides rapid healing of wounds. It is a product that should be used by diabetics who have wounds for no reason. It is a type of oil that works with its positive effects in the treatment process of foot fungus and other diseases. Ozone oil is often used in the treatment of skin problems such as psoriasis, varicose veins, wrinkles, eczema, and acne [8].

Nanofibers is a designation used for fibers with a diameter of 100 nanometers or less. Its properties such as flexibility, high porosity, small pore size, axial strength have caused it to find many different and wide application areas [9].

It is a method applied by drawing the polymer from a specially prepared solution using an electric field. In addition, nanofibers can be produced from polymers, metal oxides and ceramics with this method. With this method, one-dimensional nanostructures are formed [10].

Nanostructured wound dressings, which can be described as a new generation wound dressing, consist of nanofibers. The nanofibers with large surface have three-dimensional surface area. They have anti-bleeding feature thanks to their high surface area. Since they are nano-sized fine fibers, they can mimic the natural extracellular matrix structure (ECM), and provide a favorable environment for the attachment, development and proliferations of cells. Its high porosity gives the dressing a breathable structure that prevents the passage of bacteria and infection [11].

The electrospinning technique is one of the most used to produce nanofibers due to its simplicity and effectiveness. Electrospinning is a spinning technique which is using electrostatic force to fabricate fine fibers from polymer

solutions. In this technique, the polymer is electrically charged using a high potential voltage to induce the formation of a liquid jet. The polymer jet formed by this method flows towards the grounded source. During this flow, the polymer jet is scattered around as very thin fibers and as a result, nano-scale fine fibers are formed [12].

In the electrospinning process, many different polymers have been used to produce nanofibers. The polycaprolactone (PCL) which is synthetic polymer, is used in nanofiber production. This polymer is used in the dressings because it supports wound healing. PCL is a polymer that has some superiorities related to physicochemical aspects which covers hydrophobicity, high spinnability, preferable mechanical effects. Beside these, it degrades gradually that makes desirable for purpose of matrix to load natural products [13].

In this study, PVA nanofiber composites containing ozone oil were obtained by electrospinning technique, and the obtained membranes will be able to show ideal material properties that can appeal to all people with chronic wounds, especially diabetes patients.

2. MATERIAL AND METHOD

2.1. Materials

ANKA Biological Implant Medical Software Tourism Defense Industry and Trade Limited (Erzurum/Turkey) Sigma/Aldrich brand PVA polymer: 85,000-124,000 g/mol weight, pure water (distilled water) was used to dissolve polymer and used as fatty paper. Ozone oil was obtained from Mediazon (Istanbul/Turkey).

2.2. Method
2.2.1. Preparation of Wound Dressing Solutions

PVA, which is very useful for electrospinning method in terms of its properties such as being easily soluble in water, easy to spin, and creating quality nanofiber surfaces, was weighed on a precision balance and a 10% mass mixture of pure water was prepared. The mixture was stirred at 80 °C for 3 hours in a heated magnetic stirrer and left at room temperature for 24 hours to remove the bubbles in the solution. In addition to pure PVA, 2 different electrospinning solutions were obtained by adding 5% ozone oil to the PVA solution. Preparation of necessary solutions for dressing production is given in Table 2.1.

Table 2.1. Preparation of necessary solutions for dressing production

Polymer/Additive Matter	Solvent	Mixture Temperature (°C)	Mixture Time (Min.)
10% PVA	Distile water	30	240
10% PVA-5% Ozone Oil	Distile water	30	240

2.2.2. Biocomposite Production by Electrospinning Method

Nanofibers were obtained by depositing the nanofibers on a collecting wax paper at room temperature using a NANOFEN brand N100 model electrospinning device. Electrospinning parameters required for biocomposite production are shown in Table 2.2.

Table 2.2. Electrospinning parameters required for the production of biocomposites

Polymer/Additive Matter	Working Distance (cm)	Flow Rate (ml/hour)	Voltage (kV)
10% PVA	15	3.5	25.8
10% PVA-5% Ozone Oil	15	5	30

Suitable solvent/solvent systems for electrospinning were investigated. Pure water was used in PVA and ozone oil added PVA solutions. The stages of wound dressing production by the electrospinning method are given in Figure 2.1.
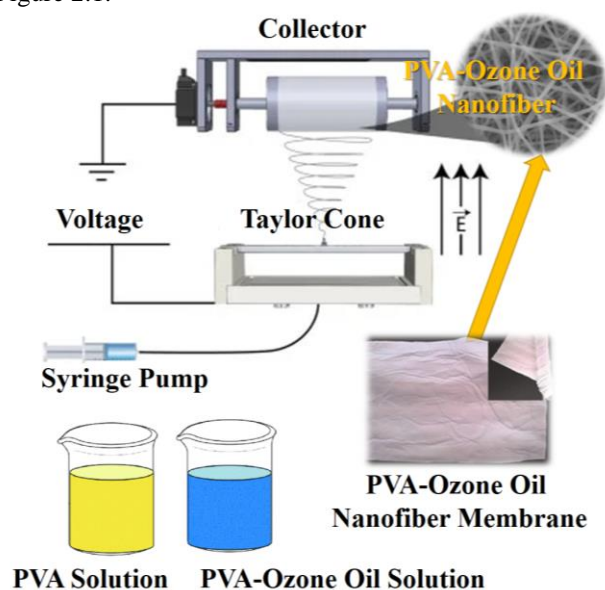
Figure 2.1. Wound dressing production by electrospinning method

2.2.2. Characterization Method
2.2.2.1. FEGSEM Analysis

During the examination of nanofiber diameters of the membranes produced on FEI FEGSEM QUANTA 450 device, the images of x1500 and x3000 enlargements were examined in the potential of 7 kV. The average nanofiber diameter ranges were determined by measuring 30 nanofiber diameters over the images and taking their arithmetic averages [14].

3.   RESULTS AND DISCUSSION

3.1. *Morphological Analysis*

3.1.1. *FEGSEM Analysis*

Nanofiber formation was observed in all samples. The fineness of nanofibers obtained by electrospinning from PVA and PVA-Ozone Oil solutions was even finer compared to pure PVA polymer. This is because; It is thought that the solution conductivity increases with the additive in the mixture. The fiber diameters in the samples were measured with the FEGSEM device. Looking at the fineness of nanofibers, it has been determined that the material produced in PVA-Ozone Oil mixtures is formed in the form of fine fibers. The PVA-Ozone Oil sample was the composite with the thinnest fiber structure compared to the PVA sample. The average diameter of the fibers was 150-300 nm, measured on the FEGSEM images obtained within the device and the arithmetic average of 30 calculated fibers was determined [15]. Figure 3.1. PVA and Figure 3.2. PVA-Ozon Oil FEGSEM images of nanofiber membranes in different magnitues are shown.
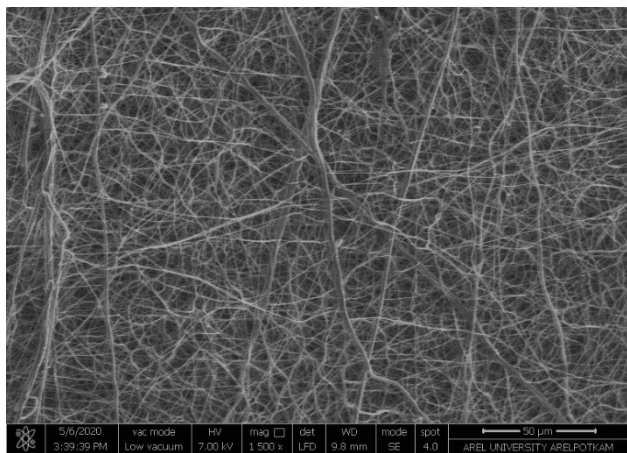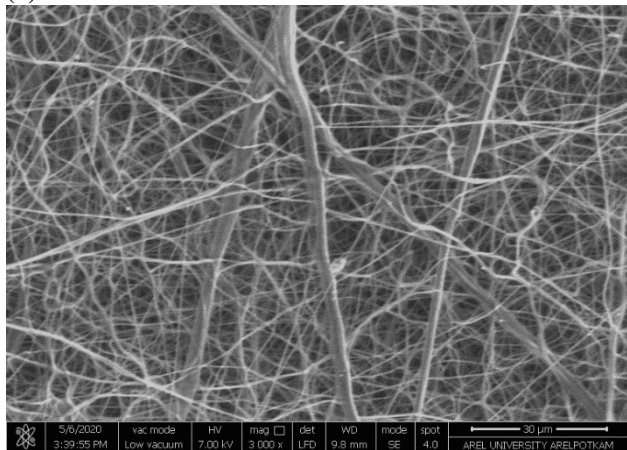
(b)
Figure 3.1. (a) x1500, (b) PVA Nanofiber FEGSEM image in x3000 magnification
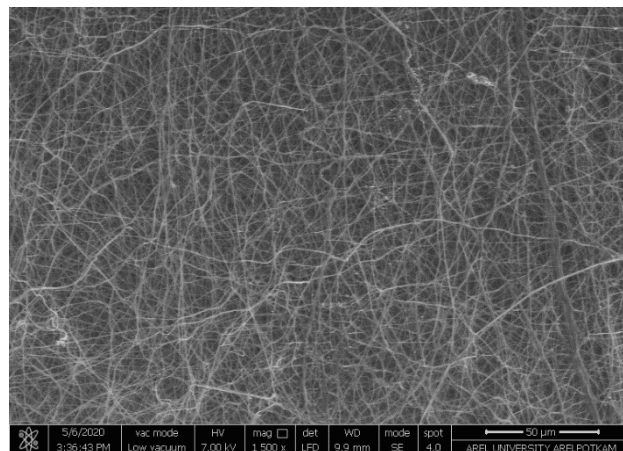
(a)
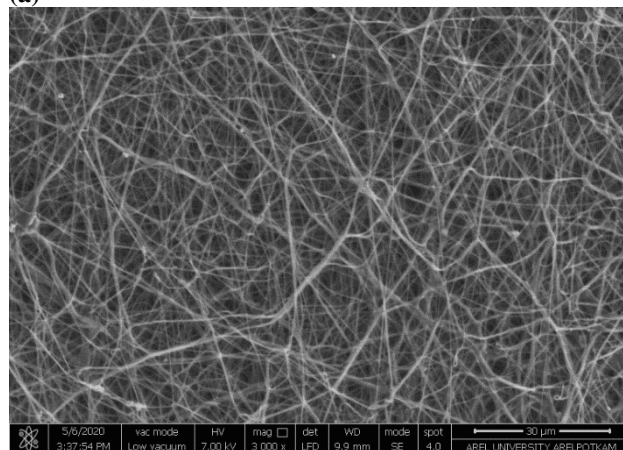
(b)

Figure 3.2. (a) x1500, (b) PVA-Ozone Oil Nanofiber FEGSEM image in x3000 magnification

Table 3.1 shows the nanofiber diameter distribution range of the samples.

(a)

Table 3.1. Nanofiber diameter distribution range of samples

Sample Name	Fiber Thickness (nm)
10% PVA	180-330
10% PVA-5% Ozone Oil	150-300

4.   CONCLUSIONS

PVA and PVA-Ozone Oil composites were successfully obtained by electrospinning technique. Wound healing tape was produced by adding 5% ozone oil to the PVA solution. When the morphological (FEGSEM) characterization tests of the produced composites are

examined, the fiber structure of the ozone oil added composite is thinner compared to the pure PVA polymer. The thinnest fibers were obtained in the PVA-Ozone Oil composite, and the fiber thicknesses are 150-300 nm on average. The obtained values may exhibit wound healing tape properties for tissue engineering and biomedical applications. The fields of application can be expanded as a result of the values obtained by carrying out mechanical, thermal and biological (antimicrobial, cell culture) characterization studies of the produced biocomposites.

5. CONFLICT OF INTEREST
The authors declare no competing financial interest.

Ethical Approval: Ethics Approval is not required for this study.

REFERENCES

[1] Cascone, S., Lamberti, G., "Hydrogel-based commercial products for biomedical applications: A review", International journal of pharmaceutics, (2020), 573, 118803.

[2] Homaeigohar, S., Boccaccini, A. R., "Antibacterial biohybrid nanofibers for wound dressings", Acta biomaterialia, (2020),107, 25-49.

[3] Mutlu, S., & Yılmaz, E., "Yara Yönetiminde Güncel Yaklaşımlar", Gümüşhane Üniversitesi Sağlık Bilimleri Dergisi, (2019), 8(4), 481–494.

[4] Dhivya, S., Vijaya, V., Santhini, E., "Review article Wound dressings – a review". Biomedicine (Taipei), (2015), 5(4), 24–28.

[5] Vowden, K., & Vowden, P., "Wound dressings: principles and practice", Surgery (United Kingdom), (2017), 35(9), 489–494.

[6] Buluş, E., Buluş, G. S., Akkaş, M., "Investigation of the Effects of Working Parameters in Electrospinning Technology on Morphology of Polymeric Nanofiber Membranes Using Reference Polymers". Journal Of Materıals And Electronıc Devıces, (2021), 2(1), 6-11.

[7] Bunn, C. W. "Crystal structure of polyvinyl alcohol", Nature, (1948),161(4102), 929-930.

[8] Buluş, E., Buluş, G. S., "The Effect of Ozone and Platelet Rich Plasma (PRP) Methods on Hip Prosthesis Healing Process", Journal Of Materials And Electronic Devices, (2020), 5(1), 17-19.

[9] Aynali, F., Balci, H., Doganci, E., & Bulus, E., "Production and characterization of non-leaching antimicrobial and hydrophilic polycaprolactone based nanofiber mats", European Polymer Journal, (2021), 149, 110368.

[10] Yan, J., Su, Q., Xiao, W., Wu, Z., Chen, L., Tang, L., Xue, H., "A review of nanofiber membranes for solar interface evaporation", Desalination, (2022), 531, 115686.

[11] Koyutürk, A., Soyaslan, D. D., "Yara ve Yanık Tedavisinde Kullanılan Örtüler". Mehmet Akif Ersoy Üniversitesi Fen Bilimleri Enstitüsü Dergisi, (2016), 0(1), 58-65–65.

[12] Bhardwaj, N., & Kundu, S.C., "Electrospinning: A fascinating fiber fabrication technique", Biotechnology Advances, (2010), 28(3):325-347.

[13] Pinzón-García, A. D., Cassini-Vieira, P., Ribeiro, C.C., "Efficient cutaneous wound healing using bixin-loaded PCL nanofibers in diabetic mice", Journal of Biomedical Materials Research - Part B Applied Biomaterials, (2017), 105(7):1938-1949.

[14] Buluş, E., Buluş, G. S., Akkaş, M., & Çetin, T. "Production and Morphological Characterization of Nanofiber Membrane with Natural Wound Healing", Journal Of Materıals And Electronıc Devıces, (2021), 2(1), 1-5.

[15] Majd, S. A., Khorasgani, M. R., Moshtaghian, S. J., Talebi, A., & Khezri, M., "Application of Chitosan/PVA Nano fiber as a potential wound dressing for streptozotocin-induced diabetic rats", International journal of biological macromolecules, (2016), 92, 1162-1168.

Paraben Substituted *Monospiro*-Cyclotriphosphazene Compounds: Synthesis and Characterization

Nagihan BAYIK TÜLÜCE[1a]*, Gönül YENİLMEZ ÇİFTÇİ[1b]*

[1]Gebze Teknik Üniversitesi, Kimya Bölümü, 41400 Kocaeli, Türkiye

ORCID: [a]0000-0001-9214-9264, [b]0000-0003-3187-7166

Abstract: Parabens are among the potential biologically active compounds due to their low toxicity potential for humans and their effective antibacterial and antifungal activity. The properties of cyclotriphosphazenes increase their efficiency according to the properties of the side groups to which they are attached. For this reason, scientists use it as a platform to design target molecules in particular. In this study, new types paraben substituted monospiro-cyclotriphosphazene compounds (**5-7**) were successfully synthesized and these compounds were fully characterized by MALDI-TOF mass, ^{1}H, ^{31}P and ^{13}C spectroscopy techniques. The molecular structure of compound **5** was also determined by single crystal X-ray crystallography.

Keywords: Cyclotriphosphazene, Paraben, NMR, X-Ray.

Paraben Sübstitüe *Monospiro*-Siklotrifosfazen Bileşikleri: Sentezi ve Karakterizasyonu

Özet: Parabenler, insanlar için düşük toksisite potansiyelleri ve etkili antibakteriyel ve antifungal aktiviteleri nedeniyle potansiyel biyolojik olarak aktif bileşikler arasındadır. Siklotrifosfazenlerin özellikleri bağlı oldukları yan grupların özelliklerine göre etkinliklerini arttırır. Siklotrifosfazenlerin göstermiş oldukları özellikler, yan gruplara bağlı olarak değişir ve etkinlikleri artar. Bu nedenle bilim adamları, özellikle hedef molekülleri tasarlamak için bir platform olarak kullanırlar. Bu çalışmada, yeni tip paraben ikameli *monospiro*-siklotrifosfazen bileşikleri (**5-7**) başarıyla sentezlendi ve bu bileşikler MALDI-TOF kütlesi, ^{1}H, ^{31}P ve ^{13}C NMR spektroskopi teknikleri ile tamamen karakterize edildi. Bileşik **5**'in moleküler yapısı da tek kristal X-ışını kristallografisi ile belirlendi.

Anahtar Kelimeler: Siklotrifosfazen, Paraben, NMR, X-Ray.

*Corresponding Author: nbayik@gtu.edu.tr (N. Bayık Tülüce and yenilmez@gtu.edu.tr (G. Yenilmez Çiftçi)

1. INTRODUCTION

Para-hydroxy benzoate (PHB) esters and their sodium salts, often called parabens, have been used as preservatives for fifty years in the food, cosmetic and pharmaceutical industries to prevent microbe growth. For the commonly used methylparaben (MP), ethylparaben (EP), propylparaben (PP), and butylparaben (BP), antimicrobial activity increases with increasing alkyl chain length, and synergy among parabens has been reported [1]. Although parabens are frequently used against many yeast, mold and bacteria species, their mechanism of action on these organisms is still not fully elucidated [2]. In a study by Nguyen et al., it was stated that parabens interacted with mechanosensitive channels in E. coli and disrupted the bacterial osmotic gradient [3]. After the antimicrobial properties of parabens were determined, their presence in human breast cancer tissue was detected. The detection of parabens in human breast cancer tissue and its association with cancer have led researchers to this issue [4, 5]. Despite the limited epidemiological evidence linking paraben exposure with breast cancer, recent in vitro and animal studies have shed light on the endocrine-modulating effects of parabens, suggesting that parabens may be implicated in breast carcinogenesis [6]. An interesting recent study investigated the toxic effects and mechanisms of four different paraben groups (MP, EP, PP, BP) on zebrafish by Lui et al. They reported that the toxic effects of parabens on the zebrafish embryos tested increased in parallel with the carbon chain length of the paraben alkyl [7]. On the other hand, estrogenic activity of parabens was investigated by in vivo experiments in mice and rats and it was reported that especially methyl, ethyl and propyl paraben did not have a negative effect. For example, Witorsch et al. have pointed out studies that the estrogenic activity of some parabens does not threaten human health [8]. While the investigation of the potential of parabens to harm human health continues, its use in the industry continues due to its antimicrobial properties. Therefore, synthesis and research of new paraben-substituted compounds is necessary. In particular, the newly synthesized compounds should not have harmful effects on human breast tissue and should not threaten human health. Cyclotriphosphazenes an important part of inorganic chemistry and they are the most preferred platform because they can give easy substitution reactions and form stable compounds [9]. Depending on the physical and chemical properties of the substituted groups, anticancer [10-14], antimicrobial [15], antitumor [16], antifungal [17], liquid crystals [18] and chemical sensors [19], flame retardants [20] etc. The reactions of phosphazenes with parabens were first studied in our laboratories. In our first study, paraben substituted cyclotetraphosphazene compounds were synthesized and their effects on DNA (genotoxicity) were investigated. Since traditional genotoxicity test methods are laborious, time-consuming and expensive, DNA damage studies were carried out with a biosensor device in this study. Propyl and benzyl substituted cyclotetraphosphazene compounds have been shown to have more effective results [21]. In a study conducted by our research group in 2017, paraben derivatives of cyclotriphosphazene compounds were synthesized and it

was determined that some derivatives could be potential anticancer agents [22]. In another study, fully paraben-substituted fluorenylidene double-bridged cyclotriphosphazenes were synthesized and their effects on DNA were evaluated by automatic biosensor device and gel electrophoresis method [23]. In our previous studies, some cyclotriphosphazene derivatives and spermine bridged cyclotriphosphazene derivatives were prepared and the in vitro cytotoxic effects (MTT) of these compounds against HT-29 (colon cancer) and Hep2 (larynx cancer) cells were investigated. As a result of studies, it was determined that some compounds showed significant effects on these cells [10, 24]. Based on these results, reactions of spermine-derived cyclotriphosphazene and parabens were carried out in 2020, and the paraben-substituted spermine-derived cyclotriphosphazene series were synthesized. DNA interactions were examined with both automatic biosensor device and gel-electrophoresis methods, and positive results were obtained [25, 26]. In recent studies by our group, new paraben-substituted compounds with mono and disipro structures were obtained and their in vitro cytotoxic activities were investigated. Some derivatives have positive results for MCF-7 and DLD-1 cells as cytotoxic agents [11,12].

All these studies encouraged us to synthesize and characterize new paraben-substituted cyclotriphosphazene compounds.

In this study *monospiro*-cyclotriphosphazene compounds decorated with different parabens that likely to show biological activity were designed and successfully synthesized for the first time (**Scheme 1**). The structures of the purified compounds (**5-7**) were elucidated by MALDI-TOF mass, ^{1}H, ^{13}C and ^{31}P NMR spectroscopic techniques. Also, the solid-state structure and geometry of compound **5** was determined by single crystal X-ray crystallography.

2. MATERIAL AND METHOD

2.1. Materials and general methods

Hexachlorocyclotriphosphazene (Otsuka Chemical Co., Ltd) was purified by fractional crystallization from n-hexane. Sodium hydride, (60% dispersion in mineral oil, Merck; prior to use the oil was removed by washing with dry heptane followed by decantation). Methyl 4-Hydroxybenzoate (99.0%), Ethyl 4-Hydroxybenzoate (99.0%) were obtained from Alfa Aesar and Benzyl 4-hydroxybenzoate (99.0%) was obtained from Aldrich. Tetrahydrofuran (99.0%), *n*-hexane (95.0%), were obtained from Merck. Silica gel 60 (230–400 mesh) for column chromatography was obtained from Merck. CDCl$_3$ for NMR spectroscopy was obtained from Merck. Mass spectra were recorded on a Bruker MALDI–TOF (Matrix-Assisted Laser Desorption/Ionization-Time-Of-Flight mass, Rheinstetten, Germany) spectrometer using DIT (1,8,9-anthrasenetriol) and DHB (2,5-Dihydroxybenzoic acid) as a matrix. All reactions were monitored using thin-layer chromatography (TLC) on Merck silica gel plates (Merck, Kieselgel 60, 0.25 mm thickness) with F$_{254}$ indicator. Column chromatography was performed on silica gel (Merck, Kieselgel 60, 230–400 mesh; for 3 g.

crude mixture, 100 g). All reactions were carried out under an argon atmosphere. ^{1}H, ^{31}P NMR and ^{13}C NMR spectra were recorded in CDCl$_3$ solutions on a Varian INOVA 500 MHz spectrometer. Melting point analyses were performed on a Stuart SMP3 melting point apparatus.
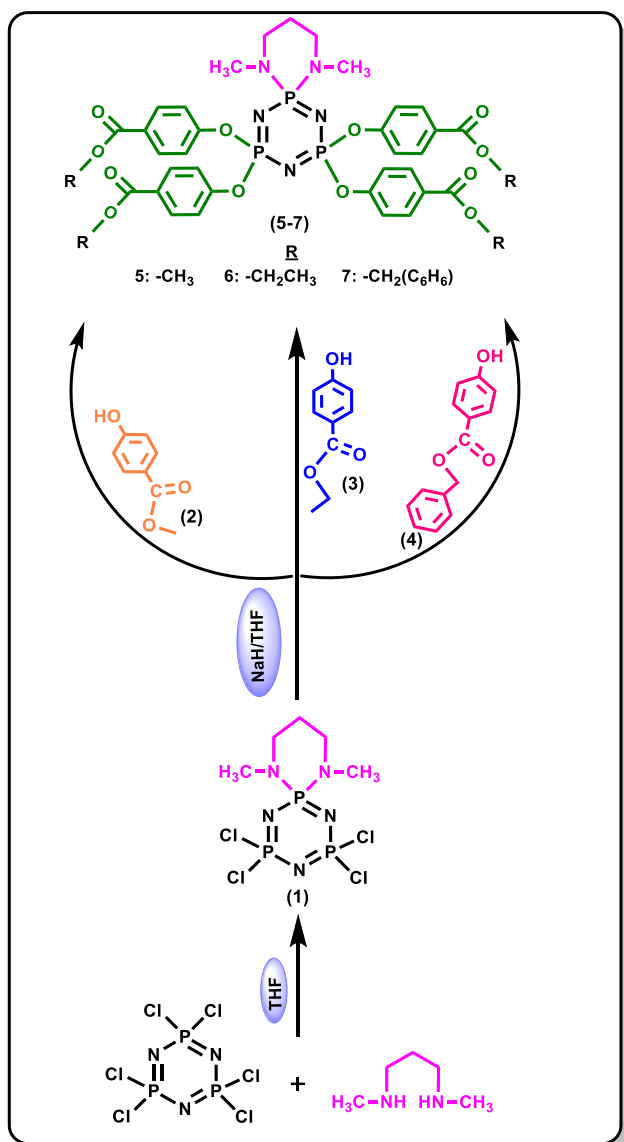
Scheme 1. Synthesis routes for paraben substituted *monospiro*-cyclotriphosphazenes.

2.2. X-ray Crystallography

The structure of the compound 5 was confirmed by X-ray crystallography. The intensity data and unit cell measurements were obtained on a Bruker APEX II QUAZAR three-circle diffractometer using monochromatized Mo-Kα X–radiation (λ = 0.71073 Å). Indexing was performed using APEX2 [27]. Data integration and reduction were carried out with SAINT [28]. Absorption correction was performed by multi-scan method implemented in SADABS [29]. The structure was solved using SHELXT [30] and then refined by full-matrix least-squares refinements on F2 using the SHELXL [31] in SHELXTL Software Package [32]. All non-hydrogen atoms were refined anisotropically using all reflections

with I > 2σ(I). The C-bound H atoms were positioned geometrically and refined using a riding mode. CCDC 2151053 (comp. 5) contains the supplementary crystallographic data for this paper. These data can be obtained free of charge from The Cambridge Crystallographic Data Centre via www.ccdc.cam.ac.uk/data_request/cif. Mercury software was used for visualization of the cif file [33].

2.3. Experimental Section

2.3.1. Syntheses of compound 1
Compound **1** was synthesized according to the literature [10].

2.3.2. Synthesis of compound 5
Methyl 4-Hydroxybenzoate (2) (0.48 g, 3.2 mmol) and NaH (0.13 g. 3.2 mmol) were dissolved in 30 mL of dry THF under an argon atmosphere in a 100 mL three-necked round-bottomed flask. The reaction mixture was cooled in an icebath and *monospiro* compound (1) (0.3 g, 0.80 mmol) in 10 mL of dry THF was dropped into the reaction medium. The reaction mixture was stirred at room temperature for 3 days, controlled by TLC. The reaction mixture was filtered to remove the formed sodium chloride and the solvent was removed under reduced pressure. The crude was subjected to column chromatography using THF:*n*-hexane (1:2) as the eluent. Compound 5 (183 mg, 28%, colorless oily, Rf = 0.32) was isolated from the crude and the product was crystallized using an *n*-hexane-THF (4:1) system (m.p:103°C). ^{1}H NMR (500 MHz, 298 K, CDCl$_3$-d1 δ, ppm): 7.96 (d, H$_a$/ H$_a$', 8H, $^3J_{Ha-Hb}$= 8.56 Hz), 7.26 (d, H$_b$/H$_b$', 8H, $^3J_{Hb-Ha}$= 8.33 Hz), 3.92 (s, -OCH$_3$, 12H), 2.97 (m, spiro-N-CH$_2$, 4H, $^3J_{H-H}$=5.50, $^3J_{H-H}$=9.15), 2.10 (d, spiro-N-CH$_3$, 6H), 1.84 (m, spiro-chain-CH$_2$- CH$_2$-CH$_2$-, 2H); ^{31}P NMR-decoupled to (202 MHz, CDCl$_3$, 298 K), δ=23.88 ppm 2[PN(Spiro)] (t, 1P, $^2J_{AX}$=59.82 Hz); δ=9.30 [PR$_2$] (R=methylparaben) (d, 2P, $^2J_{XA}$=59.85 Hz). Spin system: AX$_2$. Anal. Calc. for C$_{37}$H$_{40}$N$_5$O$_{12}$P$_3$, MALDI-TOF-MS (DHB)(*m/z*) calc: 839.67 m/z, found: 840.481 m/z [M]$^+$. ^{13}C NMR (CDCl$_3$, δ, ppm) 166.23, 154.53, 131.22,126.85, 120.90, 52.16, 50.20, 34.74, 24.54.

2.3.3. Synthesis of compound 6
Ethyl 4-Hydroxybenzoate (3) (0.53 g, 3.2 mmol) and NaH (0.13 g. 3.2 mmol) were dissolved in 30 mL of dry THF under an argon atmosphere in a 100 mL three-necked round-bottomed flask. The reaction mixture was cooled in an icebath and monospiro compound (1) (0.3 g, 0.80 mmol) in 10 mL of dry THF was dropped into the reaction medium. The reaction mixture was stirred at room temperature for 4 days, controlled by TLC. The reaction mixture was filtered to remove the formed sodium chloride and the solvent was removed under reduced pressure. The crude was subjected to column chromatography using THF:n-hexane (1:2) as the eluent. Compound 8 (181 mg, 25%, colorless oily, Rf = 0.49) was isolated from the crude.^{1}H NMR (500 MHz, 298 K, CDCl$_3$-d1 δ, ppm): 7.98 (d, H$_a$/ H$_a$', 8H, $^3J_{Ha-Hb}$= 8.17 Hz), 7.27 (d, H$_b$/H$_b$', 8H, $^3J_{Hb-Ha}$= 8.50 Hz), 4.39 (s, -OCH$_2$-, 8H, $^3J_{H-H}$=6.70, $^3J_{H-}$

H=13.51), 2.97 (m, spiro-N-CH$_2$, 4H, $^3J_{H-H}$=9.13, $^3J_{H-H}$=11.00), 2.10 (d, spiro-N-CH$_3$, 6H), 1.84 (m, spiro-chain-CH$_2$- CH$_2$- CH$_2$-, 2H), 1.41 (t, -O-CH$_2$-CH$_3$, $^3J_{H-H}$=6.81); ^{31}P NMR-decoupled to (202 MHz, CDCl$_3$, 298 K), δ=23.31 ppm [PN(Spiro)] (t, 1P, $^2J_{AX}$=58.41 Hz); δ=9.23 [PR$_2$] (R=ethylparaben) (d, 2P, $^2J_{XA}$=59.04 Hz). Spin system: AX$_2$. Anal. Calc. for C$_{41}$H$_{48}$N$_5$O$_{12}$P$_3$, MALDI-TOF-MS (DHB)(*m/z*) calc. 895.78, found: 896.367 [M]$^+$. ^{13}C NMR (CDCl$_3$, δ, ppm) 166.18, 154.45, 131.89,127.25, 120.90, 60.96, 50.23, 34.73, 24.68, 14.38.

2.3.4. Syntheses of compounds 7

Benzyl 4-Hydroxybenzoate (4) (0.73 g, 3.2 mmol) and NaH (0.13 g. 3.2 mmol) were dissolved in 30 mL of dry THF under an argon atmosphere in a 100 mL three-necked round-bottomed flask. The reaction mixture was cooled in an icebath and *monospiro* compound (1) (0.3 g, 0.80 mmol) in 10 mL of dry THF was dropped into the reaction medium. The reaction mixture was stirred at room temperature for 6 days, controlled by TLC. The reaction mixture was filtered to remove the formed sodium chloride and the solvent was removed under reduced pressure. The crude was subjected to column chromatography using THF:n-hexane (1:3) as the eluent. Compound 7 (138 mg, 15%, colorless oily, Rf = 0.17) was isolated from the crude. ^{1}H NMR (500 MHz, 298 K, CDCl$_3$-d1 δ, ppm): 8.05 (d, H$_a$/ H$_a$', 8H, $^3J_{Ha-Hb}$= 8.39 Hz), 7.51-7.34 (m, -H$_d$/-H$_c$/-H$_e$, 20H), 7.30 (d, H$_b$/H$_b$', 8H, $^3J_{Hb-Ha}$= 8.24 Hz), 5.38 (s, -OCH$_2$, 8H), 2.99 (m, spiro-N-CH$_2$, 4H, $^3J_{H-H}$=5.22, $^3J_{H-H}$=9.55), 2.13 (d, spiro-N-CH$_3$, 6H), 1.86 (m, spiro-chain-CH$_2$- CH$_2$- CH$_2$-, 2H); ^{31}P NMR- decoupled to (202 MHz, CDCl$_3$, 298 K), δ=23.66 ppm [PN(Spiro)] (t, 1P, $^2J_{AX}$=59.64 Hz); δ=9.17 [PR$_2$] (R=benzylparaben) (d, 2P, $^2J_{XA}$=59.71 Hz). Spin system: AX$_2$. Anal. Calc. for C$_{61}$H$_{56}$N$_5$O$_{12}$P$_3$, MALDI-TOF-MS (DIT)(*m/z*) calc. 1144.06, found: 1144.182 [M]$^+$. ^{13}C NMR (CDCl$_3$, δ, ppm) 165.59, 154.71, 135.97, 131.42, 128.63, 128.30, 128.19, 126.87, 120.97, 66.82, 50.23, 34.79, 24.55.

3.   RESULTS AND DISCUSSION

3.1. Synthesis and characterization of paraben substituted cyclotriphosphazenes

In the present study, hexachlorocyclotriphosphazene was reacted with N,N' -dimethyl 1,3-propane diamine under an argon atmosphere at room temperature to yield *monospiro* compound (1) according to the literature [10]. Compound **1** was reacted with methyl 4-hydroxybenzoate, ethyl 4-hydroxybenzoate and benzyl 4-hydroxybenzoate at room temperature in a ratio of 1:4 to give compounds 5-7, respectively. The final compounds (5–7) were characterized by MALDI-TOF MS, NMR (^{1}H, ^{31}P, ^{13}C) spectroscopy techniques. Also, the molecular structure of the 5 compound was also elucidated by single crystal X-ray crystallography. The spectral data of compounds 5–7 were given in the supporting information file (Fig. S1-S15). The molecular ion peaks for compounds 5–7 were

measured using MALDI-TOF MS as 840.481, 896.367 and 1144.182, respectively (Table 1, Fig. S1, S6, and S11, ESI†), which are all consistent with the proposed structures. The ^{31}P (decoupled/coupled) and ^{1}H NMR spectra of compound 5 are shown in Fig. 1a, b and c, respectively. All of the compounds showed similar signals for aromatic protons at around δ=8.05–7.26 ppm range and the aliphatic protons of the spiro groups were observed at around δ=5.38–1.84 ppm range (Fig. S2, S7, and S12, ESI†). The products formed in each reaction mixture were checked using thin-layer chromatography (TLC), proton-decoupled and proton-coupled ^{31}P NMR spectroscopy. The ^{31}P NMR chemical shifts and phosphorus-phosphorus coupling constants of the pure compounds are given in the experimental section and Table 1. The proton decoupled ^{31}P NMR spectra of compounds 5–7, as expected, were observed as AX$_2$ spin systems, due to the two different phosphorus nuclei present in the cyclotriphosphazene rings (Table 1). All of the compounds similar signals consisted of one triplet for the [PN(Spiro)] group (δ=23.88-23.31 ppm range) and one dublet for the [PR$_2$] group (δ=9.30-9.17 ppm range) (Fig. S3, S8 and S13 ESI†). Also, the multiple peak resonating at δ=23.88-23.66 ppm range in the proton-coupled ^{31}P NMR spectra of all compounds belong to the [PN(Spiro)] group and are cleaved due to protons located beyond two bonds (Fig. S4, S9 and S14 ESI†). In the ^{13}C NMR spectra of the compounds (5–7), carbonyl (C=O) carbon peaks were observed in the δ=166.23–165.59 ppm range, aromatic carbon peaks in the δ=154.71–120.90 ppm range, and aliphatic carbon peaks in the δ=66.82–14.38 ppm range (Fig. S5, S10 and S15 ESI†).
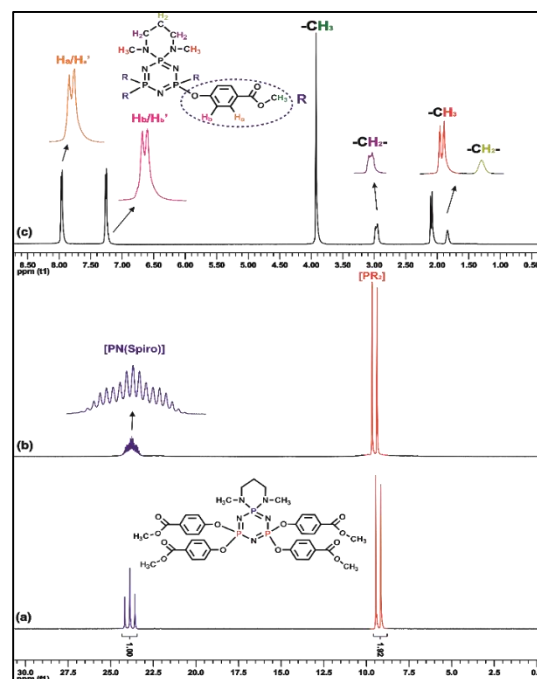
Fig. 1.   **(a)** ^{31}P decoupled NMR **(b)** ^{31}P {^{1}H} NMR **(c)** ^{1}H NMR spectrum in CDCl$_3$ of compound 5.

Table 1. ^{31}P NMR and Mass Parameters for Compounds 3[a] and 5−7[a].

Compd.	^{31}P NMR (δ, ppm)			spin system	$^2J_{P-P}$ [Hz]	Mass (m/z)
	[PCl$_2$]	[PR$_2$]	[PN(Spiro)]		$^2J_{P-P}$	[M]$^+$
3[b]	22.80	-	16.00	A$_2$X	35.04	376.137
5	-	9.30	23.88	AX$_2$	59.82	840.481
6	-	9.23	23.31	AX$_2$	58.41	896.367
7	-	9.17	23.60	AX$_2$	59.64	1144.182

[a]CDCl$_3$, [b]Reference [10].
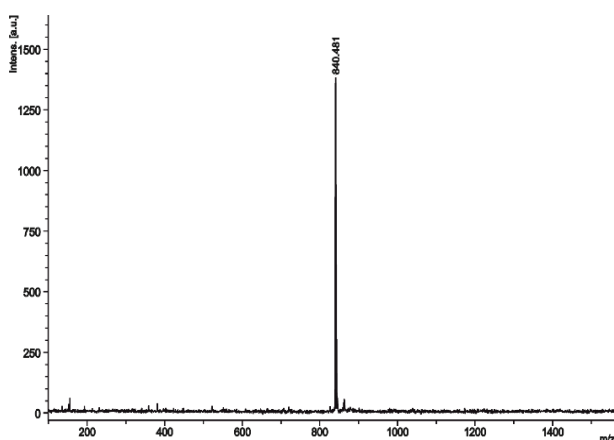
Fig. 2. Mass spectrum of compound 5.

3.2 X-Ray crystallography

The newly synthesized paraben-substituted cyclotriphosphazene (5) was crystallized in the *n*-hexane:THF solvent system, and single crystals were grown by recrystallization in the same solvent system. The solid state structure and geometry of Compound 5 was determined using single-crystal X-ray structural analysis (Fig. 3, S16). Crystallographic data and refinement details of the data collection for compound 5 is summarized in Table 2. The bond lengths and bond angles of compound **5** was given in Supplamentary Materials. Compound **5** has the triclinic crystal system with *P-1* space group. The P–N bonds in the cyclotriphosphazene ring (N$_3$P$_3$) range from 1.5674(19) Å to 1.650(2) Å and show double bond character. The P-N-P angles in the compound change range from 118.45(11)° to 123.14(12)°, and N–P–N bond angles vary range from 114.19(10)° to 118.13(10)°. The bond parameters of compound 5 are consistent with the crystallographic data of cyclotriphosphazene derivatives reported in the literatures [26, 11].
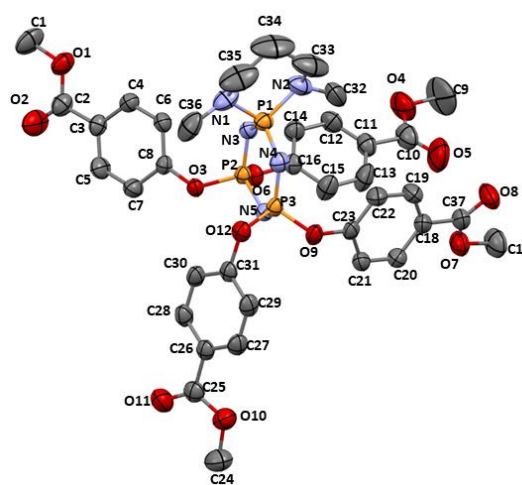
Fig. 3. The ball-stick drawings of the molecular structure of compound 5. The gray, gold, blue, and red colored atoms represent C, P, N, and O atoms, respectively. All hydrogen atoms have been omitted for clarity.

Table 2. Crystal data and refinement parameters for compound 5.

CCDC	2151053
Empirical Formula	C$_{37}$H$_{40}$N$_5$O$_{12}$P$_3$
Formula weight (g. mol^{-1})	839.65
Temperature (K)	296
Radiation	MoK$_α$ (λ = 0.71073)
Crystal system	Triclinic
Space group	P-1
a (Å), b (Å), c (Å)	10.9405(14), 11.4582(15), 17.099(2)
α(°),β(°), γ(°)	74.851(2), 85.012(2), 75.717(2)
Crystal size (mm)	0.28 × 0.13 × 0.09
V (Å^3)	2004.5 (4)
Z	2
ρ$_{calcd}$ (g. cm^{-3})	1.391
μ (mm^{-1})	0.22
F(000)	876
h, k, l max.	14,14,22
Reflections collected	9189
R[F^2 > 2σ(F^2)], wR(F^2), S	0.048, 0.131, 1.03

4. CONCLUSIONS

Although parabens show antibacterial and antifungal activity properties, their toxic effects to human health research and discussions still continue. In this case, scientists are in an effort to obtain new paraben-substituted compounds that have no toxicity effect. It is essential to synthesize and research new paraben-substituted compounds that do not have side effects on, especially human breast tissue etc. In this direction, studies continue in our laboratory. For this purpose, a series of paraben substituted *monospiro*-cyclotriphosphazene compounds have been successfully synthesized. The structural properties of all synthesized compounds (5-7) were examined by MALDI-TOF spectrometer, X-Ray (for compound 5), ^{1}H, ^{31}P and ^{13}C NMR spectroscopy. Biological activity and application studies will be continued in our laboratory in the future.

Acknowledgements

5. CONFLICT OF INTEREST

The authors declare no competing financial interest.

Ethical Approval: Ethics Approval is not required for this study.

REFERENCES

[1] Katakam, L. N. R., Ettaboina, S. K. and Dongala, T., "A simple and rapid HPLC method for determination of parabens and their degradation products in pharmaceutical dosage forms", *Biomedical Chromatography*, (**2021**), 35, 10, e5152.

[2] Matwiejczuk, N., Galicka, A. and Brzóska, M. M., ''Review of the safety of application of cosmetic products containing parabens'', *Journal of Applied Toxicology*, (**2020**), 40, 1, 176-210.

[3] Nguyen, T., Clare, B., Guo, W. and Martinac, B., ''The effects of parabens on the mechanosensitive channels of E. coli'', *European Biophysics Journal*, (**2005**), 34, 5, 389-395.

[4] Byford, J., Shaw, L., Drew, M., Pope, G., Sauer, M., Darbre, P. D., ''Oestrogenic activity of parabens in MCF7 human breast cancer cells'', *The Journal of steroid biochemistry and molecular biology,* (**2002**), 80, 1, 49-60.

[5] Darbre, P. D. and Harvey, P. W., ''Paraben esters: review of recent studies of endocrine toxicity, absorption, esterase and human exposure, and discussion of potential human health risks", *Journal of applied toxicology*, (**2008**), 28, 5, 561-578.

[6] Hager, E., Chen, J., and Zhao, L. ''Minireview: Parabens Exposure and Breast Cancer'' International Journal of Environmental Research and Public Health, (**2022**),19(3), 1873.

[7] Liang, J., Yang, X., Liu, Q. S., Sun, Z., Ren, Z., Wang, X.,, Zhang Q., Ren X., Liu X., Zhou Q., and Jiang G., ''Assessment of Thyroid Endocrine Disruption Effects of Parabens Using In Vivo, In Vitro, and In Silico Approaches'', Environmental science & technology. (**2022**), 56, 460−469.

[8] Witorsch, R. J. and Thomas, J. A., ''Personal care products and endocrine disruption: a critical review of the literature", *Critical reviews in toxicology*, (**2010**), 40, sup3, 1-30.

[9] Allen, C. W., ''Regio-and stereochemical control in substitution reactions of cyclophosphazenes", *Chemical Reviews,* (**1991**), 91, 2, 119-135.

[10] Yenilmez Çiftçi, G., Eçik, E. T., Yıldırım, T., Bilgin, K., Şenkuytu, E., Yuksel, F., Uludağ, Y. and Kılıç, A., ''Synthesis and characterization of new cyclotriphosphazene compounds", *Tetrahedron,* (**2013**), 69, 5 1454-1461.

[11] Şenkuytu, E., Akbaş, N., Yıldırım, T. and Yenilmez Çiftçi, G., Y., ''Synthesis, characterization and cytotoxic activity studies on cancer cell lines of new paraben-decorated monospiro-cyclotriphosphazenes", *New Journal of Chemistry,* (**2022**), 46(5), 2453–2464.

[12] Şenkuytu, E., Akbaş, N., Yıldırım, T. and Yenilmez Çiftçi, G., ''The Bioactive New Type Paraben Decorated Dispiro-Cyclotriphosphaze Compounds: Synthesis, Characterization and Cytotoxic Activity Studies'', *Journal of Molecular Structure*, (**2022**), 1255,132438.

[13] Yenilmez Çiftçi, G., Bayık, N., Eçik, E. T., Şenkuytu, E., Akşahin, M., and Yıldırım, T. ''Synthesis of the first 2-hydroxyanthraquinone substituted cyclotriphosphazenes and their cytotoxic properties'' *New Journal of Chemistry*, (**2020**), 44(39), 16733-16740.

[14] Yenilmez Çiftçi, G., Demir, G., Şenkuytu, E., Eçik, E. T., Aksahin, M., and Yıldırım, T. ''2-Hydroxyanthraquinone substituted cyclotriphosphazenes: Synthesis and cytotoxic activities in cancer cell lines'' *Inorganica Chimica Acta*, (**2021**), 514, 120005.

[15] İbişoğlu, H., Erdemir, E., Atilla, D., Ün, Ş. Ş., Topçu, S. and Şeker, M. G., ''Synthesis, characterization and antimicrobial properties of cyclotriphosphazenes bearing benzimidazolyl rings", *Inorganica Chimica Acta*, (**2020**), 509, 119679.

[16] Song, S.-C., Lee, S. B., Lee, B. H., Ha, H.-W., Lee, K.-T. and Sohn, Y. S., ''Synthesis and antitumor

activity of novel thermosensitive platinum (II)–cyclotriphosphazene conjugates", *Journal of controlled release*, (**2003**), 90, 3, 303-311.

[17] Koran, K., Ozkaya, A., Ozen, F., Cil, E. and Arslan, M., ''Synthesis, characterization, and biological evaluation of new oxime-phosphazenes", *Research on Chemical Intermediates*, (**2013**), 39, 3, 1109-1124.

[18] Jiménez, J., Laguna, A., Gascón, E., Sanz, J. A., Serrano, J. L., Barberá, J. and Oriol, L., ''New liquid crystalline materials based on two generations of dendronised cyclophosphazenes", *Chemistry–A European Journal*, (**2012**), 18, 52, 16801-16814.

[19] Okutan, E., Eserci, H., Şenkuytu, E., ''New perylenebisimide decorated cyclotriphosphazene heavy atom free conjugate as singlet oxygen generator", *Spectrochimica Acta Part A: Molecular and Biomolecular Spectroscopy,* (**2019**), 222, 117232.

[20] Cheng, J., Wang, J., Yang, S., Zhang, Q., Huo, S., Zhang, Q., Hu, Y. and Ding, G., ''Benzimidazolyl-substituted cyclotriphosphazene derivative as latent flame-retardant curing agent for one-component epoxy resin system with excellent comprehensive performance", *Composites Part B: Engineering*, (**2019**), 177, 107440.

[21] Yenilmez Çiftçi, G., Şenkuytu, E., İncir, S. E., Yuksel, F., Ölçer, Z., Yıldırım, T., Kılıç, A., Uludağ, Y., ''First paraben substituted cyclotetraphosphazene compounds and DNA interaction analysis with a new automated biosensor", *Biosensors and Bioelectronics*, (**2016**), 80, 331-338.

[22] Yenilmez Çiftçi, G., Şenkuytu, E., İncir, S. E., Eçik, E. T., Zorlu, Y., Ölçer, Z. and Uludağ, Y., ''Characterization of paraben substituted cyclotriphosphazenes, and a DNA interaction study with a real-time electrochemical profiling based biosensor", *Microchimica Acta,* (**2017**), 184, 7, 2307-2315.

[23] Şenkuytu, E., Yıldırım, T., Ölçer, Z., Uludağ, Y. and Yenilmez Çiftçi, G., ''DNA interaction analysis of fluorenylidene double bridged cyclotriphosphazene

derivatives", *Inorganica Chimica Acta*, (**2018**), 477, 219-226.

[24] Yıldırım, T., Bilgin, K., Yenilmez Çiftçi, G., Eçik, E. T., Şenkuytu, E., Uludağ, Y., Tomak, L. and Kılıç, A., ''Synthesis, cytotoxicity and apoptosis of cyclotriphosphazene compounds as anti-cancer agents", *European journal of medicinal chemistry*, (**2012**), 52, 213-220.

[25] Kızılkaya, P., Şenkuytu, E., Davarcı, D., Pala, U., Ölçer, Z. and Yenilmez Çiftçi, G., ''Novel paraben derivatives of tetracyclic spermine cyclotriphosphazenes: synthesis, characterization and biosensor based DNA interaction analysis", *New Journal of Chemistry*, (**2020**), 44, 43, 18942-18953.

[26] Şenkuytu, E., Kızılkaya, P., Ölçer, Z., Pala, U., Davarcı, D., Zorlu, Y., Erdoğan, H. and Yenilmez Çiftçi, G., ''Electrophoresis and biosensor-based DNA interaction analysis of the first paraben derivatives of spermine-bridged cyclotriphosphazenes", *Inorganic Chemistry*, (**2020**), 59, 4, 2288-2298.

[27] Bruker (**2007**) APEX2, Bruker AXS Inc., Madison, Wisconsin, USA.

[28] Bruker (**2007**) SAINT, Bruker AXS Inc., Madison, Wisconsin, USA.

[29] Bruker (**2001**) SADABS, Bruker AXS Inc., Madison, Wisconsin, USA.

[30] Sheldrick, G. M. SHELXT-Integrated Space-Group and Crystal-Structure Determination. *Acta Crystallographica Section A*, A71, (**2015**) 3-8.

[31] Sheldrick, G. M. Crystal Structure Refinement with SHELXL. *Acta Crystallographica* C, C71, (**2015**) 3-8.

[32] Bruker, SHELXTL, version 6.14, Bruker AXS Inc., Madison, Wisconsin, USA, 2010.

[33] Macrae, C. F.;,Edgington, P. R., McCabe, P., Pidcock, E., Shields, G. P., Taylor, R., Towler, M., Van de Streek, J. Mercury: visualization and analysis of crystal structures. *Journal of Applied Crystallography,* 39 (**2006**) 453-457

Supplamentery Materials

Contents of Figures

COMPOUND 5

Figure S1. MALDI-MS spectrum of Compound 5
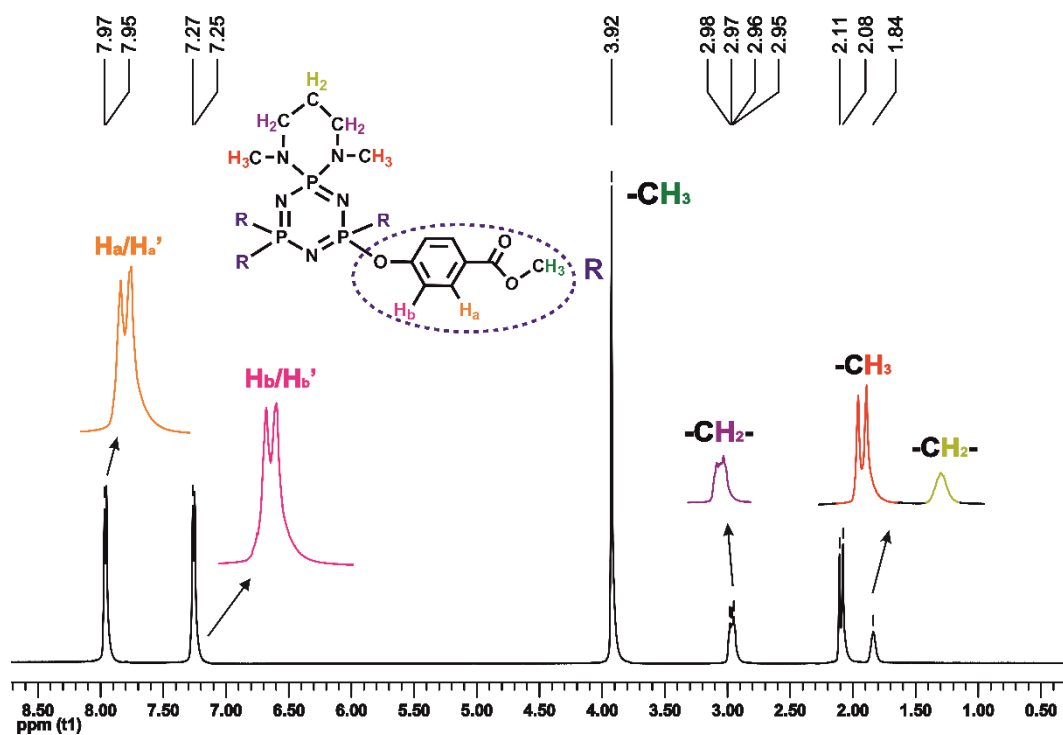
Figure S2. ^{1}H NMR spectrum of Compound 5 in CDCl$_3$
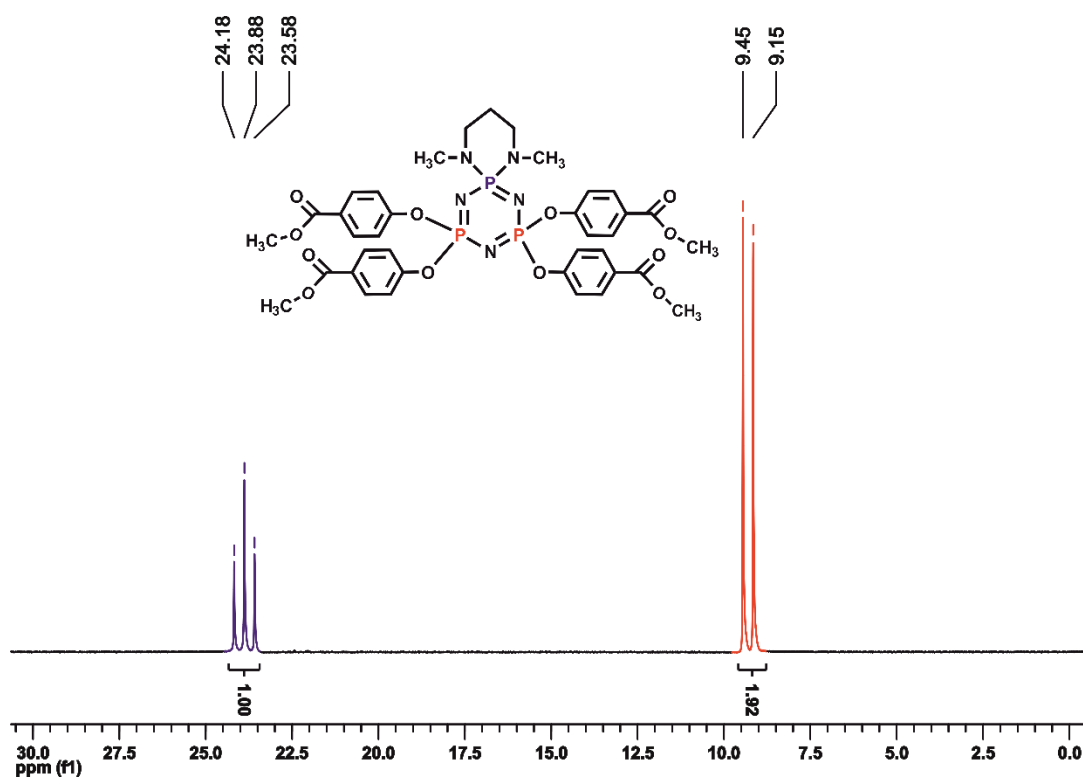
Figure S3. ^{31}P NMR decoupled spectrum of Compound 5 in CDCl$_3$
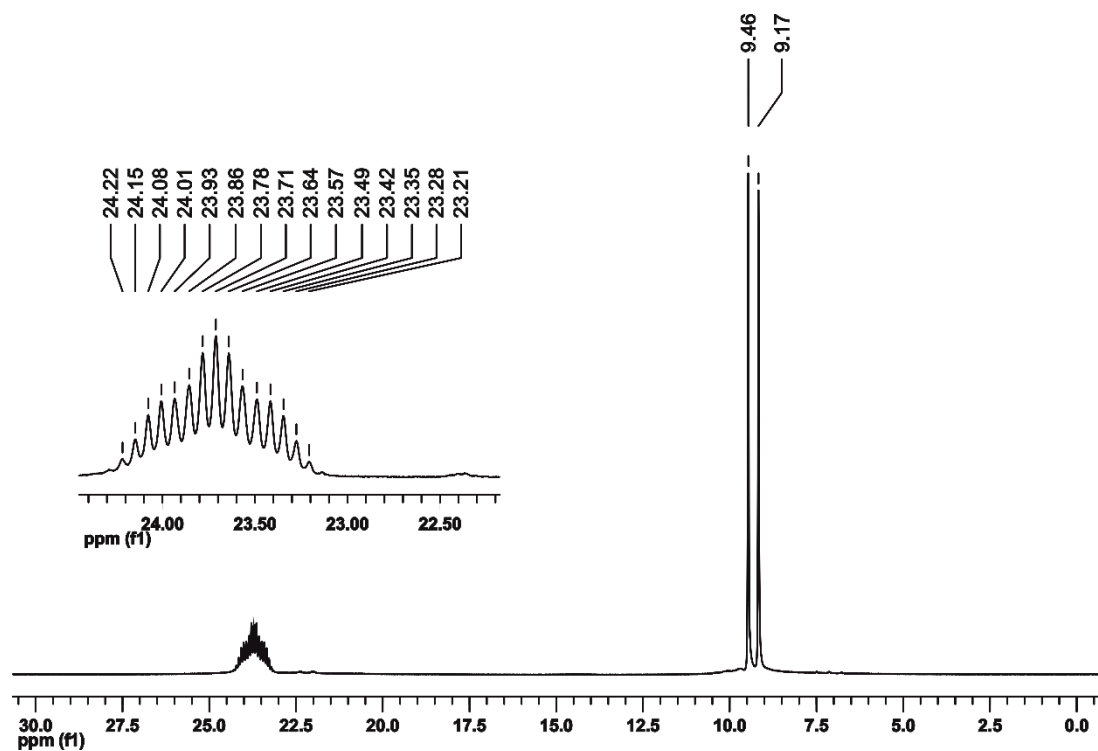
Figure S4. ^{31}P NMR coupled spectrum of Compound 5 in CDCl$_3$
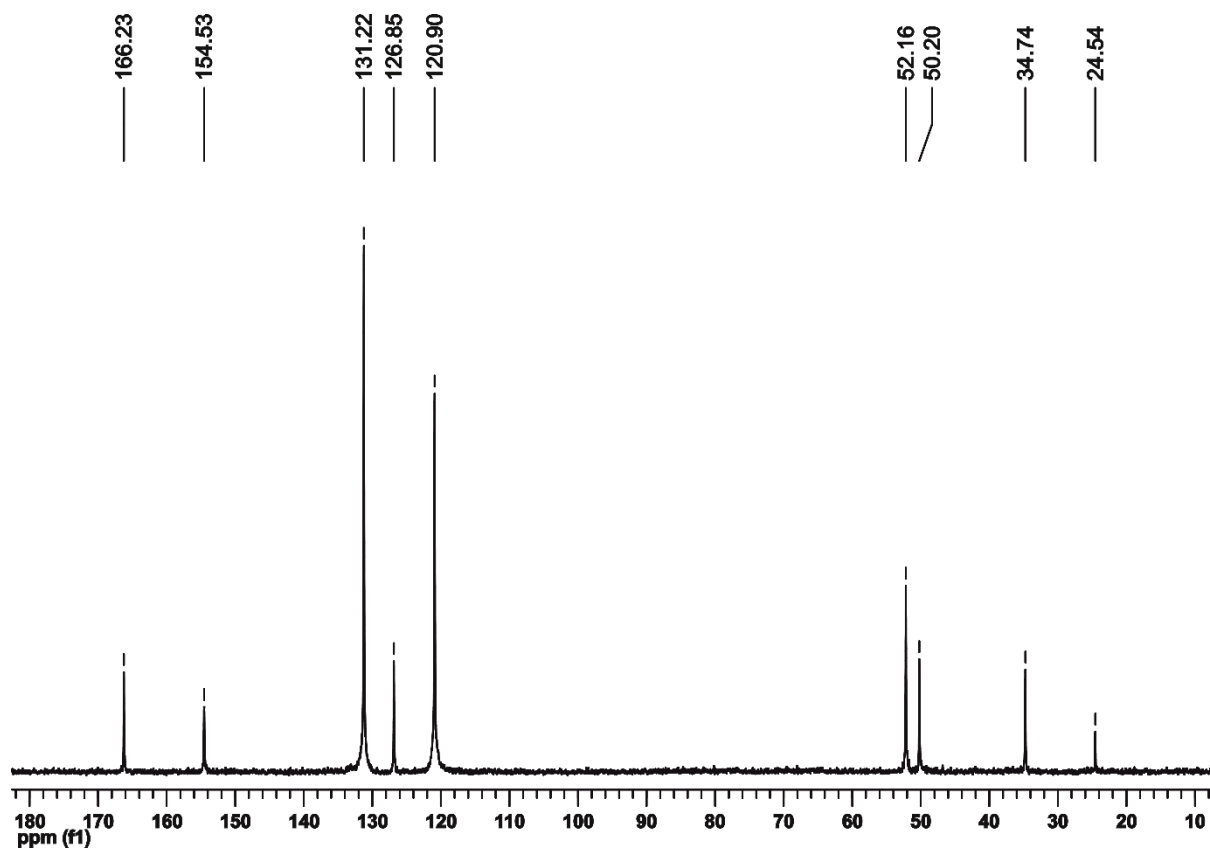
Figure S5. ^{13}C NMR spectrum of Compound **5** in CDCl$_3$

COMPOUND 6
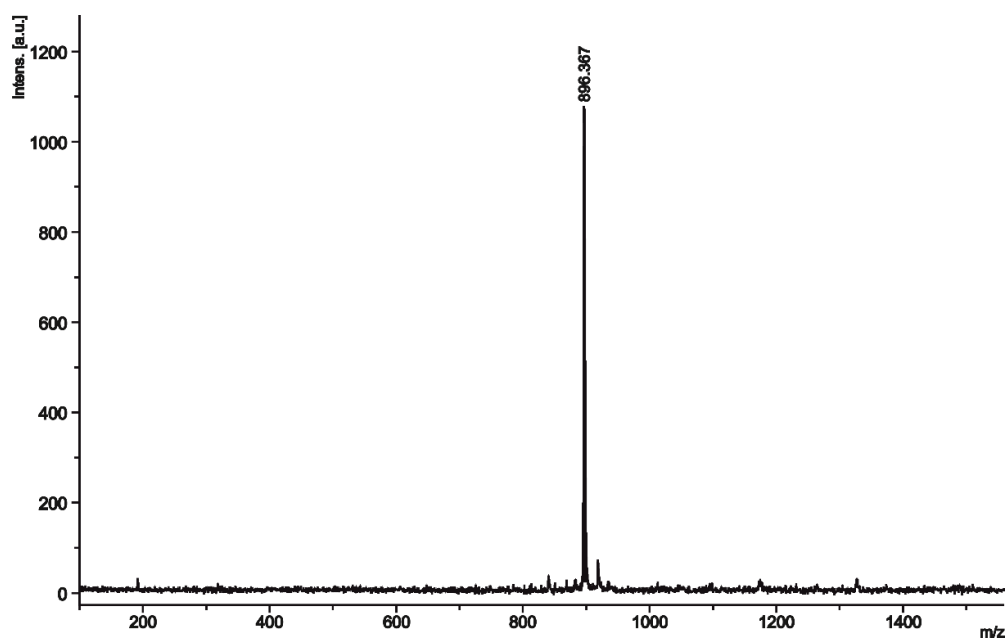
Figure S6. MALDI-MS spectrum of Compound 6
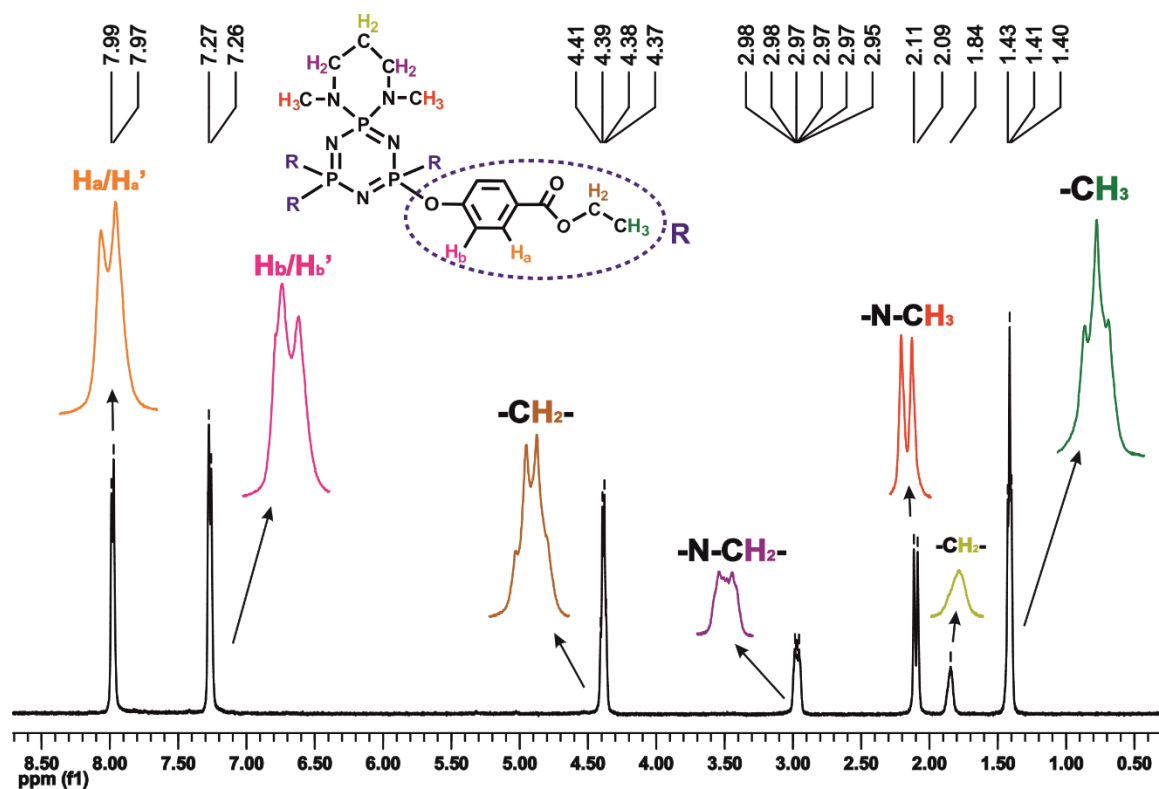
Figure S7. ^{1}H NMR spectrum of Compound 6 in CDCl$_3$

16
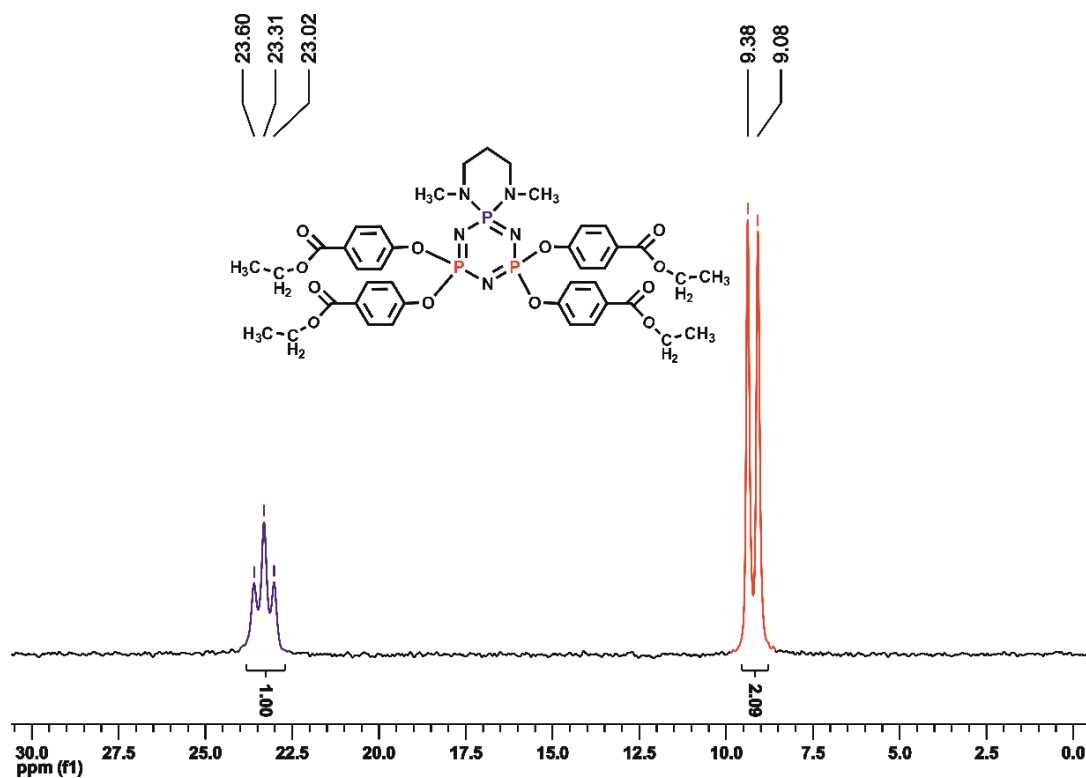
Figure S8. ^{31}P NMR decoupled spectrum of Compound 6 in CDCl$_3$
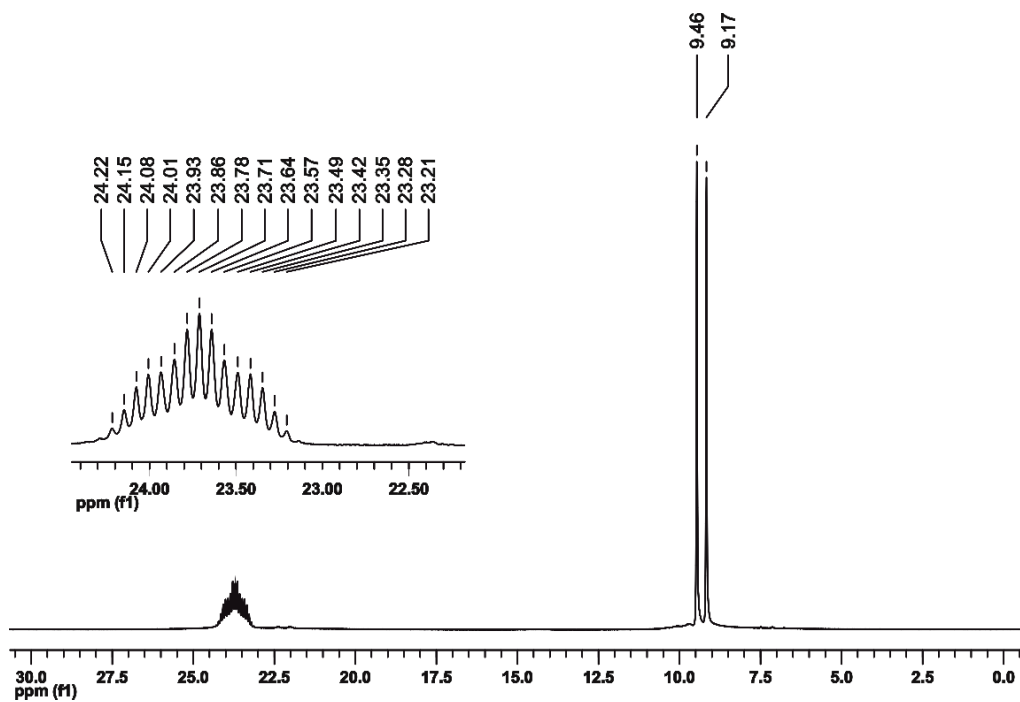
Figure S9. ^{31}P NMR coupled spectrum of Compound 6 in CDCl$_3$

17
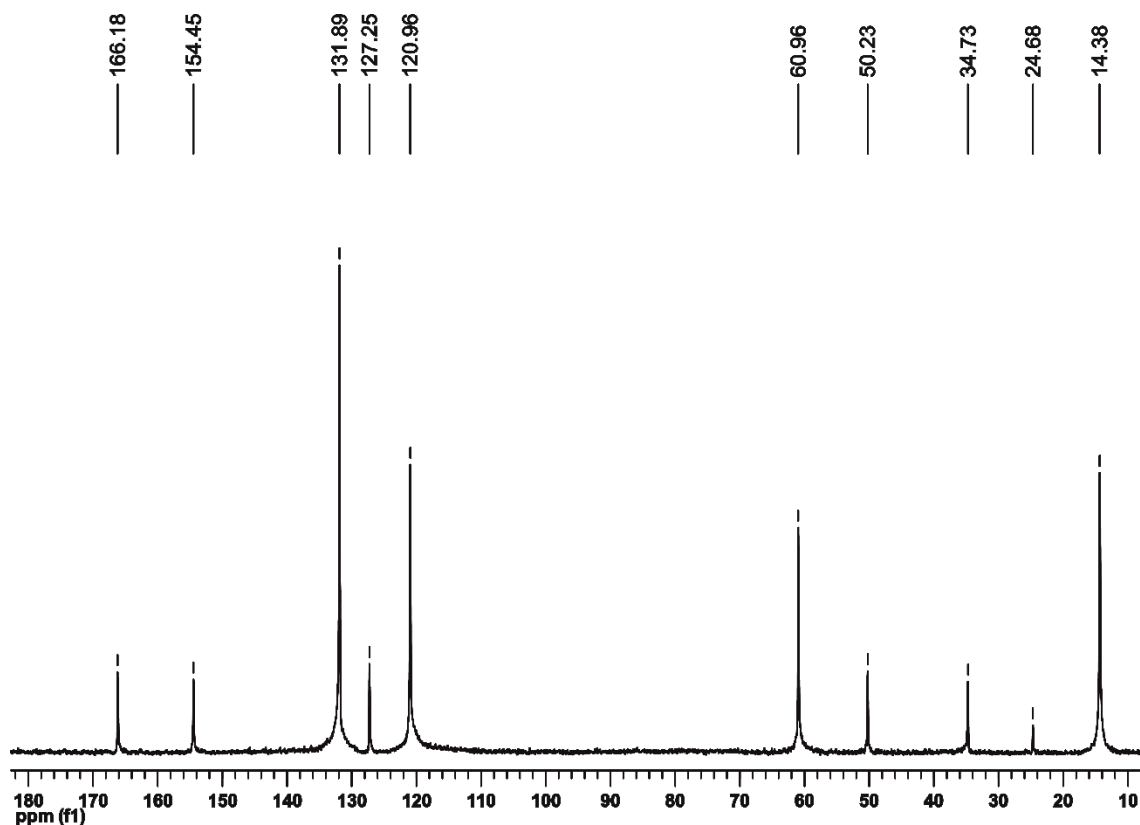
Figure S10. ¹³C NMR spectrum of Compound 6 in CDCl₃

COMPOUND 7
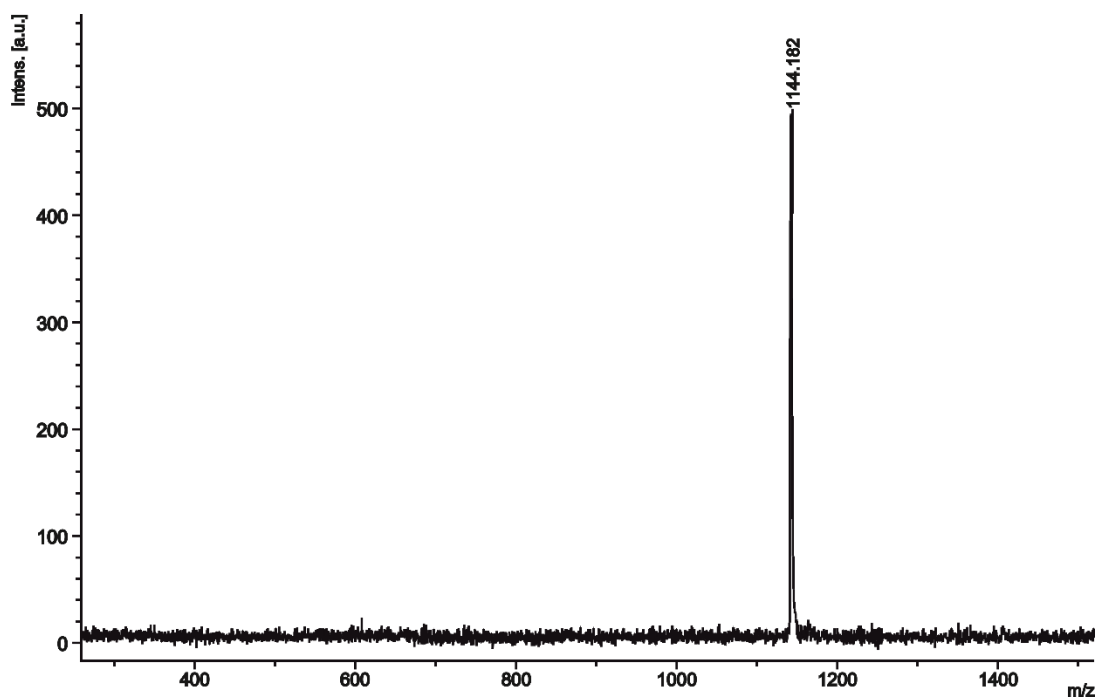
Figure S11. MALDI-MS spectrum of Compound 7
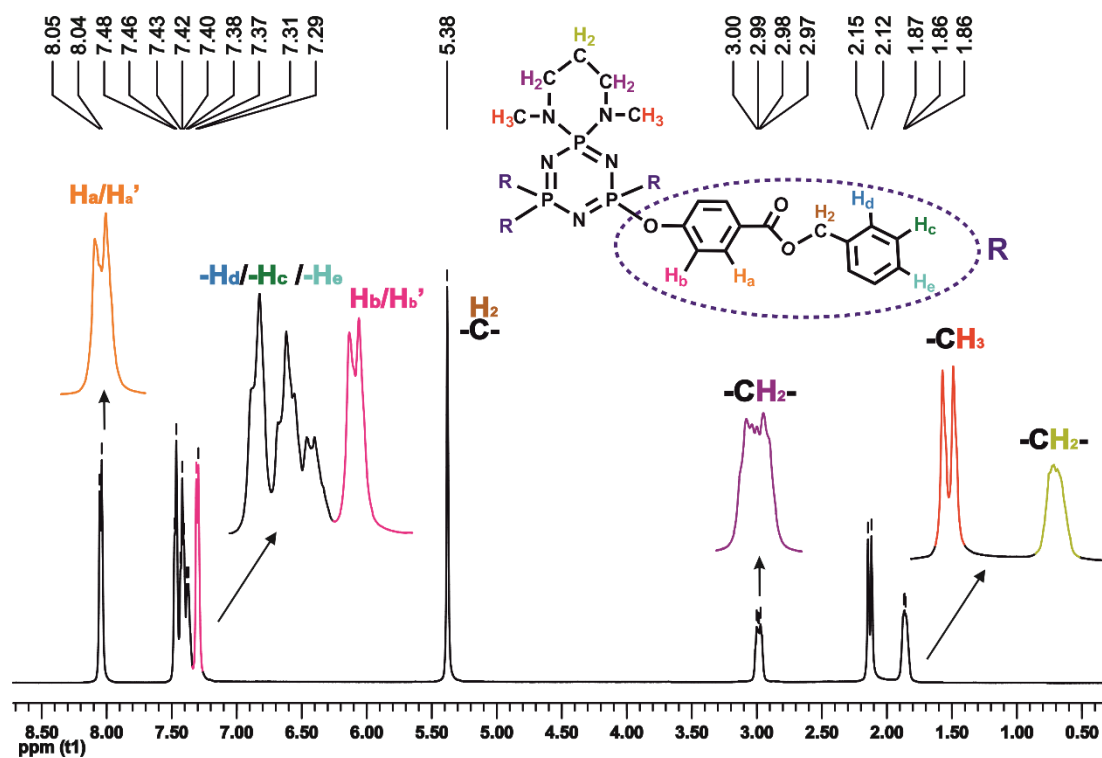
Figure S12. ^{1}H NMR spectrum of Compound 7 in CDCl$_3$
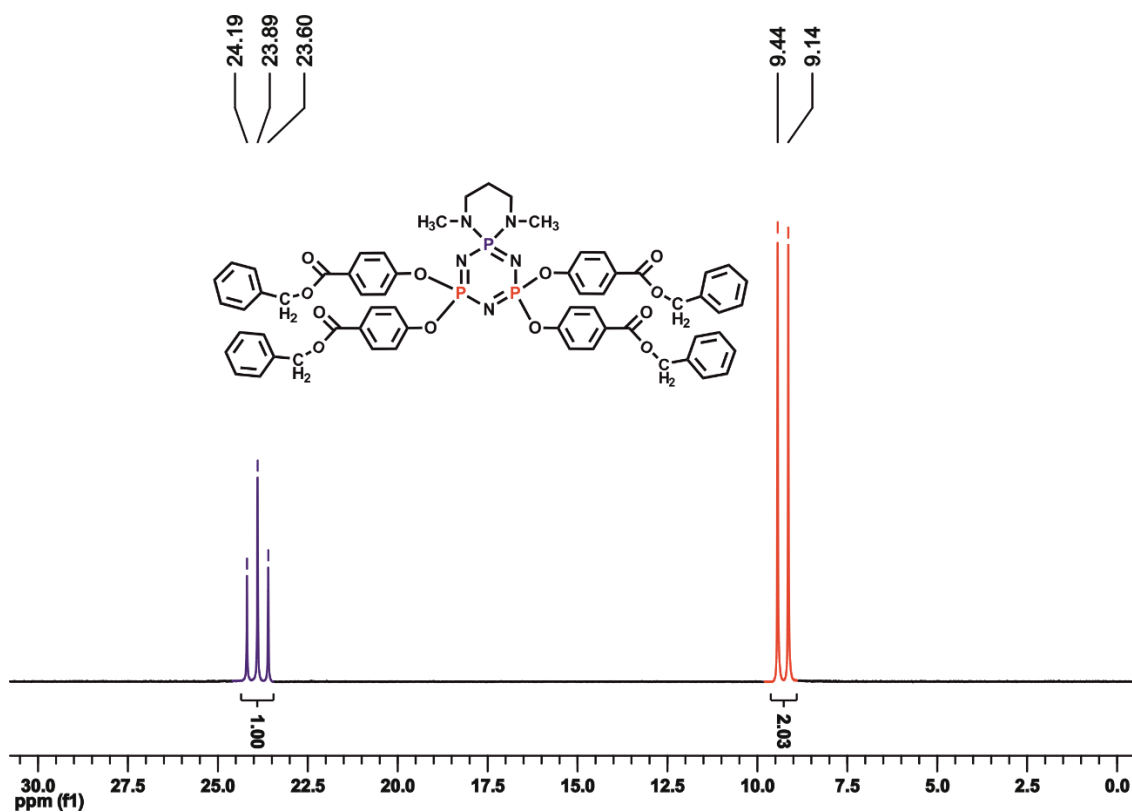
Figure S13. ^{31}P NMR decoupled spectrum of Compound 7 in CDCl$_3$

19

9.43
9.14

24.40
24.33
24.26
24.19
24.12
24.04
23.97
23.89
23.82
23.75
23.67
23.60
23.53
23.46

24.50
ppm (t1)
24.00
23.50
23.00

30.0
ppm (t1)
27.5   25.0   22.5   20.0   17.5   15.0   12.5   10.0   7.5   5.0   2.5   0.0
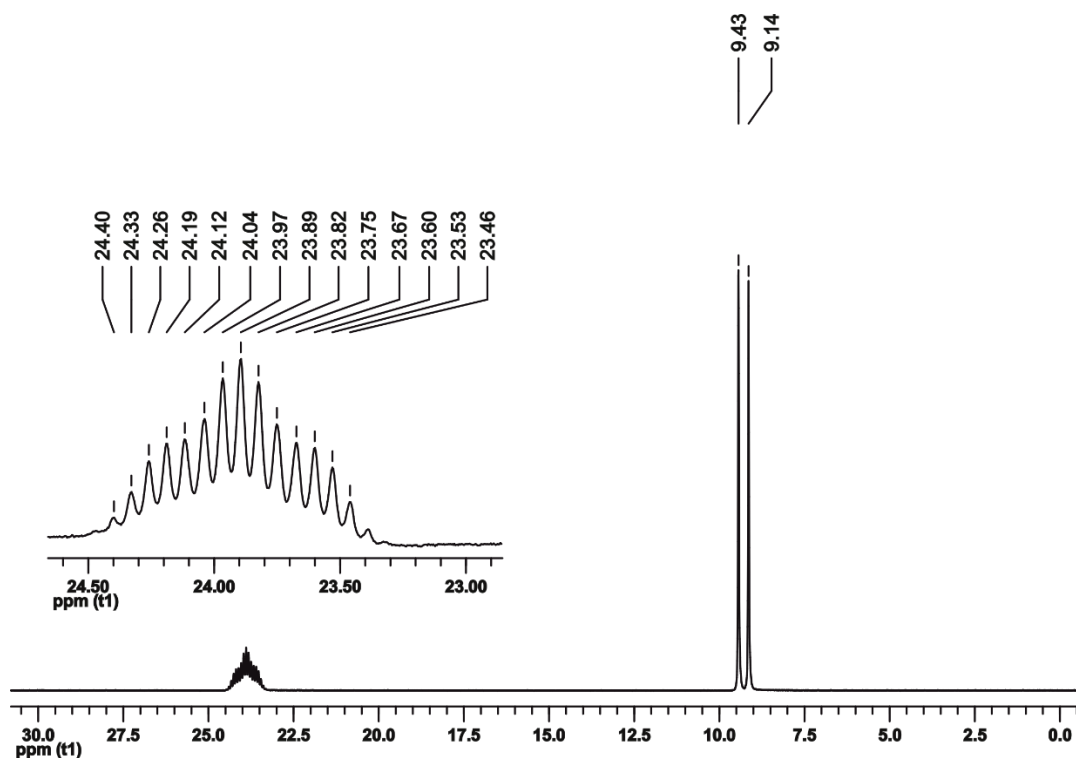
Figure S14. ^{31}P NMR coupled spectrum of Compound 7 in CDCl$_3$

165.59
154.71
135.97
131.42
128.63
128.30
128.19
126.87
120.97
66.82
50.23
34.79
24.55

180   170   160   150   140   130   120   110   100   90   80   70   60   50   40   30   20   10
ppm (f1)
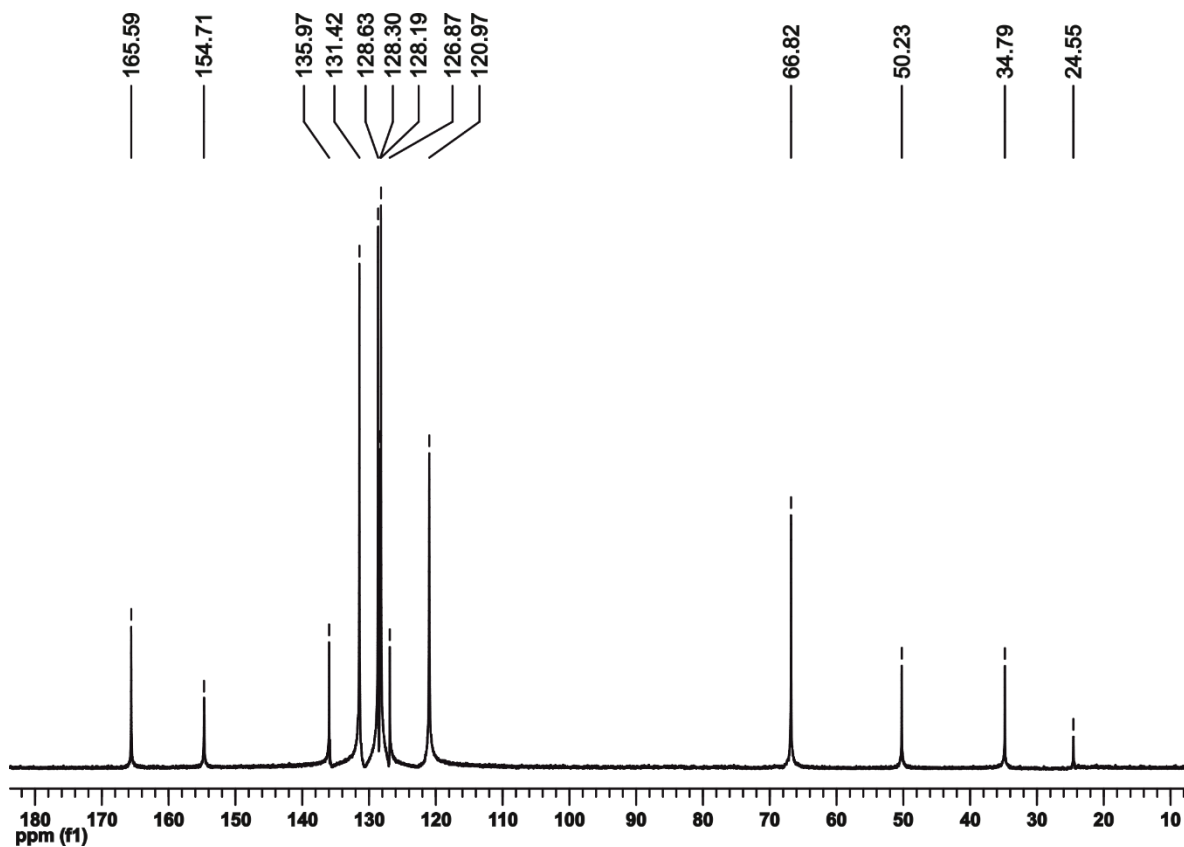
Figure S15. ^{13}C NMR spectrum of Compound 7 in CDCl$_3$
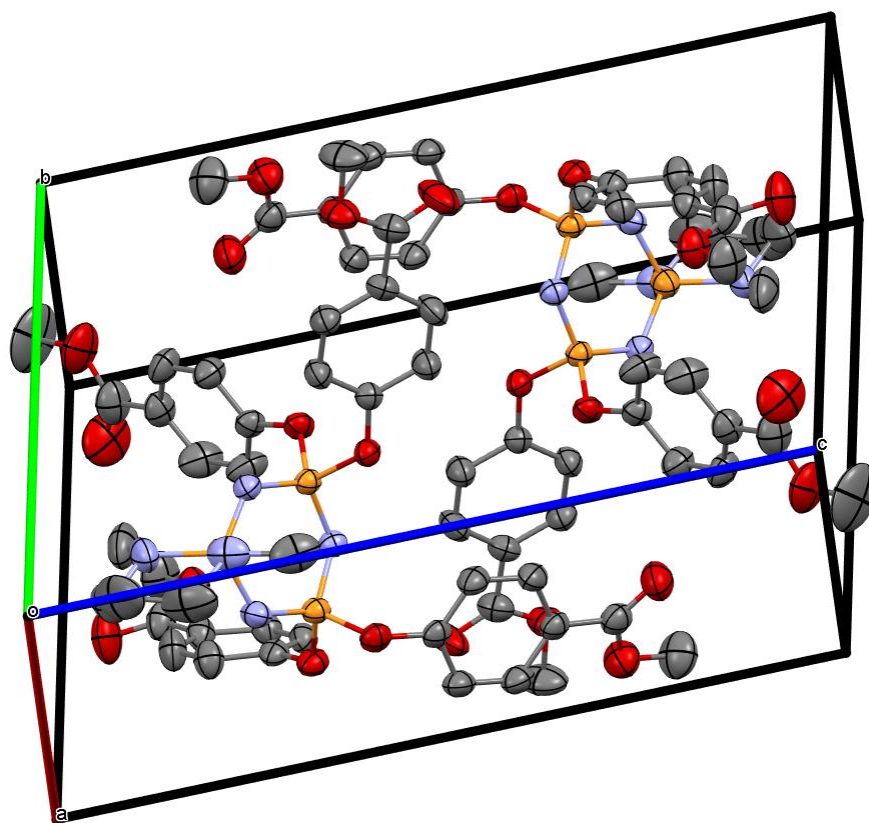
Figure S16. Perspective view of crystal packing of compound **5**

checkCIF (basic structural check) running

Checking for embedded fcf data in CIF ...
Found embedded fcf data in CIF. Extracting fcf data from uploaded CIF, please wait . . .

checkCIF/PLATON (basic structural check)

You have not supplied any structure factors. As a result the full set of tests cannot be run.

THIS REPORT IS FOR GUIDANCE ONLY. IF USED AS PART OF A REVIEW PROCEDURE FOR PUBLICATION, IT SHOULD NOT REPLACE THE EXPERTISE OF AN EXPERIENCED CRYSTALLOGRAPHIC REFEREE.

You have not supplied any structure factors. As a result the full set of tests cannot be run.

```
No syntax errors found.                        CIF dictionary
Please wait while processing ....              Interpreting this report
```

Structure factor report

Datablock: 20gtu73_20_nb_01

```
Bond precision:       C-C = 0.0040 A             Wavelength=0.71073
Cell:       a=10.9405(14)    b=11.4582(15)    c=17.099(2)
            alpha=74.851(2)  beta=85.012(2)   gamma=75.717(2)
Temperature: 273 K

                  Calculated                    Reported
Volume            2004.5(4)                     2004.5(4)
Space group       P -1                          P -1
Hall group        -P 1                          -P 1
Moiety formula    C37 H40 N5 O12 P3             C37 H40 N5 O12 P3
Sum formula       C37 H40 N5 O12 P3             C37 H40 N5 O12 P3
Mr                839.65                        839.65
Dx,g cm-3         1.391                         1.391
Z                 2                             2
Mu (mm-1)         0.216                         0.216
F000              876.0                         876.0
F000'             877.04
h,k,lmax          14,14,22                      14,14,22
Nref              9198                          9189
Tmin,Tmax         0.967,0.982
Tmin'             0.942

Correction method= Not given

Data completeness= 0.999       Theta(max)= 27.485

R(reflections)= 0.0483( 5796)      wR2(reflections)= 0.1311( 9189)

S = 1.026              Npar= 520
```

```
The following ALERTS were generated. Each ALERT has the format
        test-name_ALERT_alert-type_alert-level.
Click on the hyperlinks for more details of the test.
```

🟡 Alert level C

```
PLAT220_ALERT_2_C NonSolvent   Resd 1  C   Ueq(max)/Ueq(min) Range      4.3 Ratio
PLAT222_ALERT_3_C NonSolvent Resd 1  H   Uiso(max)/Uiso(min) Range      4.2 Ratio
PLAT241_ALERT_2_C High   'MainMol' Ueq as Compared to Neighbors of      C34 Check
PLAT241_ALERT_2_C High   'MainMol' Ueq as Compared to Neighbors of      C35 Check
PLAT242_ALERT_2_C Low    'MainMol' Ueq as Compared to Neighbors of       O4 Check
And 2 other PLAT242 Alerts
```

```
PLAT242_ALERT_2_C Low      'MainMol' Ueq as Compared to Neighbors of        N1 Check
PLAT242_ALERT_2_C Low      'MainMol' Ueq as Compared to Neighbors of        C10 Check


PLAT334_ALERT_2_C Small Aver. Benzene C-C Dist C11        -C13              1.37 Ang.
```

🌑 Alert level G

```
PLAT154_ALERT_1_G The s.u.'s on the Cell Angles are Equal ..(Note)       0.002 Degree
PLAT199_ALERT_1_G Reported _cell_measurement_temperature ..... (K)         273 Check
PLAT200_ALERT_1_G Reported   _diffrn_ambient_temperature ..... (K)         273 Check
PLAT941_ALERT_3_G Average HKL Measurement Multiplicity ...........         3.3 Low
```

```
   0 ALERT level A = Most likely a serious problem - resolve or explain
   0 ALERT level B = A potentially serious problem, consider carefully
   8 ALERT level C = Check. Ensure it is not caused by an omission or oversight
   4 ALERT level G = General information/check it is not something unexpected

   3 ALERT type 1 CIF construction/syntax error, inconsistent or missing data
   7 ALERT type 2 Indicator that the structure model may be wrong or deficient
   2 ALERT type 3 Indicator that the structure quality may be low
   0 ALERT type 4 Improvement, methodology, query or suggestion
   0 ALERT type 5 Informative message, check
```

It is advisable to attempt to resolve as many as possible of the alerts in all categories. Often the minor alerts point to easily fixed oversights, errors and omissions in your CIF or refinement strategy, so attention to these fine details can be worthwhile. In order to resolve some of the more serious problems it may be necessary to carry out additional measurements or structure refinements. However, the purpose of your study may justify the reported deviations and the more serious of these should normally be commented upon in the discussion or experimental section of a paper or in the "special_details" fields of the CIF. checkCIF was carefully designed to identify outliers and unusual parameters, but every test has its limitations and alerts that are not important in a particular case may appear. Conversely, the absence of alerts does not guarantee there are no aspects of the results needing attention. It is up to the individual to critically assess their own results and, if necessary, seek expert advice.

Publication of your CIF in IUCr journals

A basic structural check has been run on your CIF. These basic checks will be run on all CIFs submitted for publication in IUCr journals (*Acta Crystallographica*, *Journal of Applied Crystallography*, *Journal of Synchrotron Radiation*); however, if you intend to submit to *Acta Crystallographica Section C* or *E* or *IUCrData*, you should make sure that full publication checks are run on the final version of your CIF prior to submission.

Publication of your CIF in other journals

Please refer to the *Notes for Authors* of the relevant journal for any special instructions relating to CIF submission.

PLATON version of 18/09/2020; check.def file version of 20/08/2020

Datablock 20gtu73_20_nb_01 - ellipsoid plot
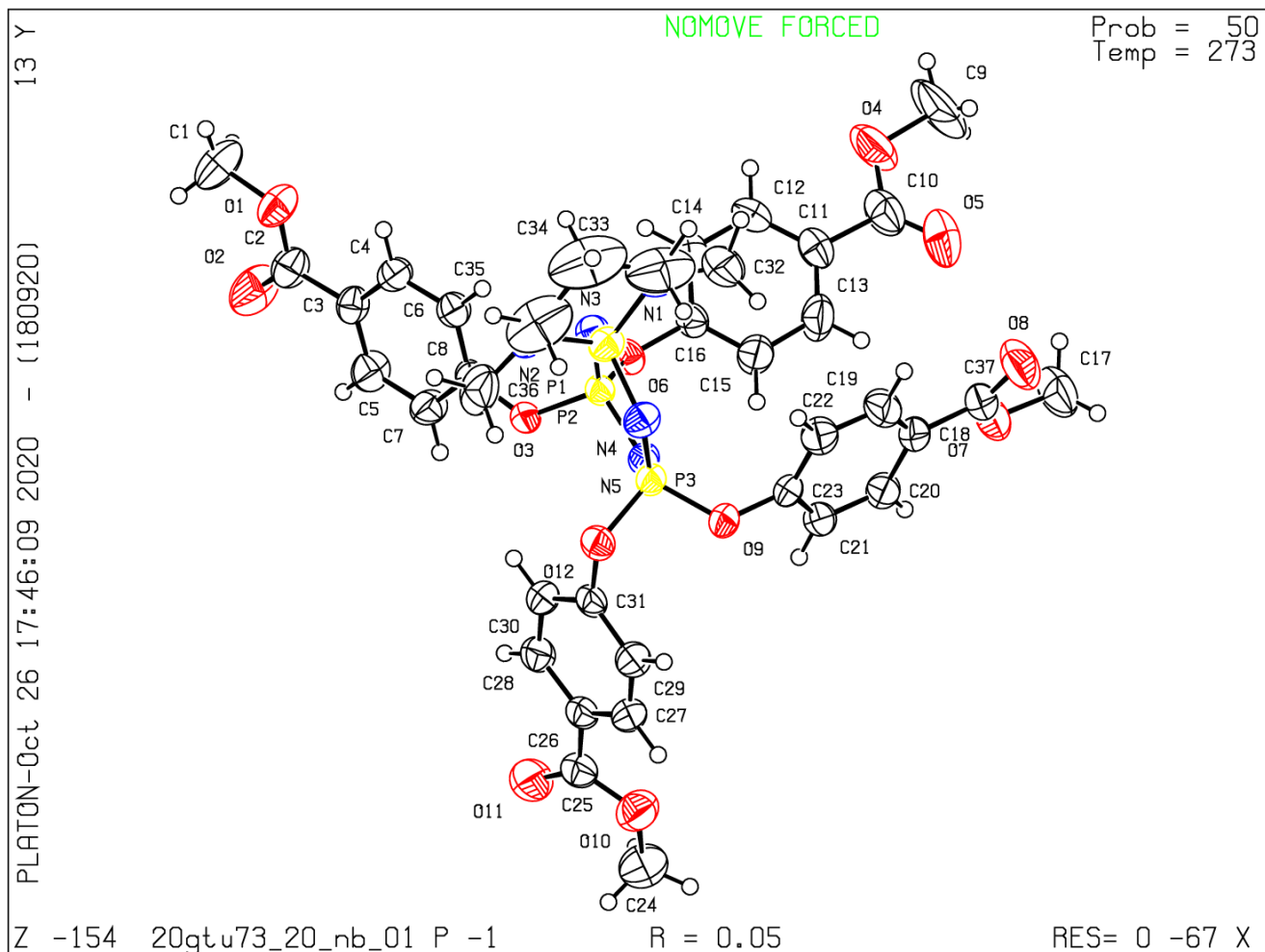
Title

Enter author details here

Abstract

Table 1

Experimental details

Crystal data	
Chemical formula	$C_{37}H_{40}N_5O_{12}P_3$
M_r	839.65
Crystal system, space group	Triclinic, $P\bar{1}$
Temperature (K)	273
a, b, c (Å)	10.9405 (14), 11.4582 (15), 17.099 (2)
α, β, γ (°)	74.851 (2), 85.012 (2), 75.717 (2)
V (Å^3)	2004.5 (4)
Z	2
Radiation type	Mo $K\alpha$
μ (mm^{-1})	0.22
Crystal size (mm)	$0.28 \times 0.13 \times 0.09$
Data collection	
Diffractometer	Bruker APEXII Quazer
Absorption correction	–
No. of measured, independent and observed [$I > 2\sigma(I)$] reflections	30322, 9189, 5796
R_{int}	0.049
$(\sin\theta/\lambda)_{max}$ (Å^{-1})	0.649
Refinement	
$R[F^2 > 2\sigma(F^2)]$, $wR(F^2)$, S	0.048, 0.131, 1.03
No. of reflections	9189
No. of parameters	520
H-atom treatment	H-atom parameters constrained
$\Delta\rho_{max}$, $\Delta\rho_{min}$ (e Å^{-3})	0.19, −0.29

Computer programs: *SHELXT* 2018/2 (Sheldrick, 2018), *SHELXL* 2018/3 (Sheldrick, 2015), Olex2 1.3 (Dolomanov *et al.*, 2009).

References

Dolomanov, O. V., Bourhis, L. J., Gildea, R. J., Howard, J. A. K. & Puschmann, H. (2009). J. Appl. Cryst. 42, 339-341.

Sheldrick, G. M. (2015). Acta Cryst. A71, 3-8.

Sheldrick, G. M. (2015). Acta Cryst. C71, 3-8.

Figure 1

Figure 1

supporting information

Title

Computing details

Program(s) used to solve structure: *SHELXT* 2018/2 (Sheldrick, 2018); program(s) used to refine structure: *SHELXL* 2018/3 (Sheldrick, 2015); molecular graphics: Olex2 1.3 (Dolomanov *et al.*, 2009); software used to prepare material for publication: Olex2 1.3 (Dolomanov *et al.*, 2009).

(20gtu73_20_nb_01)

Crystal data

$C_{37}H_{40}N_5O_{12}P_3$	$Z = 2$
$M_r = 839.65$	$F(000) = 876$
Triclinic, $P\overline{1}$	$D_x = 1.391$ Mg m^{-3}
$a = 10.9405$ (14) Å	Mo $K\alpha$ radiation, $\lambda = 0.71073$ Å
$b = 11.4582$ (15) Å	Cell parameters from 5859 reflections
$c = 17.099$ (2) Å	$\theta = 2.3–23.7°$
$\alpha = 74.851$ (2)°	$\mu = 0.22$ mm^{-1}
$\beta = 85.012$ (2)°	$T = 273$ K
$\gamma = 75.717$ (2)°	Plate, clear colourless
$V = 2004.5$ (4) Å^3	$0.28 \times 0.13 \times 0.09$ mm

Data collection

Bruker APEXII Quazer diffractometer	5796 reflections with $I > 2\sigma(I)$
Detector resolution: 8.3333 pixels mm^{-1}	$R_{int} = 0.049$
φ and ω scans	$\theta_{max} = 27.5°$, $\theta_{min} = 1.2°$
30322 measured reflections	$h = -14 \rightarrow 14$
9189 independent reflections	$k = -14 \rightarrow 14$
	$l = -22 \rightarrow 22$

Refinement

Refinement on F^2	Hydrogen site location: inferred from neighbouring sites
Least-squares matrix: full	
$R[F^2 > 2\sigma(F^2)] = 0.048$	H-atom parameters constrained
$wR(F^2) = 0.131$	$w = 1/[\sigma^2(F_o^2) + (0.0532P)^2 + 0.6682P]$
$S = 1.03$	where $P = (F_o^2 + 2F_c^2)/3$
9189 reflections	$(\Delta/\sigma)_{max} < 0.001$
520 parameters	$\Delta\rho_{max} = 0.19$ e Å^{-3}
0 restraints	$\Delta\rho_{min} = -0.29$ e Å^{-3}
Primary atom site location: dual	

Special details

Geometry. All e.s.d.'s (except the e.s.d. in the dihedral angle between two l.s. planes) are estimated using the full covariance matrix. The cell e.s.d.'s are taken into account individually in the estimation of e.s.d.'s in distances, angles and torsion angles; correlations between e.s.d.'s in cell parameters are only used when they are defined by crystal symmetry. An approximate (isotropic) treatment of cell e.s.d.'s is used for estimating e.s.d.'s involving l.s. planes.

Fractional atomic coordinates and isotropic or equivalent isotropic displacement parameters (Å^2)

	x	y	z	U_{iso}*/U_{eq}
P2	0.46982 (5)	0.56738 (5)	0.67167 (4)	0.03449 (15)

P3	0.30932 (6)	0.79245 (5)	0.66362 (4)	0.03764 (16)
P1	0.49931 (6)	0.70515 (6)	0.77738 (4)	0.04412 (17)
O3	0.55948 (14)	0.57249 (14)	0.59309 (9)	0.0393 (4)
O12	0.33325 (15)	0.89642 (14)	0.58539 (10)	0.0445 (4)
O6	0.45837 (15)	0.42760 (14)	0.68555 (9)	0.0430 (4)
O9	0.16054 (14)	0.83871 (15)	0.67240 (10)	0.0459 (4)
O1	1.13081 (17)	0.28201 (18)	0.61162 (12)	0.0630 (5)
N5	0.34068 (17)	0.66076 (17)	0.64319 (11)	0.0372 (4)
O7	−0.15543 (19)	0.45380 (19)	0.84150 (11)	0.0655 (5)
N3	0.53438 (18)	0.58162 (17)	0.74589 (11)	0.0395 (5)
O10	0.03480 (19)	0.9225 (2)	0.28410 (12)	0.0688 (6)
N4	0.37631 (19)	0.80507 (18)	0.73683 (12)	0.0452 (5)
O11	0.2252 (2)	0.8505 (2)	0.23354 (12)	0.0744 (6)
O8	−0.1507 (2)	0.5285 (2)	0.94963 (12)	0.0867 (7)
O2	1.0919 (2)	0.2716 (2)	0.48846 (14)	0.0865 (7)
C8	0.6826 (2)	0.5016 (2)	0.58781 (14)	0.0364 (5)
N2	0.6213 (2)	0.7695 (2)	0.76306 (17)	0.0643 (7)
C26	0.2068 (2)	0.8952 (2)	0.36326 (15)	0.0436 (6)
C16	0.3929 (2)	0.3667 (2)	0.75100 (14)	0.0407 (5)
O4	0.2721 (3)	0.0488 (2)	0.97601 (13)	0.0941 (8)
C3	0.9263 (2)	0.3743 (2)	0.56373 (15)	0.0435 (6)
N1	0.4825 (2)	0.6636 (2)	0.87694 (14)	0.0657 (7)
C31	0.2917 (2)	0.8974 (2)	0.50938 (14)	0.0409 (6)
C6	0.7664 (2)	0.4660 (2)	0.64938 (15)	0.0457 (6)
H6	0.741181	0.483904	0.699144	0.055*
C23	0.0899 (2)	0.7633 (2)	0.72509 (14)	0.0419 (6)
C29	0.1750 (2)	0.9677 (2)	0.48444 (16)	0.0502 (6)
H29	0.125198	1.016635	0.516301	0.060*
C21	0.0166 (2)	0.7087 (2)	0.69138 (15)	0.0465 (6)
H21	0.014492	0.722029	0.635423	0.056*
C18	−0.0516 (2)	0.6140 (3)	0.82533 (15)	0.0487 (6)
C4	0.8886 (2)	0.4031 (2)	0.63699 (15)	0.0470 (6)
H4	0.946115	0.379947	0.678409	0.056*
C28	0.3271 (2)	0.8296 (2)	0.38794 (16)	0.0514 (7)
H28	0.379625	0.785221	0.354575	0.062*
C30	0.3696 (2)	0.8295 (2)	0.46142 (16)	0.0507 (6)
H30	0.449866	0.784181	0.478342	0.061*
C7	0.7180 (2)	0.4732 (2)	0.51438 (15)	0.0505 (6)
H7	0.660488	0.497006	0.472933	0.061*
C11	0.2690 (3)	0.2279 (3)	0.87234 (16)	0.0532 (7)
C20	−0.0538 (2)	0.6339 (2)	0.74169 (15)	0.0484 (6)
H20	−0.103528	0.596154	0.719448	0.058*
C27	0.1318 (2)	0.9654 (2)	0.41171 (16)	0.0512 (7)
H27	0.051603	1.011420	0.395065	0.061*
C2	1.0561 (3)	0.3045 (2)	0.54925 (18)	0.0544 (7)
O5	0.0852 (3)	0.1822 (3)	0.94749 (17)	0.1124 (10)
C25	0.1603 (3)	0.8869 (2)	0.28700 (17)	0.0524 (7)
C5	0.8396 (3)	0.4092 (3)	0.50322 (17)	0.0568 (7)
H5	0.863658	0.389006	0.453968	0.068*
C37	−0.1245 (3)	0.5301 (3)	0.87977 (17)	0.0583 (7)
C22	0.0907 (3)	0.7480 (3)	0.80785 (16)	0.0563 (7)
H22	0.138839	0.787557	0.829802	0.068*

C14	0.4609 (3)	0.2619 (2)	0.80209 (16)	0.0530 (7)
H14	0.548143	0.238064	0.795967	0.064*
C19	0.0197 (3)	0.6735 (3)	0.85737 (16)	0.0622 (8)
H19	0.019517	0.662991	0.913179	0.075*
C12	0.3975 (3)	0.1925 (3)	0.86275 (16)	0.0598 (7)
H12	0.442405	0.120963	0.897532	0.072*
C15	0.2652 (3)	0.4042 (3)	0.75908 (19)	0.0643 (8)
H15	0.220445	0.475423	0.723904	0.077*
C10	0.1963 (4)	0.1539 (3)	0.93527 (19)	0.0709 (9)
C13	0.2034 (3)	0.3339 (3)	0.8209 (2)	0.0708 (9)
H13	0.116357	0.358832	0.827536	0.085*
C36	0.6520 (3)	0.8161 (3)	0.6777 (2)	0.0823 (10)
H36A	0.657661	0.752385	0.649724	0.123*
H36B	0.731441	0.839306	0.672839	0.123*
H36C	0.587300	0.887402	0.654325	0.123*
C17	−0.2304 (3)	0.3713 (3)	0.8877 (2)	0.0834 (10)
H17A	−0.242511	0.317199	0.856088	0.125*
H17B	−0.310849	0.419134	0.901190	0.125*
H17C	−0.187812	0.322586	0.936488	0.125*
C32	0.3905 (3)	0.5873 (4)	0.90837 (18)	0.0900 (12)
H32A	0.306705	0.639424	0.902785	0.135*
H32B	0.405686	0.547034	0.964549	0.135*
H32C	0.399019	0.525634	0.878288	0.135*
C1	1.2583 (3)	0.2114 (3)	0.6036 (2)	0.0848 (11)
H1A	1.291535	0.241867	0.550324	0.127*
H1B	1.258290	0.125273	0.611636	0.127*
H1C	1.309885	0.220089	0.643377	0.127*
C24	−0.0235 (3)	0.9119 (4)	0.2150 (2)	0.0873 (11)
H24A	−0.002722	0.970621	0.167465	0.131*
H24B	−0.113431	0.928843	0.223451	0.131*
H24C	0.006542	0.829220	0.207746	0.131*
C33	0.4820 (5)	0.7581 (4)	0.9199 (2)	0.1108 (16)
H33A	0.475920	0.722809	0.977772	0.133*
H33B	0.408658	0.826230	0.904680	0.133*
C35	0.6178 (4)	0.8611 (4)	0.8114 (3)	0.1121 (16)
H35A	0.549466	0.933281	0.793005	0.135*
H35B	0.696173	0.888388	0.802422	0.135*
C34	0.5993 (5)	0.8069 (5)	0.9006 (3)	0.128 (2)
H34A	0.671826	0.739711	0.919779	0.154*
H34B	0.595139	0.870339	0.929409	0.154*
C9	0.2079 (5)	−0.0286 (5)	1.0390 (3)	0.155 (2)
H9A	0.151069	−0.059783	1.014533	0.233*
H9B	0.161211	0.019923	1.074512	0.233*
H9C	0.269006	−0.097037	1.069430	0.233*

Atomic displacement parameters (Å²)

	U^{11}	U^{22}	U^{33}	U^{12}	U^{13}	U^{23}
P2	0.0344 (3)	0.0316 (3)	0.0351 (3)	−0.0075 (2)	0.0019 (2)	−0.0053 (2)
P3	0.0324 (3)	0.0354 (3)	0.0418 (4)	−0.0052 (2)	0.0015 (3)	−0.0070 (3)
P1	0.0413 (4)	0.0488 (4)	0.0435 (4)	−0.0061 (3)	−0.0036 (3)	−0.0169 (3)
O3	0.0364 (9)	0.0410 (9)	0.0351 (9)	−0.0054 (7)	0.0030 (7)	−0.0045 (7)

O12	0.0467 (10)	0.0364 (9)	0.0484 (10)	−0.0126 (7)	0.0009 (8)	−0.0049 (7)
O6	0.0500 (10)	0.0313 (8)	0.0455 (10)	−0.0104 (7)	0.0066 (8)	−0.0071 (7)
O9	0.0334 (9)	0.0463 (9)	0.0497 (10)	−0.0027 (7)	0.0046 (7)	−0.0055 (8)
O1	0.0418 (11)	0.0682 (13)	0.0779 (14)	0.0023 (9)	−0.0042 (10)	−0.0294 (11)
N5	0.0336 (11)	0.0372 (10)	0.0400 (11)	−0.0079 (8)	−0.0011 (8)	−0.0088 (8)
O7	0.0691 (14)	0.0768 (14)	0.0533 (12)	−0.0336 (11)	0.0130 (10)	−0.0096 (10)
N3	0.0376 (11)	0.0400 (11)	0.0376 (11)	−0.0040 (9)	−0.0033 (9)	−0.0080 (9)
O10	0.0560 (13)	0.0824 (15)	0.0671 (13)	−0.0103 (11)	−0.0086 (10)	−0.0204 (11)
N4	0.0434 (12)	0.0420 (11)	0.0501 (12)	−0.0027 (9)	−0.0021 (10)	−0.0176 (10)
O11	0.0723 (15)	0.0930 (16)	0.0517 (12)	−0.0078 (12)	0.0034 (11)	−0.0197 (11)
O8	0.0926 (18)	0.131 (2)	0.0459 (13)	−0.0560 (16)	0.0165 (11)	−0.0165 (13)
O2	0.0649 (14)	0.1080 (18)	0.0882 (16)	0.0164 (12)	−0.0012 (12)	−0.0621 (15)
C8	0.0344 (13)	0.0351 (12)	0.0389 (13)	−0.0099 (10)	0.0037 (10)	−0.0077 (10)
N2	0.0507 (15)	0.0596 (15)	0.093 (2)	−0.0167 (12)	−0.0140 (13)	−0.0289 (14)
C26	0.0431 (15)	0.0377 (13)	0.0419 (14)	−0.0067 (11)	0.0035 (11)	0.0002 (11)
C16	0.0442 (14)	0.0329 (12)	0.0445 (14)	−0.0123 (11)	0.0033 (11)	−0.0071 (10)
O4	0.117 (2)	0.0920 (18)	0.0637 (14)	−0.0503 (16)	0.0075 (14)	0.0187 (13)
C3	0.0397 (14)	0.0400 (13)	0.0517 (15)	−0.0064 (11)	0.0050 (11)	−0.0178 (11)
N1	0.0713 (17)	0.0790 (17)	0.0439 (13)	0.0025 (14)	−0.0102 (12)	−0.0261 (13)
C31	0.0422 (14)	0.0329 (12)	0.0417 (14)	−0.0103 (10)	0.0044 (11)	0.0006 (10)
C6	0.0442 (15)	0.0541 (15)	0.0380 (14)	−0.0074 (12)	0.0030 (11)	−0.0151 (12)
C23	0.0288 (12)	0.0456 (14)	0.0436 (14)	0.0002 (10)	0.0023 (10)	−0.0068 (11)
C29	0.0458 (16)	0.0409 (14)	0.0536 (16)	0.0024 (12)	0.0053 (12)	−0.0075 (12)
C21	0.0412 (14)	0.0561 (15)	0.0375 (14)	−0.0049 (12)	0.0025 (11)	−0.0105 (12)
C18	0.0376 (14)	0.0645 (17)	0.0396 (14)	−0.0094 (12)	0.0026 (11)	−0.0089 (12)
C4	0.0401 (14)	0.0514 (15)	0.0473 (15)	−0.0062 (12)	−0.0048 (11)	−0.0115 (12)
C28	0.0480 (16)	0.0506 (15)	0.0448 (15)	0.0012 (12)	0.0078 (12)	−0.0078 (12)
C30	0.0374 (14)	0.0522 (15)	0.0501 (16)	0.0013 (12)	0.0036 (12)	−0.0036 (12)
C7	0.0459 (16)	0.0612 (16)	0.0430 (15)	−0.0029 (13)	−0.0041 (12)	−0.0185 (13)
C11	0.0615 (19)	0.0522 (16)	0.0492 (16)	−0.0254 (14)	0.0081 (13)	−0.0097 (13)
C20	0.0422 (15)	0.0586 (16)	0.0453 (15)	−0.0118 (12)	−0.0004 (11)	−0.0147 (13)
C27	0.0417 (15)	0.0455 (14)	0.0545 (17)	0.0007 (12)	−0.0004 (12)	−0.0023 (12)
C2	0.0476 (16)	0.0496 (15)	0.0664 (19)	−0.0051 (12)	0.0005 (14)	−0.0215 (14)
O5	0.086 (2)	0.128 (2)	0.114 (2)	−0.0534 (18)	0.0305 (16)	0.0021 (17)
C25	0.0541 (18)	0.0463 (15)	0.0494 (17)	−0.0095 (13)	0.0004 (14)	−0.0016 (12)
C5	0.0537 (17)	0.0696 (18)	0.0494 (16)	−0.0028 (14)	0.0044 (13)	−0.0316 (14)
C37	0.0460 (16)	0.079 (2)	0.0440 (17)	−0.0177 (15)	0.0035 (13)	−0.0037 (15)
C22	0.0506 (17)	0.0760 (19)	0.0465 (16)	−0.0211 (15)	−0.0046 (13)	−0.0153 (14)
C14	0.0462 (16)	0.0511 (15)	0.0539 (16)	−0.0076 (12)	0.0007 (13)	−0.0036 (13)
C19	0.0599 (19)	0.092 (2)	0.0368 (15)	−0.0247 (17)	0.0001 (13)	−0.0126 (15)
C12	0.066 (2)	0.0547 (17)	0.0475 (16)	−0.0156 (14)	−0.0028 (14)	0.0087 (13)
C15	0.0466 (17)	0.0466 (15)	0.084 (2)	−0.0071 (13)	0.0031 (15)	0.0068 (15)
C10	0.084 (3)	0.076 (2)	0.060 (2)	−0.045 (2)	0.0079 (18)	−0.0090 (17)
C13	0.0449 (17)	0.0634 (19)	0.096 (2)	−0.0189 (15)	0.0148 (16)	−0.0048 (17)
C36	0.054 (2)	0.066 (2)	0.123 (3)	−0.0277 (16)	0.0040 (19)	−0.007 (2)
C17	0.093 (3)	0.088 (2)	0.073 (2)	−0.050 (2)	0.0168 (19)	−0.0055 (18)
C32	0.077 (2)	0.126 (3)	0.0452 (18)	−0.006 (2)	0.0081 (16)	−0.0017 (19)
C1	0.0470 (19)	0.082 (2)	0.122 (3)	0.0119 (16)	−0.0120 (19)	−0.041 (2)
C24	0.077 (2)	0.111 (3)	0.077 (2)	−0.028 (2)	−0.0203 (19)	−0.019 (2)
C33	0.139 (4)	0.115 (3)	0.074 (3)	0.026 (3)	−0.038 (3)	−0.058 (2)
C35	0.111 (3)	0.082 (3)	0.167 (5)	−0.019 (2)	−0.049 (3)	−0.060 (3)
C34	0.157 (5)	0.115 (4)	0.136 (4)	0.004 (3)	−0.075 (4)	−0.081 (3)

C9	0.186 (5)	0.159 (5)	0.102 (3)	−0.102 (4)	0.022 (3)	0.051 (3)

Geometric parameters (Å, º)

P2—O3	1.5904 (16)	C18—C20	1.390 (3)
P2—O6	1.5913 (16)	C18—C37	1.486 (4)
P2—N5	1.5747 (19)	C18—C19	1.380 (4)
P2—N3	1.5674 (19)	C4—H4	0.9300
P3—O12	1.5928 (17)	C28—H28	0.9300
P3—O9	1.5895 (16)	C28—C30	1.377 (4)
P3—N5	1.5861 (19)	C30—H30	0.9300
P3—N4	1.559 (2)	C7—H7	0.9300
P1—N3	1.592 (2)	C7—C5	1.375 (4)
P1—N4	1.609 (2)	C11—C12	1.371 (4)
P1—N2	1.649 (2)	C11—C10	1.488 (4)
P1—N1	1.650 (2)	C11—C13	1.374 (4)
O3—C8	1.400 (3)	C20—H20	0.9300
O12—C31	1.410 (3)	C27—H27	0.9300
O6—C16	1.397 (3)	O5—C10	1.194 (4)
O9—C23	1.399 (3)	C5—H5	0.9300
O1—C2	1.333 (3)	C22—H22	0.9300
O1—C1	1.445 (3)	C22—C19	1.373 (4)
O7—C37	1.338 (3)	C14—H14	0.9300
O7—C17	1.438 (3)	C14—C12	1.381 (4)
O10—C25	1.334 (3)	C19—H19	0.9300
O10—C24	1.437 (4)	C12—H12	0.9300
O11—C25	1.206 (3)	C15—H15	0.9300
O8—C37	1.201 (3)	C15—C13	1.386 (4)
O2—C2	1.198 (3)	C13—H13	0.9300
C8—C6	1.369 (3)	C36—H36A	0.9600
C8—C7	1.378 (3)	C36—H36B	0.9600
N2—C36	1.458 (4)	C36—H36C	0.9600
N2—C35	1.487 (4)	C17—H17A	0.9600
C26—C28	1.385 (3)	C17—H17B	0.9600
C26—C27	1.382 (3)	C17—H17C	0.9600
C26—C25	1.474 (4)	C32—H32A	0.9600
C16—C14	1.372 (3)	C32—H32B	0.9600
C16—C15	1.363 (4)	C32—H32C	0.9600
O4—C10	1.338 (4)	C1—H1A	0.9600
O4—C9	1.455 (4)	C1—H1B	0.9600
C3—C4	1.381 (3)	C1—H1C	0.9600
C3—C2	1.483 (3)	C24—H24A	0.9600
C3—C5	1.378 (4)	C24—H24B	0.9600
N1—C32	1.470 (4)	C24—H24C	0.9600
N1—C33	1.458 (4)	C33—H33A	0.9700
C31—C29	1.368 (3)	C33—H33B	0.9700
C31—C30	1.374 (3)	C33—C34	1.501 (7)
C6—H6	0.9300	C35—H35A	0.9700
C6—C4	1.381 (3)	C35—H35B	0.9700
C23—C21	1.373 (3)	C35—C34	1.506 (6)
C23—C22	1.380 (3)	C34—H34A	0.9700
C29—H29	0.9300	C34—H34B	0.9700

C29—C27	1.377 (4)	C9—H9A	0.9600
C21—H21	0.9300	C9—H9B	0.9600
C21—C20	1.376 (3)	C9—H9C	0.9600
O3—P2—O6	97.35 (8)	O2—C2—O1	122.8 (3)
N5—P2—O3	106.00 (9)	O2—C2—C3	124.6 (3)
N5—P2—O6	110.58 (9)	O10—C25—C26	111.6 (2)
N3—P2—O3	112.78 (10)	O11—C25—O10	122.9 (3)
N3—P2—O6	109.99 (9)	O11—C25—C26	125.5 (3)
N3—P2—N5	118.13 (10)	C3—C5—H5	119.4
O9—P3—O12	98.76 (9)	C7—C5—C3	121.1 (2)
N5—P3—O12	110.06 (9)	C7—C5—H5	119.4
N5—P3—O9	108.83 (10)	O7—C37—C18	111.3 (2)
N4—P3—O12	108.86 (10)	O8—C37—O7	123.8 (3)
N4—P3—O9	110.77 (10)	O8—C37—C18	124.9 (3)
N4—P3—N5	117.88 (10)	C23—C22—H22	120.4
N3—P1—N4	114.19 (10)	C19—C22—C23	119.2 (3)
N3—P1—N2	109.59 (12)	C19—C22—H22	120.4
N3—P1—N1	107.52 (12)	C16—C14—H14	120.6
N4—P1—N2	110.01 (12)	C16—C14—C12	118.8 (3)
N4—P1—N1	111.31 (12)	C12—C14—H14	120.6
N2—P1—N1	103.68 (14)	C18—C19—H19	119.6
C8—O3—P2	126.90 (14)	C22—C19—C18	120.8 (2)
C31—O12—P3	119.74 (13)	C22—C19—H19	119.6
C16—O6—P2	123.85 (14)	C11—C12—C14	120.8 (3)
C23—O9—P3	120.67 (14)	C11—C12—H12	119.6
C2—O1—C1	116.3 (2)	C14—C12—H12	119.6
P2—N5—P3	118.45 (11)	C16—C15—H15	120.7
C37—O7—C17	116.1 (2)	C16—C15—C13	118.6 (3)
P2—N3—P1	122.95 (12)	C13—C15—H15	120.7
C25—O10—C24	117.4 (2)	O4—C10—C11	110.9 (3)
P3—N4—P1	123.14 (12)	O5—C10—O4	123.9 (3)
C6—C8—O3	123.4 (2)	O5—C10—C11	125.2 (3)
C6—C8—C7	120.8 (2)	C11—C13—C15	120.9 (3)
C7—C8—O3	115.8 (2)	C11—C13—H13	119.6
C36—N2—P1	113.16 (19)	C15—C13—H13	119.6
C36—N2—C35	112.6 (3)	N2—C36—H36A	109.5
C35—N2—P1	115.3 (2)	N2—C36—H36B	109.5
C28—C26—C25	119.5 (2)	N2—C36—H36C	109.5
C27—C26—C28	119.1 (2)	H36A—C36—H36B	109.5
C27—C26—C25	121.3 (2)	H36A—C36—H36C	109.5
C14—C16—O6	117.1 (2)	H36B—C36—H36C	109.5
C15—C16—O6	120.9 (2)	O7—C17—H17A	109.5
C15—C16—C14	121.8 (2)	O7—C17—H17B	109.5
C10—O4—C9	114.2 (3)	O7—C17—H17C	109.5
C4—C3—C2	121.9 (2)	H17A—C17—H17B	109.5
C5—C3—C4	118.8 (2)	H17A—C17—H17C	109.5
C5—C3—C2	119.3 (2)	H17B—C17—H17C	109.5
C32—N1—P1	115.9 (2)	N1—C32—H32A	109.5
C33—N1—P1	116.3 (3)	N1—C32—H32B	109.5
C33—N1—C32	114.7 (3)	N1—C32—H32C	109.5
C29—C31—O12	119.0 (2)	H32A—C32—H32B	109.5

C29—C31—C30	121.4 (2)	H32A—C32—H32C	109.5
C30—C31—O12	119.6 (2)	H32B—C32—H32C	109.5
C8—C6—H6	120.3	O1—C1—H1A	109.5
C8—C6—C4	119.4 (2)	O1—C1—H1B	109.5
C4—C6—H6	120.3	O1—C1—H1C	109.5
C21—C23—O9	117.6 (2)	H1A—C1—H1B	109.5
C21—C23—C22	121.3 (2)	H1A—C1—H1C	109.5
C22—C23—O9	121.1 (2)	H1B—C1—H1C	109.5
C31—C29—H29	120.3	O10—C24—H24A	109.5
C31—C29—C27	119.4 (2)	O10—C24—H24B	109.5
C27—C29—H29	120.3	O10—C24—H24C	109.5
C23—C21—H21	120.5	H24A—C24—H24B	109.5
C23—C21—C20	118.9 (2)	H24A—C24—H24C	109.5
C20—C21—H21	120.5	H24B—C24—H24C	109.5
C20—C18—C37	120.8 (2)	N1—C33—H33A	109.4
C19—C18—C20	118.9 (2)	N1—C33—H33B	109.4
C19—C18—C37	120.2 (2)	N1—C33—C34	111.3 (3)
C3—C4—H4	119.7	H33A—C33—H33B	108.0
C6—C4—C3	120.7 (2)	C34—C33—H33A	109.4
C6—C4—H4	119.7	C34—C33—H33B	109.4
C26—C28—H28	119.7	N2—C35—H35A	109.2
C30—C28—C26	120.6 (2)	N2—C35—H35B	109.2
C30—C28—H28	119.7	N2—C35—C34	111.9 (3)
C31—C30—C28	119.0 (2)	H35A—C35—H35B	107.9
C31—C30—H30	120.5	C34—C35—H35A	109.2
C28—C30—H30	120.5	C34—C35—H35B	109.2
C8—C7—H7	120.4	C33—C34—C35	113.0 (3)
C5—C7—C8	119.1 (2)	C33—C34—H34A	109.0
C5—C7—H7	120.4	C33—C34—H34B	109.0
C12—C11—C10	122.6 (3)	C35—C34—H34A	109.0
C12—C11—C13	119.2 (2)	C35—C34—H34B	109.0
C13—C11—C10	118.2 (3)	H34A—C34—H34B	107.8
C21—C20—C18	120.8 (2)	O4—C9—H9A	109.5
C21—C20—H20	119.6	O4—C9—H9B	109.5
C18—C20—H20	119.6	O4—C9—H9C	109.5
C26—C27—H27	119.8	H9A—C9—H9B	109.5
C29—C27—C26	120.4 (2)	H9A—C9—H9C	109.5
C29—C27—H27	119.8	H9B—C9—H9C	109.5
O1—C2—C3	112.6 (2)		
P2—O3—C8—C6	−34.2 (3)	C16—C14—C12—C11	−0.5 (4)
P2—O3—C8—C7	148.50 (18)	C16—C15—C13—C11	−0.8 (5)
P2—O6—C16—C14	−119.4 (2)	N1—P1—N3—P2	134.00 (15)
P2—O6—C16—C15	66.3 (3)	N1—P1—N4—P3	−131.14 (16)
P3—O12—C31—C29	92.5 (2)	N1—P1—N2—C36	−178.9 (2)
P3—O12—C31—C30	−88.5 (2)	N1—P1—N2—C35	−47.3 (3)
P3—O9—C23—C21	−107.0 (2)	N1—C33—C34—C35	57.8 (5)
P3—O9—C23—C22	75.2 (3)	C31—C29—C27—C26	−1.6 (4)
P1—N2—C35—C34	54.1 (4)	C6—C8—C7—C5	−0.6 (4)
P1—N1—C33—C34	−56.2 (4)	C23—C21—C20—C18	0.3 (4)
O3—P2—O6—C16	176.80 (17)	C23—C22—C19—C18	0.3 (4)
O3—P2—N5—P3	−103.03 (13)	C29—C31—C30—C28	−2.1 (4)

O3—P2—N3—P1	106.15 (14)	C21—C23—C22—C19	2.0 (4)
O3—C8—C6—C4	−175.7 (2)	C4—C3—C2—O1	−4.4 (3)
O3—C8—C7—C5	176.8 (2)	C4—C3—C2—O2	176.1 (3)
O12—P3—O9—C23	168.15 (17)	C4—C3—C5—C7	1.0 (4)
O12—P3—N5—P2	101.92 (13)	C28—C26—C27—C29	−1.5 (4)
O12—P3—N4—P1	−109.84 (15)	C28—C26—C25—O10	161.1 (2)
O12—C31—C29—C27	−177.6 (2)	C28—C26—C25—O11	−17.6 (4)
O12—C31—C30—C28	179.0 (2)	C30—C31—C29—C27	3.5 (4)
O6—P2—O3—C8	−63.41 (18)	C7—C8—C6—C4	1.4 (4)
O6—P2—N5—P3	152.50 (11)	C20—C18—C37—O7	18.7 (4)
O6—P2—N3—P1	−146.36 (13)	C20—C18—C37—O8	−162.6 (3)
O6—C16—C14—C12	−173.8 (2)	C20—C18—C19—C22	−2.2 (4)
O6—C16—C15—C13	174.2 (3)	C27—C26—C28—C30	2.9 (4)
O9—P3—O12—C31	−70.12 (17)	C27—C26—C25—O10	−17.6 (3)
O9—P3—N5—P2	−150.88 (11)	C27—C26—C25—O11	163.7 (3)
O9—P3—N4—P1	142.61 (14)	C2—C3—C4—C6	−178.6 (2)
O9—C23—C21—C20	179.9 (2)	C2—C3—C5—C7	179.5 (2)
O9—C23—C22—C19	179.7 (2)	C25—C26—C28—C30	−175.8 (2)
N5—P2—O3—C8	−177.34 (16)	C25—C26—C27—C29	177.2 (2)
N5—P2—O6—C16	−73.00 (19)	C5—C3—C4—C6	−0.2 (4)
N5—P2—N3—P1	−18.15 (18)	C5—C3—C2—O1	177.2 (2)
N5—P3—O12—C31	43.70 (19)	C5—C3—C2—O2	−2.3 (4)
N5—P3—O9—C23	53.37 (19)	C37—C18—C20—C21	−178.1 (2)
N5—P3—N4—P1	16.4 (2)	C37—C18—C19—C22	177.8 (3)
N3—P2—O3—C8	51.94 (19)	C22—C23—C21—C20	−2.3 (4)
N3—P2—O6—C16	59.3 (2)	C14—C16—C15—C13	0.1 (4)
N3—P2—N5—P3	24.56 (17)	C19—C18—C20—C21	1.9 (4)
N3—P1—N4—P3	−9.17 (19)	C19—C18—C37—O7	−161.3 (3)
N3—P1—N2—C36	66.6 (2)	C19—C18—C37—O8	17.4 (5)
N3—P1—N2—C35	−161.8 (2)	C12—C11—C10—O4	−3.3 (4)
N3—P1—N1—C32	−55.8 (2)	C12—C11—C10—O5	177.9 (3)
N3—P1—N1—C33	165.0 (3)	C12—C11—C13—C15	0.8 (5)
N4—P3—O12—C31	174.30 (16)	C15—C16—C14—C12	0.5 (4)
N4—P3—O9—C23	−77.75 (19)	C10—C11—C12—C14	178.1 (3)
N4—P3—N5—P2	−23.71 (17)	C10—C11—C13—C15	−177.6 (3)
N4—P1—N3—P2	9.97 (18)	C13—C11—C12—C14	−0.2 (4)
N4—P1—N2—C36	−59.7 (2)	C13—C11—C10—O4	175.0 (3)
N4—P1—N2—C35	71.8 (3)	C13—C11—C10—O5	−3.8 (5)
N4—P1—N1—C32	69.9 (2)	C36—N2—C35—C34	−174.0 (3)
N4—P1—N1—C33	−69.3 (3)	C17—O7—C37—O8	3.5 (4)
C8—C6—C4—C3	−1.0 (4)	C17—O7—C37—C18	−177.8 (2)
C8—C7—C5—C3	−0.7 (4)	C32—N1—C33—C34	164.1 (3)
N2—P1—N3—P2	−113.94 (16)	C1—O1—C2—O2	−2.0 (4)
N2—P1—N4—P3	114.52 (17)	C1—O1—C2—C3	178.4 (2)
N2—P1—N1—C32	−171.9 (2)	C24—O10—C25—O11	2.3 (4)
N2—P1—N1—C33	48.9 (3)	C24—O10—C25—C26	−176.4 (2)
N2—C35—C34—C33	−57.0 (5)	C9—O4—C10—C11	179.8 (3)
C26—C28—C30—C31	−1.2 (4)	C9—O4—C10—O5	−1.3 (5)

Inhibitory effects of some additives on LOX activity in Santa Maria pear puree

Arzu ÖZTÜRK KESEBİR[1a*], Işıl Nihan KORKMAZ[1b], Ö. İrfan KÜFREVİOĞLU[1c]

[1]Atatürk University, Faculty of Science, Department of Chemistry, Erzurum, Turkey

ORCID: [a] 0000 0003 26037509, [b]0000 0003 4896 5226, [c]0000 0002 18773154

Abstract: Lipoxygenase (EC 1.13.11.34.; LOX) enzymes; They are iron carrier dioxygenases that oxidize fatty acids with two or more unsaturated bonds in their structure and do not contain heme groups in their structure. LOXs are found in plants, animal tissues, and cyanobacteria. In this study, the change of LOX enzyme activity in Santa Maria pear puree depending on different concentrations of fumaric acid, syringic acid and rosmarinic acid and cooking process was followed for 7 days. It has been observed that fumaric acid increases LOX activity. This increase was not prevented by the cooking process. It was observed that syringic acid and rosmarinic acid decreased LOX activity day by day, and a faster decrease in activity was observed in the samples that were additionally cooked. At the end of 7 days, it was observed that rosmarinic acid caused approximately 60% inhibition, while syringic acid caused approximately 80% inhibition. Based on these results, we can say that the cooking process with the addition of rosmarinic acid or syringic acid to the medium in order to prevent the loss of taste, smell and flavor of the pear, which is frequently used in baby complementary foods and fruit juices, extends the shelf life.

Keywords: LOX, rosmarinic acid, syringic acid, fumaric acid, shelf life.

Santa Maria armudu püresinde LOX aktivitesi üzerine bazı katkı maddelerinin inhibisyon etkileri

Özet: Lipoksigenaz (EC 1.13.11.34.; LOX) enzimleri; yapısında iki ya da daha fazla doymamış bağ bulunduran yağ asitlerini oksitleyen, yapılarında hem grubu bulundurmayan demir taşıyıcı dioksigenazlardır. LOX'lar bitkiler, hayvan dokuları ve siyanobakterilerde bulunurlar. Bu çalışmada Santa Maria armudu püresindeki LOX enzimi aktivitesinin fumarik asit, sirinjik asit ve rosmarinik asitin farklı konsantrasyonlarına ve pişirme işlemine bağlı olarak değişimi 7 gün boyunca takip edilmiştir. Fumarik asitin LOX aktivitesini artırdığı gözlenmiştir. Bu artışa pişirme işlemi de engel olamamıştır. Sirinjik asit ve rosmarinik asitin LOX aktivitesini gün geçtikçe azalttığı, ek olarak pişirme uygulanan örneklerde daha hızlı bir aktivite azalışı olduğu görülmüştür. 7 gün sonunda rosmarinik asitin yaklaşık % 60'lık inhibisyona sebep olduğu, sirinjik asitin ise yaklaşık %80'lik bir inhibisyona sebep olduğu görülmüştür. Bu sonuçlardan yola çıkarak bebek ek gıdaları ve meyve sularında sıkça kullanılan armudun tat, koku ve lezzet kaybının önlenmesi için ortama rosmarinik asit ya da sirinjik asitin eklenmesiyle birlikte pişirme işlemi uygulanması raf ömrünü uzatmaktadır diyebiliriz.

Anahtar Kelimeler: LOX, rosmarinik asit, sirinjik asit, fumarik asit, raf ömrü.

*Corresponding Author: arzuozturk_20@hotmail.com (A. Öztürk Kesebir)

1   INTRODUCTION

Lipoxygenases (LOXs) are a family of monomeric proteins that produce hydroperoxide by oxidation of polyunsaturated fatty acids (PUFA) such as linoleic, linoleic, and arachidonic acids [1]. LOXs are found in plants, animals, fungi and cyanobacteria [2]. 5-LOX is ubiquitous in the mammalian body, its job is to oxidize the number 5 carbon atom. 9-LOX and 13-LOX are found in plants and they catalyze the oxidation of linoleic and linolenic acid [2, 3]. Lipoxygenases play an important role in stimulating inflammatory reactions in the human body. The excessive reactive oxygen species formed in the body first stimulates the release of cytokines and then the activation of the LOX enzyme, the result may be inflammation. Inflammation in the body is associated with many diseases such as cancer, stroke, cardiovascular and neurodegenerative diseases. LOXs are involved in the synthesis of prostaglandins and leukotrienes, therefore they are associated with diseases and their inhibition is considered important for disease treatment [4].

LOXs are also abundant in grains, legumes and potato tubers [5, 6]. The products produced in the LOX metabolic pathways have various effects. LOX acts as a storage protein in vegetative growth and also mobilizes storage lipids during germination [7]. LOX protects plants from pathogens and insects. It also plays a role in the production of substances such as jasmonates, divinyl ethers, leaf aldehydes that help protect during abiotic stress [8, 9].

On the other hand, the reaction between unsaturated fatty acids and LOX can cause bad taste and odour, resulting in food spoilage. Therefore, investigation of LOX inhibition has gained importance [10]. Plant phytochemicals play an important defensive role in preventing diseases caused by oxidative stress. Plants have been used as medicine for centuries. Today, many drugs are isolated from plants and there is increasing interest in plant-derived therapeutics [11].

Fumaric acid ((E)-2-butenedioic acid or trans-1,2-ethylenedicarboxylic acid) (Fig. 1) is a naturally occurring organic acid originally obtained from the plant Fumaria officinalis. Since it is synthesized as a key intermediate in the citrate cycle, it is produced in many living things, albeit in small amounts [12]. Fumaric acid esters have been used for many years in the treatment of chronic plaque psoriasis [13] and multiple sclerosis [14] diseases.

Syringic acid (SA) (Fig. 1) is a phenolic compound found in many natural foods (pumpkin, grapes, dates, various spices, olives, acai palm, honey and wine) [15, 16] with important effects such as antioxidant, antiinflammation, antimicrobial, anticancer, antidiabetic, heart, liver and brain / CNS (central nervous system) protection [17].

SA is also used in industry. Syringic acid is among the many phenolic compounds that contribute to the structural integrity of lignin. Syringic acid in lignin acts as a good substrate for laccase, an important enzyme in the pulp and bioremediation industry [18].

Although rosmarinic acid (Fig. 1) got its name because it was first obtained from rosemary, it is also found in a wide variety of herbs such as sage, mint, thyme, lemon balm,

basil and thyme [19, 20]. Studies show that herbal medicines containing RA do not have serious side effects and have many positive effects on the body. In addition to in vitro studies, it has been reported to be effective in the treatment of metabolic syndrome, increasing cognitive performance, osteoarthritic disorders, various otolaryngological treatments and dermatological treatments in clinical studies. It has been targeted in many studies that RA is also used for long-term treatments by prolonging the elimination process from the body [21-28].
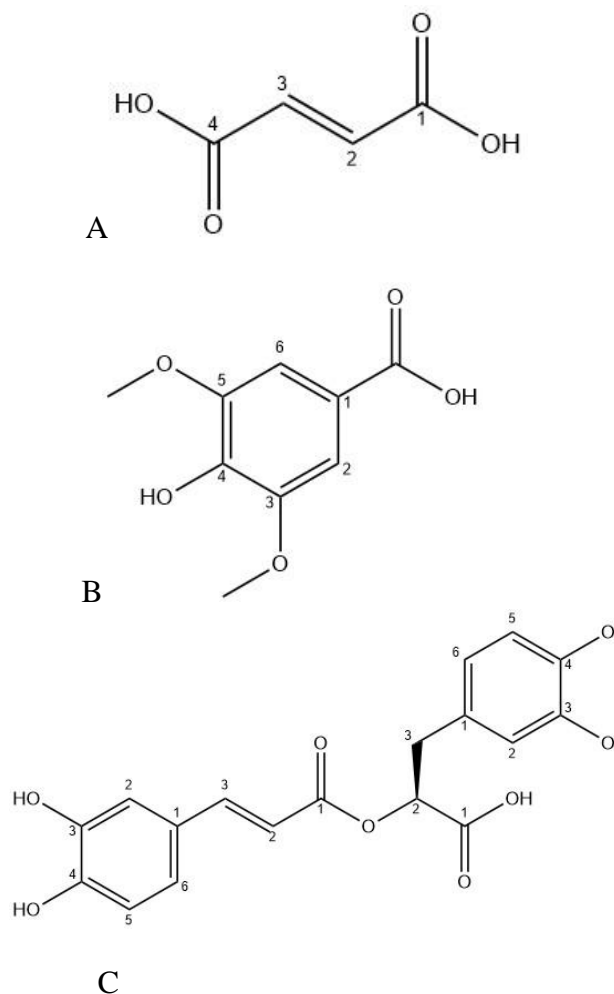
Fig. 1. Structure of fumaric acid (A), syringic acid (B) and rosmarinic acid (C).

In this study, fumaric acid, syringic acid and rosmarinic acid were added to pear puree and activity measurement was made for 7 days to examine the effects of these chemicals on LOX activity. The effects of this chemicals on the bitterness of pear puree provide important ideas for the shelf life of the puree.

The inhibitors used in the study were chosen because they are natural substances obtained from plants. so its use as an additive in the food industry will also be beneficial for human health. The use of such natural products in the sector is more preferred than artificially produced chemicals.

We think that it would be beneficial to add natural inhibitors that reduces LOX activity to the literature.

2   MATERIALS AND METHODS

2.1   Materials

The Santa Maria pear used in the study was obtained from greengrocers. The chemicals used were purchased from Merck, Sigma-Aldrich. (Fumaric acid CAS Number: 110-17-8, syringic acid CAS number: 530-57-4, roamarinic acid CAS number: 20283-92-5, linoleic acid CAS number: 60-33-3). In the study, activity measurements were made with the Beckman coulter DU730 UV-Vis spectrophotometer.

2.2. Preparetion of pear puree

Santa Maria pears washed and grated. The seed zone was not used in the study. Purees were taken into 10 mL glass jars. Weighings were made to correspond to 1mM, 2mM, 3mM, 4mM and 5 mM concentrations for each inhibitor and added to the jars and mixed.

Some of the grated pears were cooked at 100°C for 15 minutes and placed in 10 mL jars. After cooling, 3 mM inhibitory substance was added to each jar (Figure 2). Here, 3 mM was chosen so that the inhibitor concentration was not too high or too low. Jars were stored at 4°C for 7 days. For each measurement, 500 µL of sample was taken from the jar, centrifuged at 1000 x g for 10 minutes, and activity with the supernatant was measured.

Fig. 2. Pear puree jar

2.3. Activity measurement procedure of LOX

For the activity measurement, the substrate solution was first prepared by dissolving 0.04 mM linoleic in 5 mL of methanol.

3 mL of 5mM phosphate buffer (pH 6.5) was added to 90 µL of substrate solution. It was incubated at 20°C for 5 minutes. After incubation, 30 µL of enzyme was added and the change in absorbance was measured at 234 nm for 3 minutes [29].

Enzyme unit was defined as the amount of enzyme that converts 1 µmol of substrate to product in 1 minute under optimal conditions.

3   RESULTS

In this study, the effects of rosmarinic acid, fumaric acid, syringic acid and cooking process on the shelf life of pear puree was investigated. Activity measurement of LOX enzyme was performed for 7 days.

When the graph of rosmarinic acid is examined (Fig.3), the first thing to notice will be that the cooking process negatively affects the LOX activity and decreases the activity rapidly. Although there is no change in activity in the first 4 days at 5 mM concentration, a rapid decrease is observed in the following days. In other cases, no effective reduction in LOX activity was observed. This will cause the pear puree to deteriorate and deteriorate its taste. Based on these results, it can be said that 5 mM concentration of rosmarinic acid in raw pear puree and 3 mM concentration in cooked pear puree can be effective on LOX activity and prolong shelf life.

Fig. 3. Effects of rosmarinic acid on LOX
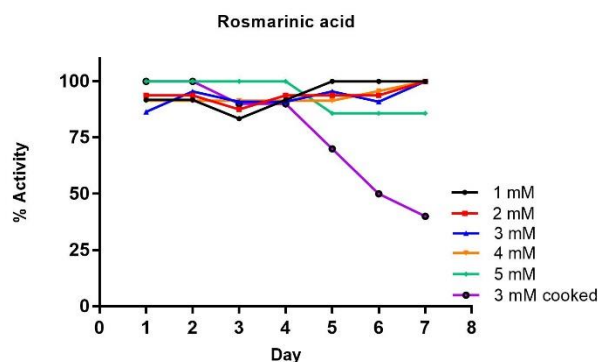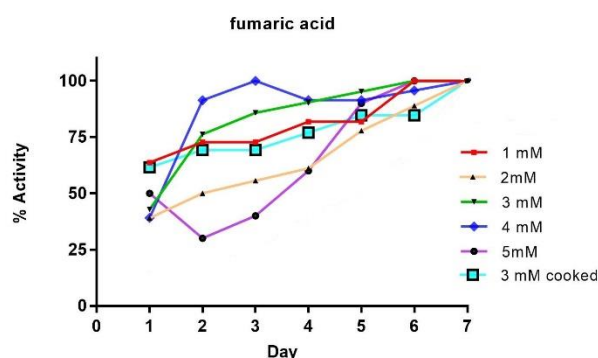

Fig. 4. Effects of fumaric acid on LOX

When Figure 4 is examined, it is seen that all concentrations of fumaric acid increase the LOX activity in pear puree for 7 days, even when cooked. Based on these results, it can be said that fumaric acid does not inhibit the LOX enzyme, but activates it and shortens its shelf life.
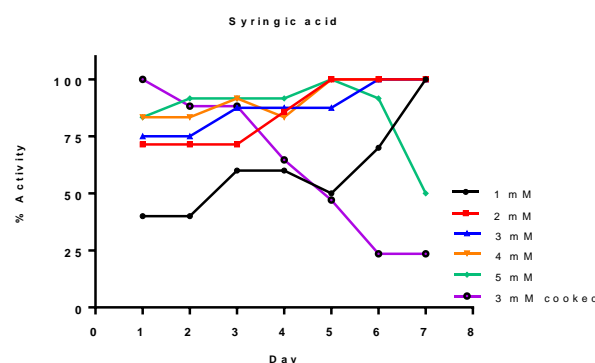

Fig. 5. Effects of syringic acid on LOX

Figure 5 shows that syringic acid has a similar effect to rosmarinic acid. It is seen that the LOX activity in the cooked pear puree containing 3 mM syringic acid experienced a rapid decrease from the first day. At the end of 7 days, approximately 75% of activity loss is observed. Pear puree containing 5 mM syringic acid appears to have half as much LOX activity as at the end of 7 days. Looking at the results obtained in the study, it can be said that the best inhibitor of LOX enzyme is syringic acid. rosmarinic acid also appears to be effective, but fumaric acid appears to increase LOX activity continuously. In addition, it is seen that the cooking process is very effective in extending the shelf life. A longer shelf life can be achieved by adding less additives.

4   DISCUSSION

For this reason, there are studies investigating LOX inhibitors in the literature. Yashanswinj et al. investigated the effect of sesame derivatives on LOX inhibition and reported that 51.84 µM amount of sesamol reduced LOX activity to half of the initial activity [30].
The effects of salicylic acid, eupatorin, eupatilin, gardenin A substances on LOX activity isolated from bovine liver in 2019 were investigated and the highest inhibition effect was seen in Eupatilin (IC_{50}=0.46 mM), and the lowest inhibition effect was seen in Gardenin A (IC_{50}= 5.31 mM) has been reported [22].
There are studies indicating that the correlation between lipoxygenase activity and quality changes such as color change and off-flavor formation in vegetables may be better [31-33] In a study carried out, it was determined that boiling at 100°C for 20 minutes was sufficient for LOX inactivation and no LOX regeneration was detected during the storage period. The tomato puree produced without the boiling process was stored at two different temperatures, -7 and -18°C. It was reported that the activity of the enzyme decreased gradually during 130 days of storage in these samples and no activity was observed when this period was extended [34]. This study with tomatoes could be explored for other foods as well.
Studies show that LOX is a very important enzyme for food quality and storage, and its inhibition can be done by various methods such as additives, heating and cold storage. It is thought that extensive studies should be carried out on LOX, especially in the food and health industry.

5   CONCLUSIONS

LOX is a very important enzyme for the health and food industry, which can be obtained from plants, animal tissues and microorganisms. In this paper we measured LOX activity in pear puree for 7 days. We saw that the chemicals added to the environment and the applied heat were quite effective on the LOX activity. The LOX activity in the pear, which is widely used especially in fruit juices and baby supplements, causes a great change in the color, smell and taste of the food. The important results we obtained as

a result of our study are that adding syringic acid or rosmarinic acid to the medium or cooking the puree is beneficial in maintaining the shelf life and therefore the product quality for a long time. We think that LOX inhibition and longer shelf life can be achieved by developing different additives, cooking times or methods.

Conflicts of Interest: The authors declare no conflict of interest.

Ethical Approval: No experiments were performed on any living creature in this study, it does not need ethical approval

References

[1] Chedea, V.S., Jisaka, M., ''Lipoxygenase and carotenoids: A co-oxidation story'', Afr. J. Biotechnol. (2013), 12, 2786–2791.

[2] Newcomer, M.E., Brash, A.R., ''The structural basis for specificity in lipoxygenase catalysis'', Protein Sci. (2015), 24, 298–309.

[3] Pallavi, P.C., Singh, A.K., Singh, S., Singh, N.K, ''In Silico Structural and Functional Insights into the Lipoxygenase Enzyme of Legume Cajanus Cajan'', Int. J. Recent Innov. Trends Comput. Commun. (2014), 5, 87–91.

[4] Srivastava, P., Vyas, V.K., Variya, B., Patel, P., Qureshi, G., Ghate, M,. ''Synthesis, anti-inflammatory, analgesic, 5-lipoxygenase (5-LOX) inhibition activities, and molecular docking study of 7-substituted coumarin derivatives'', Bioorg. Chem. (2016), 67, 130–138.

[5] Baysal, T., Demirdöven, A., ''Lipoxygenase in fruits and vegetables: A review'', Enzym. Microb. Technol. (2007), 40, 491–496.

[6] Lampi, A.M., Yang, Z., Mustonen, O., Piironen, V., ''Potential of faba bean lipase and lipoxygenase to promote formation of volatile lipid oxidation products in food models'', Food Chem. (2020), 311, 125982.

[7] Porta, H., Rocha-Sosa, M., ''Plant lipoxygenases. Physiological and molecular features'', Plant Physiol. (2002), 130, 15–21

[8] Kermasha, S., Dioum, N., Bisakowski, B., ''Biocatalysis of lipoxygenase in selected organic solvent media'', J. Mol. Catal. B Enzym, (2001), 11, 909–919.

[9] Ogorodnikova, A.V., Mukhitova, F.K., Grechkin, A.N., ''Oxylipins in the spikemoss Selaginella martensii: Detection of divinyl ethers, 12-oxophytodienoic acid and related cyclopentenones'', Phytochemistry, (2015), 118, 42–50.

[10] Padilla, M.N., Hernández, M.L., Sanz, C., ''Martínez-Rivas, J.M. Stress-dependent regulation of 13 lipoxygenases and 13-hydroperoxide lyase in

38

olive fruit mesocarp'', Phytochemistry, (2014), 102, 80–88.

[11] Dzoyem, J.P., Eloff, J.N., ''Anti-inflammatory, anticholinesterase and antioxidant activity of leaf extracts of twelve plants used traditionally to alleviate pain and inflammation in South Africa'', J. Ethnopharmacol. (2015), 160, 194–201

[12] Car, E., Straathof, A.J.J., Zijlmans, T.W., van Gulik, W.M., van der Wielen, L.A.M., ''Fumaric acid production by fermentation'', Appl Microbiol Biotechnol (2008), 78:379–389 DOI 10.1007/s00253-007-1341-x

[13] Nast, A., Kopp, I., Augustin, M., et al. ''German evidence-based guidelines for the treatment of Psoriasis vulgaris'', Arch Dermatol Res (2007), 299: 111–138

[14] Linker, R.A., Haghikia, A., ''Dimethyl fumarate in multiple sclerosis: latest developments, evidence and place in therapy'', Ther Adv Chronic Dis (2016), 7: 198–207

[15] Pacheco-Palencia, L.A., Mertens-Talcott, S., Talcott, S.T., ''Chemical composition, antioxidant properties, and thermal stability of a phytochemical enriched oil from Acai (Euterpe oleracea Mart.)'', J Agric Food Chemistry, 56 (2008), pp. 4631-4636

[16] Pezzuto, J.M., ''Grapes and human health: a perspective'', J Agric Food Chemistry, 56 (2008), pp. 6777-6784

[17] Kiran, P., Denni, M., Daniel, M., ''Antidiabetic principles, phospholipids and fixed oil of kodo millet (Paspalum scrobiculatum Linn)'', Ind J Appl Res., 4 (2014), pp. 13-15.

[18] Abe, T., Masai, E., Miyauchi, K., Katayama, Y., Fukuda, M., ''Tetrahydrofolate-Dependent O-Demethylase, LigM, Is Crucial for Catabolism of Vanillate and Syringate in Sphingomonas paucimobilis SYK-6'', J of Bacteriology. (2005), pp. 2030-2037.

[19] Petersen, M., Simmonds, M.S., ''Rosmarinic acid. Phytochemistry'', (2003), 62: 121–125

[20] Petersen, M., Abdullah, Y., Benner, J., Eberle, D., Gehlen, K., Hucherig, S., Janiak, V., Kim, K.H., Sander, M., Weitzel, C., Wolters, S., ''Evolution of rosmarinic acid biosynthesis,'' Phytochemistry, (2009), 70: 1663–1679.

[21] Hiti, M., Kladar, N., Gavaric, N., Bozin, B., ''Rosmarinic Acid–Human Pharmacokinetics and Health Benefits'', Planta Med (2021), 87: 273–282. https://doi.org/10.1055/a-1301-8648.

[22] Budhiraja, A., Dhingra, G., ''Development and characterization of a novel antiacne niosomal gel of rosmarinic acid,'' Drug Deliv (2015), 22: 723–730

[23] Tundis, R., Loizzo, MR., ''Bonesi M, Menichini F. Potential role of natural compounds against skin aging,'' Curr Med Chem (2015), 22: 1515–1538.

[24] Yucel, C., Seker Karatoprak, G., Degim, IT., ''Anti-aging formulation of rosmarinic acid-loaded ethosomes and liposomes,'' J Microencapsul (2019), 36: 180–191

[25] Bhatt, R., Singh, D., Prakash, A., Mishra, N., ''Development, characterization and nasal delivery of rosmarinic acid-loaded solid lipid nanoparticles for the effective management of Huntington's diseas,''. Drug Deliv., (2015), 22: 931–939

[26] Lu, P., Xing, Y., Xue, Z., Ma, Z., Zhang, B., Peng, H., Zhou, QT., Liu, H., Liu, Z., Li, J., ''Pharmacokinetics of salvianolic acid B, rosmarinic acid and Danshensu in rat after pulmonary administration of Salvia miltiorrhiza polyphenolic acid solutio,'' Biomed Chromatogr., (2019), 33: e4561

[27] da Silva, SB., Ferreira, D., Pintado, M., Sarmento, B., ''Chitosan-based nanoparticles for rosmarinic acid ocular delivery–in vitro tests,'' Int J Biol Macromol., (2016), 84: 112–120

[28] Jia, JY., Lu, YL., Li, XC., Liu, GY., Li, SJ., Liu, Y., Liu, YM., Yu, C., Wang, YP., ''Pharmacokinetics of depside salts from Salvia miltiorrhiza in healthy Chinese volunteers: a randomized, open-label, single-dose study,'' Curr Ther Res Clin Exp., (2010), 71: 260–271

[29] Ozturk Kesebir, A., Kilic, D., Kufrevioglu O.I., '' Partial Purification and Characterization of Lipoxygenase Enzyme From Bovine Liver, Effects of Salicylic Acid and Some Flavons on the Enzyme'', Journal of the Institute of Science and Technology, (2019), 9(3): 1452-1459. DOI: 10.21597/jist.510855.

[30] Yashaswini, P.S., Rao, A.G., Singh, S.A., ''Inhibition of lipoxygenase by sesamol corroborates its potential anti-inflammatory activity'', Int J Biol Macromol., (2017), 94(Pt B):781-787.

[31] Barrett, D.M., Theerakulkait, C., ''Quality indicators in blanched, frozen, stored vegetables'',Food Technology, (1995), 49(62):64–65.

[32] Barrett, D.M., Garcia, E.L., Russell, G.F., Ramirez, E., Shirazi, A., ''Blanch time and cultivar effects on quality of frozen and stored corn broccoli'', Journal of Food Science, (2000), 65(3): 534-540.

[33] Cabibel, M., Nicolas, J., ''Lipoxygenase from tomato fruit (Lycopersicon esculentum L.). Partial purification, some properties and in vitro cooxidation of some carotenoid pigments''. Sciences des Aliments, (1990), 11(2): 277-290.

[34] Calligaris, S., Falcone, P., Anese, M., ''Color changes of tomato purees during storage at freezing temperatures''. Journal of Food Science, (2002), 67(6): 2432-2435.

Synthesis and structure analysis of the novel 4-(2-aminoethyl)morpholine substituted cyclotriphosphazene

Elif YILDIZ GÜL[1a], Merve BAL[1b], Buse KÖSE[1c], Esra TANRIVERDİ EÇİK*[1d]

[1]*Atatürk University, Department of Chemistry, Faculty of Science, Erzurum, Turkey*

ORCID: [a]0000-0001-7422-5665, [b]0000-0003-0069-0286, [c]0000-0001-8121-0875, [d]0000-0003-2953-6872

Abstract: In this study, the reaction of hexachlorocyclotriphosphazene with 4-(2-aminoethyl) morpholine which is a primary amine was carried out in the presence of Trimethylamine in THF. The molecular structure of the final compound was confirmed by mass spectrometry, FT-IR, ^{31}P, ^{1}H and ^{13}C NMR spectroscopies. The possible progress mechanism of the reaction was proposed using the structure analysis of the product formed.

Keywords: Cyclotriphosphazene, aminoethylmorpholine, NMR

Yeni 4-(2-aminoetil)morfolin substitüe siklotrifosfazenin sentezi ve yapı analizi

Özet: Bu çalışmada, hekzaklorosiklotrifosfazenin primer bir amin olan 4-(2-aminoetil) morfolin ile reaksiyonu THF içerisinde trimetilamin varlığında gerçekleştirilmiştir. Final bileşiğin moleküler yapısı, kütle spektrometresi, FT-IR ^{31}P, ^{1}H ve ^{13}C NMR spektroskopi teknikleri ile doğrulandı. Oluşan ürünün yapı analizi kullanılarak, reaksiyon için olası ilerleme mekanizması önerildi.

Anahtar Kelimeler: Siklotrifosfazen, aminoetilmorfolin, NMR

*Corresponding Author: esra.ecik@atauni.edu.tr (E.Tanrıverdi-Eçik)

1   INTRODUCTION

Hexachlorocyclotriphosphazene ring is an important member of inorganic ring systems [1-3]. This ring is renowned for the robustness of the phosphorus-nitrogen backbone and active phosphorus-chlorine bonds that enable nucleophilic substitution reactions [1-5]. The planar molecular geometry of the cyclotriphosphazene ring, its resistance to heat, light and different reaction conditions, and its ability to combine multiple groups with the same or different properties in the same molecule make this ring an indispensable carrier framework for new material designs [1, 2, 6-8]. Depending on the number, type and properties of the functional group carried by the cyclotriphosphazene ring, fluorescence chemosensor [6, 7], anticancer [8, 9], antimicrobial agents [10], organic light emitting diodes [11,12], biosensor [13] and photosensitizer [14, 15] applications have been successfully demonstrated. Therefore, the nucleophilic substitution reactions of the cyclotriphosphazene ring with different functional groups, the diversity of the products formed and the potential application areas attract attention.

The progression pathway of the substitution reactions in the cyclotriphosphazene ring depends on many parameters, especially electronic, steric and mechanistic effects [16-21]. Thus, a great deal of effort has been devoted to elucidate the preference of geminal and non-geminal reaction pathways in cyclotriphosphazene derivatives [4, 19, 20, 22-24]. When electron-donating units are attached to the cyclotriphosphazene core, the positive charge on the P atoms decreases and then their reaction with monofunctional alkoxy groups proceeds in the non-geminal route [19]. The substitution reactions of cyclotriphosphazenes with secondary amines generally tend to form non-geminal product, while the formation of geminal products with primary amines predominate due to polar environment or steric factor [4, 18, 24-26].

Morpholine is a heterocyclic ring containing oxygen and nitrogen atoms in its structure, and it is a bioactive molecule often preferred in medical applications [27-29]. The reactions of morpholine, a secondary amine, and cyclotriphosphazene were investigated and it was reported that non-geminal products were dominant [23]. The di-, tri- and tetra-non-geminal replacements in cyclotriphosphazenes often lead to a mixture of *cis-* and *trans-* isomers [19, 23, 26, 30]. In this study, the reaction of hexachlorocyclotriphosphazene (**1**) with 4-(2-aminoethyl) morpholine (**2**) which is a primary amine was carried out and the progression route of the reaction was investigated from the structure analysis of the obtained product.

2   MATERIALS VE METHODS

2.1. General methods

All the precursors chemical reagents and solvents were procured from commercial suppliers. Analytical thin layer chromatography (TLC) was performed on silica gel plates (Merck, Kieselgel 60 Å, 0.25 mm thickness) with F_{254}

indicator. Column chromatography was performed on silica gel (200-400 mesh). Mass spectra were acquired in linear modes with average of 50 shots on a Bruker Daltonics Microflex mass spectrometer (Bremen, Germany) equipped with a nitrogen UV- Laser operating at 337 nm. ^{31}P, ^{1}H and ^{13}C NMR spectra were measured with a 400 MHz spectrometer (Varian 400 MHz).
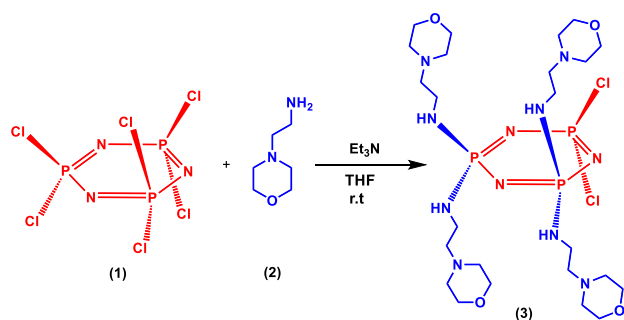
2.2. Synthesis of 4-(2-aminoethyl)morpholine substituted cyclotriphosphazene (3)

4-(2-aminoethyl)morpholine (**2**) (3 mL, 23.0 mmol) was dissolved in 20 mL of dry THF in a 100 mL three-necked round-bottomed flask. The reaction mixture was cooled in an ice-bath and triethylamine (3.2 mL, 23.0 mmol) was quickly added to the stirred solution. Then, hexachlorocyclotriphosphazene (**1**) (1.0 g, 2.9 mmol) in dry THF (10.0 mL) was added to the medium. The reaction mixture was stirred for 4 days at room temperature and followed by TLC silica gel plate. The triethylamine hydrochloride (NEt$_3$.HCl) and any other in soluble materials were filtered off. The solvent was removed under reduced pressure. The crude product was subjected to column chromatography using THF:methanole: *n* - hexane (90:9:1) as the mobile phase. The product (0.40 g, 17 %) was obtained as oily. MALDI TOF (m/z) Calc. 721.08, Found: 721.28 [M]$^{+}$, 1076.85. ^{31}P NMR (162 MHz, CDCl$_3$, ppm) δ_P 24.1 (t, 1P), 14.3 (d, 2P). ^{1}H NMR (400 MHz, CDCl$_3$, ppm) δ_H 3.6 (m, 16H) (-OCH$_2$), 3.1 (s, 4H) (-NH), 3.0 (m, 8H) (-NCH$_2$), 2.4 (m, 8H) (-NCH$_2$), 2.4 (m, 16H) (-NCH$_2$). ^{13}C NMR (101 MHz, CDCl$_3$, ppm) δ_C 66.8, 58.9, 53.3, 37.0. FT-IR (ν : cm^{-1}): 3110.13 (N-H); 2954.91, 2856.20 and 2813.54 (C-H)$_{aliphatic}$; 1655.19 (N-H); 1222.77 and 1176.74 (P=N) ; 1116.48 (C-O) and 971.69 (P-N-C).

3   RESULT AND DISCUSSION

3.1. Synthesis and structural characterization of 4-(2-aminoethyl)morpholine substituted cyclotriphosphazene derivative

Cyclotriphosphazene ring is an important class of molecules consisting of six peripheral arms [1-3]. Cyclotriphosphazene derivatives are easily prepared by the nucleophilic substitution of reactive chlorine atoms with different reagents, and their structural, physical and chemical properties can be easily modulated by substituents [4, 5, 19-23]. In this study, the 4-(2-aminoethyl)morpholine substituted cyclotriphosphazene derivative (**3**) was synthesized (Scheme 1). The compound **3** was prepared by treating hexachlorocyclotriphosphazene (**1**) with 4-(2-aminoethyl) morpholine (**2**) in the presence of Et$_3$N in THF. The product was purified by column chromatography and then the molecular structure of the final compound was confirmed by mass spectrometry, FT-IR, ^{31}P, ^{1}H and ^{13}C NMR spectroscopies. The molecular ion peak of the compound was marked as 721.07 Da by MALDI-TOF mass spectrometer (Fig.1). The MS data of the novel compound confirmed that the four chlorine atoms on the cyclotriphosphazene core had been replaced by the morpholine group.

Scheme 1. Synthesis pathway of 4-(2-aminoethyl) morpholine substituted cyclotriphosphazene derivative

FT-IR spectrum of compound **3** exhibited characteristic stretching bands for P=N- at 1222.77 and 1176.74 cm^{-1}. The vibration band assignable to the stretching of the N-H was observed at 3110.13 cm^{-1}. The stretching bands of aliphatic C-H was seen about 2856 cm^{-1} and peaks of C-O

was observed about 1116.48 cm^{-1} (Fig.2). However, these analyses were insufficient about whether the displacement occurred via geminal or non-geminal. The NMR spectra of the novel compound were examined to explain this situation. The proton decoupled ^{31}P NMR spectrum of the compound **3** was observed as an AX_2 spin system due to two different phosphorus environments within the molecule (Fig. 3). The signals of the compound **3** consisted of one triplet for the [PCl$_2$] group at 24.1 ppm and a doublet for the [P(NR)$_2$] groups at 14.3 ppm. The coupling constant for phosphorus atoms was calculated as 47.5 Hz. The ^{31}P NMR data confirmed the geminal displacement of four 4-(2-aminoethyl) morpholine groups with chlorine atoms. Further structural verification was obtained via ^{1}H and ^{13}C NMR spectroscopies. The -OCH$_2$ and -NCH$_2$ protons of morpholine ring were marked at 3.6 and 2.4 ppm, respectively. The characteristic -NH protons were observed at 3.1 ppm as broad signal. The other aliphatic -NCH$_2$ protons gave signals at 3.0 and 2.4 ppm (Fig. 4).
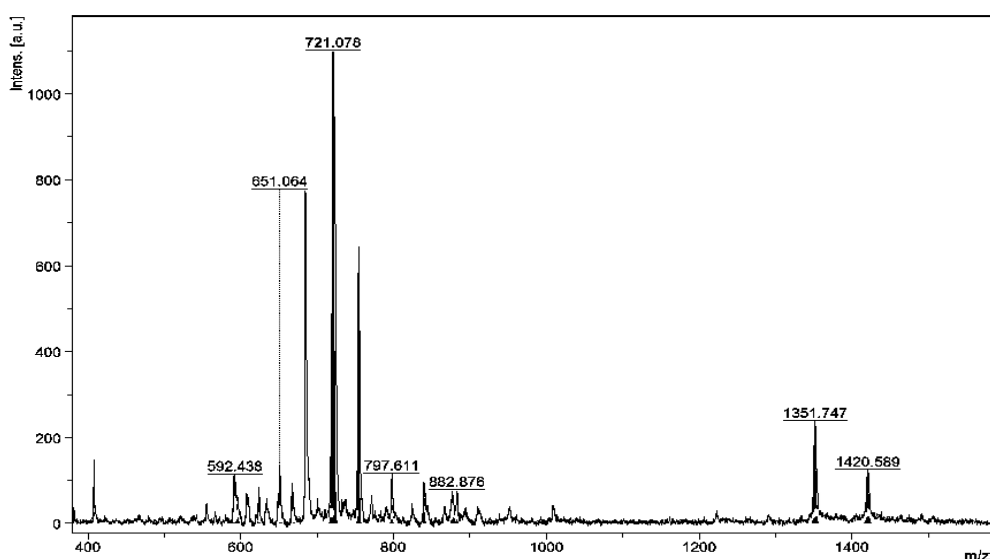

Figure 1. The MALDI-TOF mass spectrum of compound **3**
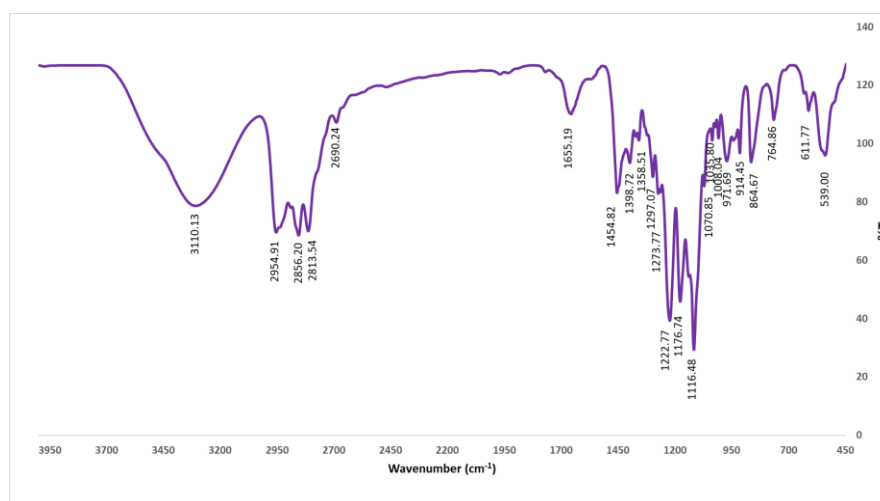

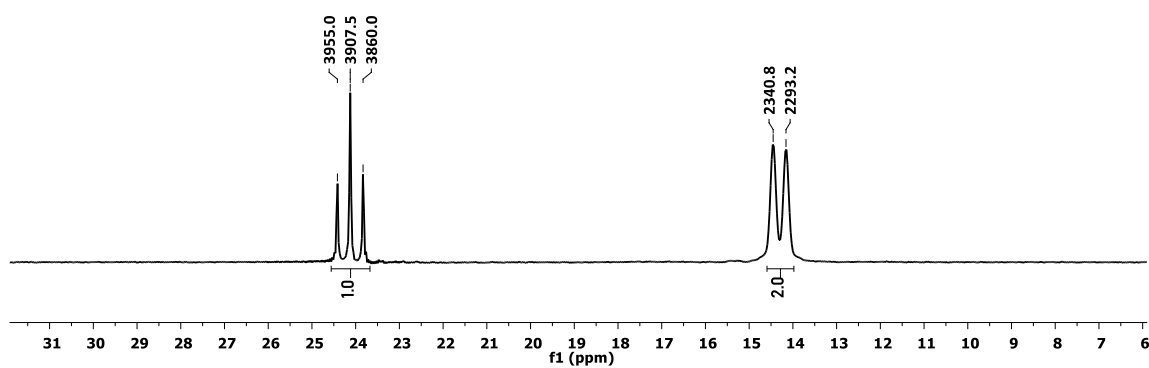**Figure 2.** FT-IR spectrum of compound **3**

Figure 3. The ^{31}P NMR (^{1}H decoupled) spectrum of compound **3**
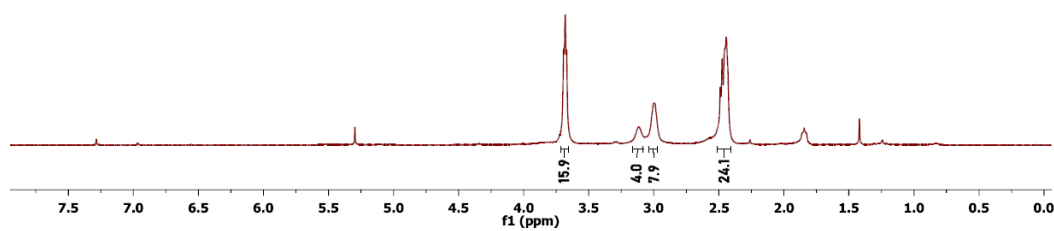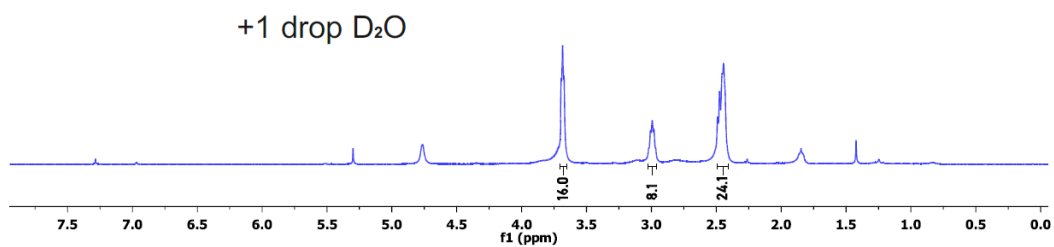

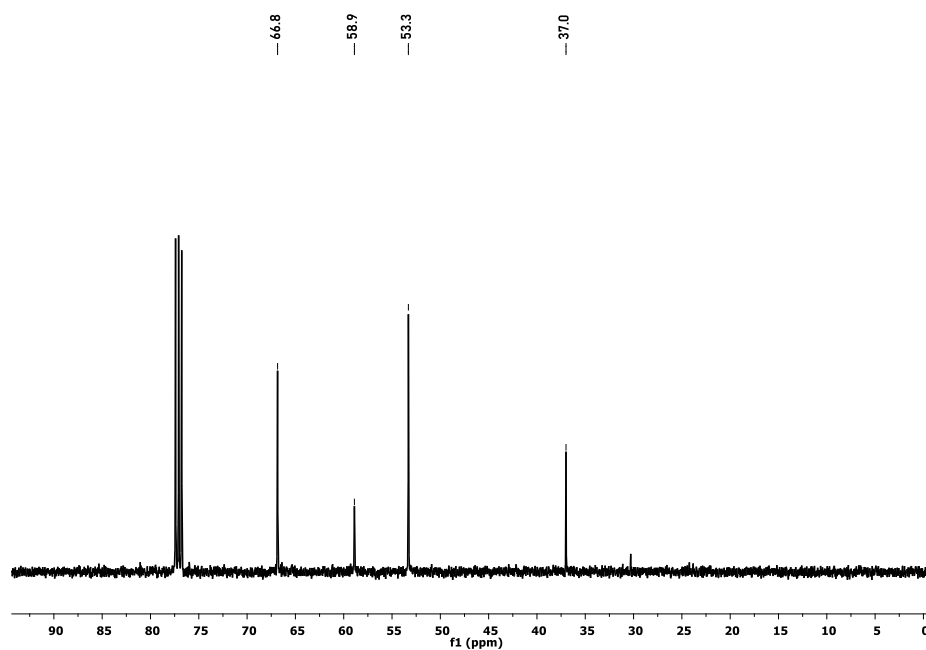**Figure 4.** The ^{1}H NMR spectrum of compound **3** in CDCl$_3$

Figure 5. The ^{13}C NMR spectrum of compound **3**

The location of the NH- protons was also confirmed by D_2O exchange in ^1H NMR (Fig 4). As expected, four different carbon signals (66.8, 58.9, 53.3, 37.0) were seen in the ^{13}C NMR spectrum (Fig. 5). All NMR spectra of the final compound (**3**) was consistent with molecular structure.

3.2. Chlorine replacement pattern

The nucleophilic displacement reactions of cyclotriphosphazene derivatives result in the formation of geminal and non-geminal *cis-* or *trans-* isomers due to kinetic, thermodynamic and steric effects [4, 18-24]. Previous works have shown that the non-geminal *trans-*product is formed as the predominant product and the *cis-*isomer was a minor product at the di-substitution stage of the reaction of hexachlorocyclotriphosphazene with morpholine, a secondary amine [23]. In the current work, outcomes from ^{31}P NMR and MALDI-TOF mass data of the cyclotriphosphazene derivative including 4-(2-aminoethyl) morpholine units pointed to the formation of geminal product (**3**). Similar product formations with primary amines such as aniline, cyclopropanemethlyamine and *t*-butylamine are available in the literature [4, 25, 31]. It can be said that S_N1 and proton abstraction-chloride elimination mechanism go together for the formation of the compound **3**. In this reaction pathway, triethylamine used as the base abstracted a proton from the PCl(NHR) center in the cyclotriphosphazene ring, resulting in loss of chloride ion and a three-coordinate phosphoranimine intermediate is formed. With the attack of another amine group on this phosphoranimine, a geminal substitution product is formed.

4 CONCLUSIONS

In this work, the synthesis of 4-(2-aminoethyl) morpholine substituted cyclotriphosphazene derivative was described. The final compound was isolated in moderate yield by simple column chromatography. The molecular structure of the compound (**3**) was confirmed by mass spectrometry, FT-IR, ^{31}P, ^1H and ^{13}C NMR spectroscopies. The formation of the geminal product was explained by the combined action of S_N1 and proton abstraction-chloride elimination mechanisms. The new compound may be useful as antimicrobial or antifungal agents owing to containing its morpholine moieties.

Conflict of interest
The authors declare no competing financial interest.

Ethical Approval
Ethics Approval is not required for this study.

References

[1] Wang, L., Yang. Y.X., Shi. X., Mignani S., Caminde, A.M., Majoral, J.P., "Cyclotriphosphazene core-based dendrimers for biomedical applications: an update on recent advances", J.Mater.Chem.B, (**2018**), 6,884-895.

[2] Caminade, A.M., Hameauaand, A., Majorala J.P., "The specific functionalization of cyclotriphosphazene for the synthesis of smart dendrimers", Dalton Trans., (**2016**), 45,1810-1822.

[3] Ainscough, E.W., Brodiei A.M., Derwahl, A., Kirk, S., Otter, C.A. "Conformationally Rigid Chelate Rings in Metal Complexes of Pyridyloxy-Substituted 2,2′-Dioxybiphenyl-Cyclotetra- and Cyclotriphosphazene Platforms", Inorg. Chem., (**2007**), 46, 9841-9852.

[4] Allen, C.W., **"**Regio- and stereochemical control in substitution reactions of cyclophosphazenes", Chem Rev., (**1991**), 91,119-135.

[5] Beşli, S., Coles, S.J., Davies, D.B., Kılıç, A., Shaw, R.A., "Bridged cyclophosphazenes resulting from deprotonation reactions of cyclotriphophazenes bearing a P–NH group", Dalton Trans., (**2011**), 40, 5307-5315.

[6] Kagit, R., Yildirim, M., Ozay, O., Yesilot, S., Ozay, H. "Phosphazene Based Multicentered Naked-Eye Fluorescent Sensor with High Selectivity for Fe^{3+} Ions", Inorg. Chem., (**2014**), 53, 4, 2144-2151.

[7] Tümay S. O., A Novel Selective "Turn-On" Fluorescent Chemosensor Based on Thiophene Appended Cyclotriphosphazene Schiff Base for Detection of Ag^+ Ions, Chemistry Select, (**2021**), 6, 39, 10561-10572.

[8] Yıldırım, T., Bilgin, K., Yenilmez Çiftçi, G., Tanrıverdi Eçik, E., Senkuytu, E., Uludag, Y., Tomak, L., Kılıç, A., "Synthesis, cytotoxicity and apoptosis of cyclotriphosphazene compounds as anti-cancer agents", Eur. J. Med. Chem., (**2012**), 52, 213-220.

[9] Bozkurt B., Elmas G., Yakut M., Okumuş A., Çerçi N. A., Zeyrek C. T., Kılıç Z., Açık L., T. Hökelek, "Phosphorus-nitrogen compounds part 59. The syntheses of tetrachloro and tetraamino-2-pyridylmethylspiro(N/N)ethylenediaminocyclotriph osphazenes: Structural characterization, bioactivity, and molecular docking studies", J. Chin. Chem. Soc., (**2021**), 69, 310-331.

[10] Elmas G., Okumuş A., Kılıç Z., Özbeden P., Açık L., Tunalı B. Ç., Türk M., Çerçi N. A., Hökelek T., "Phosphorus-nitrogen compounds. Part 48. Syntheses of the phosphazenium salts containing 2-pyridyl pendant arm: Structural characterizations, thermal analysis, antimicrobial and cytotoxic activity studies", Indian J. Chem. Sec. A, (**2020**), 59A, 533-550.

*Corresponding Author: esra.ecik@atauni.edu.tr (E.Tanrıverdi-Eçik)

[11] Mucur S. P., Canımkurbey B., Kavak P., Akbaş H., Karadağ A., "Charge carrier performance of phosphazene-based ionic liquids doped hole transport layer in organic light-emitting diodes", Appl. Phys. A, (**2020**), 126, 923.

[12] Rao, M. R., Bolligarla, R., Butcher, R.J., Ravikanth, M., "Hexa Boron-Dipyrromethene Cyclotriphosphazenes: Synthesis, Crystal Structure, and Photophysical Properties", Inorg. Chem., (**2010**), 40, 10606-10616.

[13] Çiftçi, G.Y., Şenkuytu, E, İncir, S.E., Tanrıverdi-Eçik, E., Zorlu, Y, Ölçer, Z., Uludağ, Y., "Characterization of paraben substituted cyclotriphosphazenes, and a DNA interaction study with a real-time electrochemical profiling based biosensor", Microchim Acta, (**2017**), 184, 2307–2315.

[14] Sarıkaya, S.Y., Yeşilot, S., Kılıç, A., Okutan, E., "Novel BODIPY-Cyclotriphosphazene- Fullerene triads: Synthesis, characterization and singlet oxygen generation efficiency", Dyes and Pigments, (**2018**), 153, 26–34.

[15] Şenkuytu E., Okutan E., Tanrıverdi-Eçik E., "Cyclotriphosphazene-BODIPY Dyads: Synthesis, halogen atom effect on the photophysical and singlet oxygen generation properties" Inorg. Chem Acta., (**2020**), 502, 119342.

[16] Ainscough, E.W., Brodie, A.M., Derwahl, A., Kirk, S., Otter, C.A. "Conformationally Rigid Chelate Rings in Metal Complexes of Pyridyloxy-Substituted 2,2′-Dioxybiphenyl-Cyclotetra- and Cyclotriphosphazene Platforms", Inorg. Chem., (2007), 46, 9841-9852.

[17] Chaplin, A.B., Harrison, J.A., Dyson, P.J. "Revisiting the Electronic Structure of Phosphazenes", Inorg. Chem., (**2005**), 44, 8407−8417.

[18] Chandrasekhar, V., Thilagar, P., Pandian, B. M., "Cyclophosphazene-based multi-site coordination ligands", Coord. Chem. Rev., (**2007**), 251, 1045-1074.

[19] Eçik, E.T., Beşli, S., Çiftçi, G.Y., Davies, D.B., Kılıç, A., Yuksel, F. "Stereo-selectivity in a cyclotriphosphazene derivative bearing an exocyclic P–O moiety". Dalton Trans., (**2012**), 41, 6715-6725.

[20] Ganapathiappan, S., Krishnamurthy, S. S., "Studies of phosphazenes. Part 30. Reactions of hexachlorocyclotriphosphazene with aromatic primary amines: interplay of geminal and non-geminal modes of chlorine replacement", J. Chem. Soc., Dalton Trans., (**1987**), 579-584.

[21] Lee, S. B., Song, S.-C., Jin, J.-I., Sohn, Y. S. " Thermosensitive Cyclotriphosphazenes", J. Am. Chem. Soc., (**2000**), 122, 8315-8316.

[22] Uslu, A., Yeşilot, S., "Chiral configurations in cyclophosphazene chemistry", Coord. Chem. Rev., (**2015**), 291, 28-67.

[23] Uslu, A., Özcan, E., Dural, S., Yuksel, F., "Synthesis and characterization of cyclotriphosphazene derivatives bearing azole groups", Polyhedron, (**2016**), 117, 394-403.

[24] Ibisoglu, H., Besli, S., Yuksel, F., Un, I., Kılıç, A., "Investigation of nucleophilic substitution pathway for the reactions of 1,4-benzodioxan-6-amine with chlorocyclophosphazenes", Inorganica Chimica Acta (**2014**), 409, 216-226.

[25] Bartlett, S.W., Coles, S.J, Davies, D.B., Hursthouse, M.B., Ibisoglu H., et al. "Structural investigations of phosphorus–nitrogen compounds. 7. Relationships between physical properties, electron densities, reaction mechanisms and hydrogen-bonding motifs of $N_3P_3Cl_{(6-n)}(NHBut)_n$ derivatives" Acta Crystallographica Section B (**2006**), B62, 321-329.

[26] Besli, S., Balcı, C. M., Doğan S., Allen, C.W.," Regiochemical Control in the Substitution Reactions of Cyclotriphosphazene Derivatives with Secondary Amines" Inorg. Chem., (**2018**), 57, 19, 12066-12077.

[27] Kourounakis A.P., Xanthopoulos D., Tzara A. "Morpholine as a Privileged Structure: A Review on the Medicinal Chemistry and Pharmacological Activity of Morpholine Containing Bioactive Molecules" Med. Res. Rev., (**2019**), 1-44.

[28] Tzara A., Kourounakis A.P., Xanthopoulos D. "Morpholine As a Scaffold in Medicinal Chemistry: An Update on Synthetic Strategies" ChemMedChem, (**2020**), 15, 392-403.

[29] Kumari A., Singh R.K. "Morpholine as ubiquitous pharmacophore in medicinal chemistry: Deep insight into the structure-activity relationship (SAR)" Bioorganic Chem., (**2020**), 96, 103578

[30] Uslu, A., Güvenaltın, S., "The investigation of structural and thermosensitive properties of new phosphazene derivatives bearing glycol and amino acid" Dalton Trans., (**2010**), 39, 10685–10691.

[31] Tanrıvedi-Eçik, E., İbisoğlu, H., Yenilmez-Çiftçi, G., Demir, G., Erdemir, E., Yuksel, F., "Nucleophilic subtitution reactions of mono-functional nucleophilic reagents with cyclotriphosphazenes containing 2, 2′-dioxybiphenyl units", Turkish Journal of Chemistry, (**2020**), 44, 87-98.

Cu(II) Katkılı 6,7-Dihidroksi-3-(3-klorofenil)kumarin Bileşiğinin Dielektrik Özelliklerinin İncelenmesi

Fatih BİRYAN[1a], Kenan KORAN[1b,*], Ahmet Orhan GÖRGÜLÜ[2a]

[1]Fırat Üniversitesi, Kimya Bölümü, Elazığ, Türkiye
[2]Marmara Üniversitesi, Kimya Bölümü, Elazığ, Türkiye

ORCID: [a]0000-0001-9198-3329 [b]0000-0002-2218-7211, [c]0000-0003-0632-4834

Özet: Bu çalışmada, Cu(II) metal iyonlarının farklı mol oranlarında 6,7-dihidroksi-3-(3-klorofenil)kumarin bileşiğinin (DPCl-Kum) dielektrik sabiti, dielektrik kayıp faktörü ve ac iletkenliğinin frekansın bir fonksiyonu olarak incelenmesi amaçlanmıştır. DPCl-Kum için dielektrik ölçümleri, frekansın bir fonksiyonu olarak bir empedans analizörü kullanılarak belirlenmiştir. DPCl-Kum ve kompozitlerinin dielektrik özellikleri, oda sıcaklığında 100 Hz ile 20 kHz arasındaki frekansta ölçülmüş ve birbirleriyle karşılaştırılarak verilmiştir. DPCl-Kum bileşiğindeki polarize olan serbest –OH fonksiyonel gruplarının Cu(II) iyonları ile etkileşimi sonucu polarizasyonun azalmasından dolayı Cu (II) iyonunun artan mol oranlarında dielektrik özelliklerinde de azalma olduğu görüldü. Ayrıca DPCl-Kum ve kompozitlerinin TGA analizleri gerçekleştirildi. Cu(II) oranı arttıkça hem termal kararlılığın arttığı hem de artık miktarlarının arttığı görüldü.

Anahtar Kelimeler: Kumarin, Dielektrik Özellik, Bakır (II) İyonları

Investigation of Dielectric Properties of Cu(II) Doped 6,7-Dihydroxy-3-(3-chlorophenyl)coumarin Compound

Abstract: We aimed to investigate the dielectric constant, dielectric loss factor and ac conductivity of 6,7-dihydroxy-3-(3-chlorophenyl)coumarin compound (DPCl-Kum) at different mole ratios of Cu(II) metal ions as a function of frequency. Dielectric measurements for DPCl-Kum were determined using an impedance analyzer as a function of frequency. Dielectric properties of DPCl-Kum and its composites were measured at 25 °C over the frequency from 100 Hz to 20 kHz and given as compared with each other. It was observed that the dielectric properties of the Cu (II) ion decreased with increasing mole ratios due to the decrease in polarization as a result of the interaction of polarized free –OH functional groups with Cu(II) ions in the DPCl-Kum compound. In addition, TGA analyzes of DPCl-Kum and its composites were performed. It was observed that as the Cu(II) ratio increased, both the thermal stability increased and the residual amount increased.

Keywords: Coumarin, Dielectric Properties, Copper (II) Ions

*Corresponding Author: kenan.koran@gmail.com (Kenan Koran)

1 GİRİŞ

Kumarin kimyası 200 yıllık bir geçmişe sahiptir. 1820'lerde kumarin ilk kez Tonka fasulyesinin çiçeklerinden izole edilmiştir. Daha sonra bu bileşiğe tonka fasulyesinin Fransızca "coumarou" kumarin adı verilmiştir [1-5].

W. H. Perkin, 1868'de salisilaldehitin sodyum tuzunu asetik asitle ısıtarak kumarini yapay sentezleyen ilk kişi olmuştur ve bu yöntem Perkin reaksiyonu olarak kabul edilmiştir [6]. Kumarin yapısı, 1872'de Strecker, Fittig ve Tiemann tarafından 1-benzopiran-2-on yapısında olarak önerilmiştir. Ayrıca 1741'de Rama Swamy, 1973'te Myasnikova [1] kumarinin kristal yapısıyla ilgili araştırmalarda bulunmuştur. Kumarin floroforları, antiviral [7], antikanser [8], antilösemi [9], anti-diyabetik [10], anti-inflamatuar [11] gibi çeşitli farmakolojik uygulamalarda katkı maddesi olarak kullanılmakta ve adenosin reseptör antagonistleri [12, 13] olarak işlev gördüğü belirlenmiştir. Bunun dışında kumarin ve ürünleri pestisitlerde [14], gıda katkı maddelerinde [15], parfüm sanayisinde [16], kozmetiklerde [17], boya ve kauçuklarda koku maskeleyicilerde [18], uçucu yağların güçlendiricilerinde [19] olarak kullanılmaktadır [20].

Kumarin, bir benzen halkası ile bir piran halkası içeren iki halkalı bir sistemdir. 3 ve 4 numaralı karbon arasındaki C=C, *cis-/trans-* izomerizasyonunu sınırlamaktadır ve bu şekilde tüm kumarin çekirdeği bir planya haline gelir. Kumarinin planer yapısından dolayı mükemmel yük transferi özelliği gösterir ve üstün fotofiziksel özelliklere sahiptirler. Kumarin, 1 ve 2 konumlarında bir lakton grubuna ve C-3'ten C-8'e kadar altı çevresel hidrojen atomuna sahiptir. Periferal hidrojenler uygun şekilde süstitüe edilebilir. Doğal olarak oluşan kumarin türevleri 7. pozisyonda bir hidroksil grubuna sahipken, bazı temel floresan kumarin aynı pozisyonda amino- veya hidroksil-gruplarına sahiptir [1, 20].

Kumarin, Perkin kondenzasyonu [6], Knoevenagel kondenzasyonu [21] ve Pechmann reaksiyonu [22] gibi çeşitli yöntemlerle sentezlenebilmektedir. Son zamanlarda mikrodalga destekli kumarin sentezi geliştirilmiştir [23, 24]. Metal katalizli siklizasyon da kumarin omurgasının sentezi için tercih edilen yöntemdir [25].

Kumarin halkasına bağlı olan süstitüe grupların yeri ve konumunun değişmesi, kumarinlerin farklı fiziksel, kimyasal ve biyolojik özellikler gösterebilmesine olanak sağlamaktadır. Bu durum kumarin türevlerinin yeni uygulama alanlarının keşfedilmesini önemli kılmıştır.

Bu amaçla, bu çalışmada 6,7-dihidroksi-3-(3-klorofenil)kumarin bileşiği (DPCl-Kum) literatürdeki metoda göre sentezlendi [24] ve yapısı FT-IR, ^{1}H ve ^{13}C-APT NMR spektroskopi yöntemleri ile aydınlatıldı. Ayrıca DPCl-Kum bileşiği farklı mol oranlarında bakır (II) iyonu ile katkılandı. Elde edilen Cu(II) iyonu ile doplanmış kumarin karışımlarının dielektrik sabiti, dielektrik kayıp faktörü ve ac iletkenlik özellikleri oda sıcaklığında 100 Hz ile 20 kHz frekans aralığında frekansın bir fonksiyonu olarak incelendi.

2 MATERYAL VE METOD

2,4,5-trimetoksibenzaldehit, 3-kloroakrilonitril bileşikleri Sigma-Aldrich firmasından temin edilmiştir. Silikajel, n-hekzan, aseton, etanol, kloroform ve tetrahidrofuran ve NMR çalışmalarında döteryumlu çözücü olarak kullanılan DMSO-d6 Merck firmasından satın alınmıştır.

Bileşiklerin karakterizasyonunda FT-IR spektrumları Perkin Elmer SpectrumOne FT-IR spektrometre cihazı ile NMR Spektrumları Bruker DPX–400 High Performance Digital FT-NMR cihazı ile ve dielektrik parametrelerin ölçümlerinde Quadtech 7600 Precision LCR meter cihazı kullanılmıştır.

2.1 Sentez ve Karakterizasyon

2-(2,4,5-trimetoksifenil)-1-(3-klorofenil)akrilonitrile (TM-CN) [26] ve 6,7-dihidroksi-3-(3-klorofenil)kumarin (DPCl-Kum) [24] bileşikleri literatüre göre sentezlenmiştir. Genel sentez şeması Şekil 1'de verilmiştir.

2.1.1 2-(2,4,5-trimetoksifenil)-1-(3-klorofenil) akrilonitrile (TM-CN) Bileşiğinin Karakterizasyonu

2,4,5-trimetoksibenzaldehit (TM) (2.7 mmol) ve 3-klorobenzilsiyanit (AC) (2.7 mmol) kullanıldı. Yeşil renkli katı madde: Verim: 70%, E.N. 164-165 ºC. FT-IR (KBr, cm^{-1}) ν: ν: 1612, 1580, 1510 (C=C), ν: 2196 (C≡N), 3049, 3008 (Ar-CH). ^{1}H-NMR (400 MHz, CDCl$_3$) δ 6.53 (1H, s, H^2), 7.66 (1H, s, H^5), 3.94 (3H, s, H^7), 3.98 (3H, s, H^8), 3.97 (3H, s, H^9), 7.95-7.99 (2H, s, H^{14}, H^{10}), 7.33-7.40 (2H, m, H^{16} ve H^{17}), 7.58 (1H, d, H^{18}). ^{13}C-NMR (CDCl$_3$) δ 154.12 C^1, 96.14 C^2, 152.65 C^3, 143.02 C^4, 110.11 C^5, 113.92 C^6, 56.81 C^7, 56.11 C^8, 56.42 C^9, 137.44 C^{10}, 106.10 C^{11}, 118.81 C^{12}, 137.10 C^{13}, 124.01 C^{14}, 134.92 C^{15}, 125.71 C^{16}, 130.13 C^{17}, 128.42 C^{18}.

2.1.2 DPCl-Kum Bileşiğinin Karakterizasyonu

Açık kahverenkli katı madde DPCl-Kum, Verim:90%, FT-IR (KBr, cm^{-1}): 1580, 1602 ve 1621, $\nu_{C=C}$, 1661 $\nu_{C=O}$, 3059 $\nu_{C-H(Ar)}$, 3370, 3168 ν_{O-H}. ^{1}H NMR (400 MHz, DMSO-d$_6$): δ, 7.07 (1H, s, H^2), 6.79 (1H, s, H^5), 9.55 (1H, s, H^7), 10.36 (1H, s, H^8), 7.73 (1H, s, H^9), 8.16 (1H, s, H^{13}), 7.50 (1H, d, J=8.4 Hz, H^{15}), 7.52 (1H, t, J=8.0 Hz, H^{16}), 7.76 (1H, d, J=6.8 Hz, H^{17}). ^{13}C-NMR (DMSO-d$_6$): δ, 143.6 C^1, 102.6 C^2, 151.2 C^3, 148.6 C^4, 112.9 C^5, 111.8 C^6, 141.9 C^9, 121.2 C^{10}, 160.65 C^{11}, 132.9 C^{12}, 128.6 C^{13}, 134.6 C^{14}, 130.4 C^{15}, 132.2 C^{16}, 128.6 C^{17}.

Şekil 1. TM-AC ve **DPCl-Kum** Bileşiklerinin genel sentez reaksionu

2.2 DPCl-Kum Bileşiğinin Cu(II) Kompozitlerinin Hazırlanması

100 ml lik reaksiyon balonunda **DPCl-Kum** bileşiği ve kütlece farklı oranlarda tartılan (%10, %20, %28) bakır (II) klorür etanol/su karışımında çözüldü ve oda sıcaklığında 12 saat boyunca karıştırıldı. Daha sonra ultrasonic homojenizatör ile 30 dk dispers edildi (300 kw). Daha sonar çözücünün fazlası uzaklaştırıldıktan sonra ürünler vakum altında 40 °C'de kurutuldu.

2.3 Dielektrik Özelliklerin Belirlenmesi

DPCl-Kum bileşiği ve Cu (II) ile doplanmış **DPCl-Kum** bileşiğinin karışımlarının dielektrik özelliklerinin belirlenmesi için öncelikle numuneler basınç altında (yaklaşık 4 ton) tablet haline getirildi. Tablet kalınlığı ölçüldü. Kapasitans değerleri (Cp) ve dielektrik kayıp faktörü (DF) ve Gp değerleri belirlendi. Ölçümler 100 Hz ile 20 kHz aralığında oda sıcaklığında frekansa karşı yapıldı. Dielektrik sabitleri aşağıda belirtilen formüller ile hesaplandı[27-30].

$$\varepsilon' = C_p \frac{d}{A\varepsilon_0} \qquad (1)$$

$$\varepsilon'' = \varepsilon' DF \qquad (2)$$

$$\sigma = G_p \frac{d}{A} \qquad (3)$$

A: Numunenin alanı (m²);   ε': Dielektrik sabiti

C: Numunenin kapasitansı(F);   ε″: Dielektrik kayıp

d: Numunenin çapı (m)

ε₀: Boşluğun dielektrik sabiti (8.85x10⁻¹² F/m)

3 BULGULAR

3.1 Sentez ve Karakterizasyon

Çalışmanın sentez basamağında ilk olarak TM, 3-klorobenzilsiyanit (AC) ile etanol içerisinde ve %20'lik NaOH varlığında 70 °C'de, argon atmosferi altında etkileştirilerek **TM-AC** bileşiği literatüre benzer metotla elde edildi. Elde edilen **TM-AC** bileşiği havası alınmış bir balona ilave edildi ardından silikajel:piridinyum hidroklorür (3:1) karışımı eklenerek ev tipi bir mikro dalga fırın içinde etkileştirilerek **DPCl-Kum** bileşiği elde edildi. Bileşiklerin yapıları FT-IR, ¹H- ve ¹³C-NMR teknikleri ile aydınlatıldı ve elde edilen veriler literatürle uyumlu olduğu gözlendi [24]. Bileşiklerin ¹H ve ¹³C-NMR spektrumları Şekil 2 ve 3'de verilmiştir. Detaylı veriler deneysel bölümde açıklanmıştır. Bileşik **TM-AC** de 2196 cm⁻¹ deki -CN pikinin, **DPCl-Kum** bileşiğinin FT-IR spektrumunda gözlenmemesi halkanın oluştuğunu göstermektedir. **TM-AC** Bileşiğinin yapısındaki –CN'e komşu 1612 cm⁻¹ deki C=C bağlarının **DPCl-Kum** bileşiğinin oluşumuyla 1622 cm⁻¹'e kaydığı gözlenmiştir. **TM-AC** Bileşiğindeki –OCH₃ gruplarının -OH a dönüştüğü ve –OH gerilme titreşimleri **DPCl-Kum** bileşiğinin FT-IR spektrumunda gözlenmiştir. ¹H-NMR spektrumunda 9.5 ve 10.3 ppm'de görülen singlet 1 protonluk pikler yapıda bulunan –OH protonlarına aittir. **TM-AC** bileşiğinde aromatik halkaya bağlı 3.5-4 ppm arasında olan –OCH₃ protonlarının **DPCl-Kum** bileşiğinde gözlenmemesi yapının oluştuğunu göstermektedir. –OCH₃ Gruplarının –OH'a dönüşmesinin bir sonucu olarak –OH protonlarının varlığı ve integral yüksekliklerinin yapıya uygun olması önerilen yapıyı desteklemektedir. ¹³C-NMR spektrumunda da **DPCl-Kum** bileşiğine ait karakteristik lakton karbonili ve diğer karbon atomlarına ait pikler spektrumda görülmektedir.

Şekil 2. TM-AC Bileşiğinin ^{1}H ve ^{13}C-NMR spektrumu (Kloroform-d)

49

*Corresponding Author: kenan.koran@gmail.com (Kenan Koran)

Şekil 3. DPCl-Kum Bileşiğinin ^{1}H ve ^{13}C-NMR spektrumu (DMSO-d$_6$)
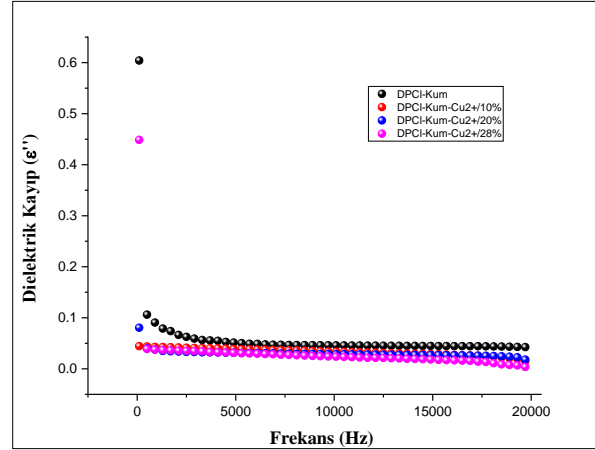
3.2 Dielektrik ve Termal Özellikleri

DPCl-Kum bileşiği ve ağırlıkça %10, %20 ve %28 oranlarında Cu(II) klorür ile hazırlanan kompozitlerinin dielektrik sabiti, dielektrik kayıp faktörü ve ac iletkenlikleri incelendi ve bileşiğin saf hal ile farklı oranlardaki kompozitleri bir birleri ile karşılaştırıldı (Şekil 4-6). DPCl-Kum ve hibrit yapıların termal özelliklerini incelemek amacıyla Shimadzu marka DTG-60 birleşik sistemi kullanıldı. Toz halindeki numunelerden 5 mg örnek alınarak azot atmosferinde oda sıcaklığından 600 °C'ye kadar 10 °C dk^{-1} ısıtma hızıyla analiz edildi. Sonuçlar aynı sıcaklık ekseninde karşılaştırmalı olarak Şekil 7'de gösterilmiştir.

Şekil 5. DPCl-Kum Bileşiği ve kompozitlerinin artan frekansa karşı dielektrik kayıp faktörlerinin karşılaştırılması
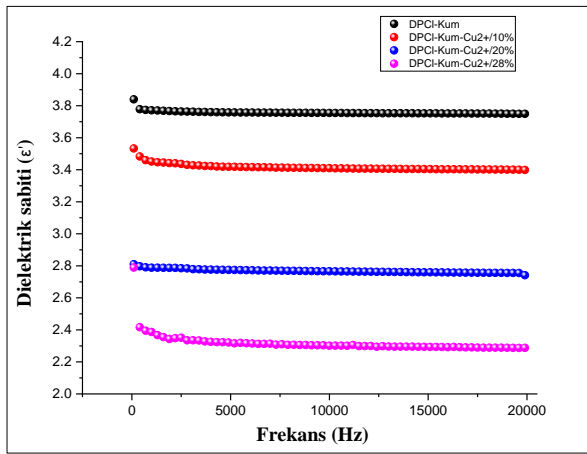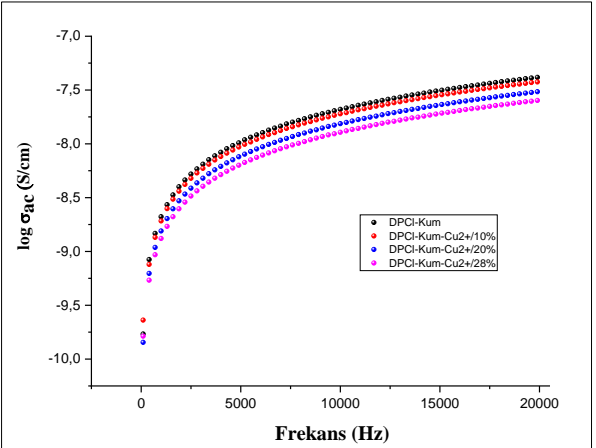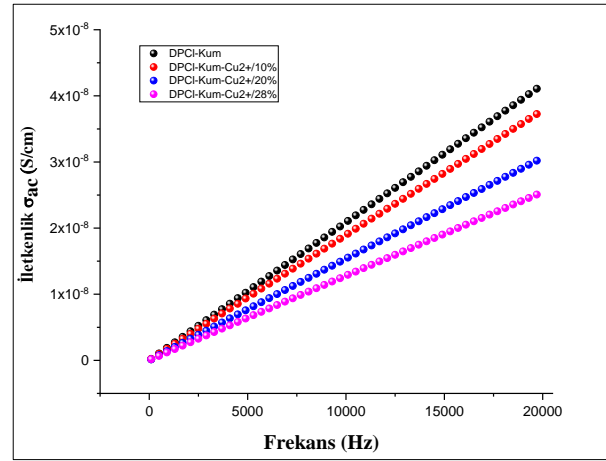

**Şekil 4. DPCl-Kum** bileşiği ve **Cu(II)** kompozitlerinin artan frekansa karşı dielektrik sabitlerinin değişimi

Dielektrik özellikler üzerinde artan Cu^{2+} yüzdesinin etkisi frekansın bir fonksiyonu olarak oda sıcaklığında incelendi. **DPCl-Kum** bileşiğinin 2 kHz'deki dielektrik sabiti 3.77 iken Cu(II) kompozitlerinde bu değer konsantrasyona bağlı olarak azalmış ve %28 kompozit oranına 2.28'e düşmüştür. **DPCl-Kum** ve kompozitlerin değerleri artan frekansla azaldığı tespit edildi (Şekil 4). Genellikle düşük frekanslarda bu azalma oldukça belirgindir. Yüksek frekans değerlerine doğru dielektrik sabitindeki azalma eğilimi yavaşlamakta ancak düşüş yine de devam etmektedir. Düşük frekanslardaki ani azalmalar, muhtemelen bu frekanslarda uygulanan elektriksel alan yönünde maddenin yapısında bulunan yüklü dipollerin kendi eksenleri etrafında ve alan yönünde hareket etme eğilimlerinin yüksek olmasındandır. Benzer durum Şekil 5'teki dielektrik kayıp grafiğinde de görülmektedir.

DPCl-Kum ve Cu(II) kompozitleri için Şekil 6'da, AC iletkenliğin frekans ile değişimini de gösterilmektedir. Buna göre, iletkenlik düşük frekans bölgelerinde oldukça hızlı artarken, yüksek frekans bölgelerine doğru artış hızı azalmakta ve sabit bir değişim durumuna yaklaşmaktadır. Elde edilen kompozitlerin için 1 kHz'de ölçülen dielektrik sabiti (ε'), dielektrik kayıp faktörü (ε″) ve iletkenlik (logσ) sonuçları Tablo 1'de özetlenmiştir.

Şekil 6. DPCl-Kum Bileşiği ve kompozitlerinin artan frekansa karşı AC iletkenliğinin değişimi

Tablo 1. DPCl-Kum Bileşiği ve kompozitlerinin 25 ^{0}C ve 1 kHz'deki Dielektrik Sonuçları

	ε'	ε″	log σ
DPCl-Kum	3.77	0.086	-8.67
DPCl-Kum-Cu^{2+}/10%	3.45	0.042	-8.71
DPCl-Kum-Cu^{2+}/20%	2.78	0.037	-8.80
DPCl-Kum-Cu^{2+}/28%	2.38	0.036	-8.87

4   TARTIŞMA

Bu çalışmada, 6,7-Dihidroksi-3-(3-klorofenil)kumarin (**DPCl-Kum**) bileşiği ve ağırlıkça %10, 20 ve 28 oranlarında Cu (II) klorür ile hazırlanan kompozitlerinin dielektrik özelliklerinin belirlenmesi amaçlanmıştır.

Sentezleri gerçekleştirilen bu **DPCl-Kum** bileşiğinin dielektrik sabiti, dielektrik kayıp faktörü ve AC iletkenlik değerleri sabit sıcaklıkta frekansın bir fonksiyonu olarak (100 Hz ile 20 kHz arasında) empedans analizörü ile belirlendi. Bu bileşiklerde artan frekans ile dielektrik özellikleri değişmektedir. Dielektrik sabitinin frekans arttıkça bir miktar azaldığı ve yüksek frekans değerlerinde sabit kaldığı görülmüştür. Ayrıca, dielektrik kayıp faktörleri frekansla bir azalış eğilimi gösterdiği, AC iletkenlik değerlerinin ise frekansla arttığı gözlenmiştir. Bu artışlar literatürde yapılan çalışmalarla kıyaslandığında sonuçların artan frekansla uyumluluk gösterdiği bulunmuştur[28, 30, 31]. Ayrıca, Cu(II) iyonunun artan mol oranlarında dielektrik özelliklerinde de azalma olduğu görüldü. Bunun nedeni **DPCl-Kum** bileşiğindeki polarize olan serbest –OH fonksiyonel gruplarının Cu(II) iyonları ile etkileşimi sonucu polarizasyonun azalmasından kaynaklandığı düşünülmektedir. Bu sonuçlar incelendiğinde bileşiklerin iletkenliği hem frekansa hem de Cu(II) iyonlarına duyarlı olup bu ölçütlerin artışıyla azaldığı görülmüştür.
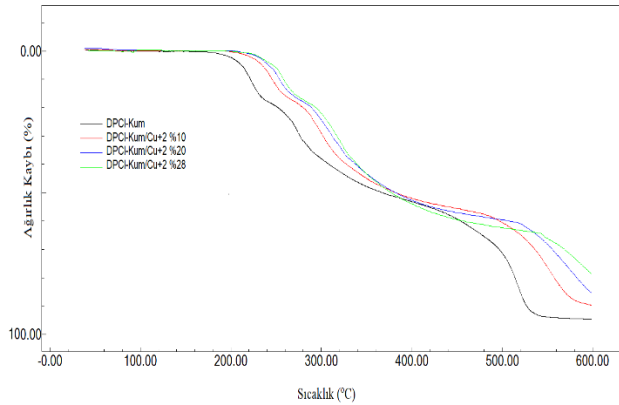
Şekil 7. DPCl-Kum Bileşiği ve kompozitlerinin TGA eğrileri

TGA eğrilerindeki sonuçlara göre $CuCl_2$ oranı arttıkça yapının termal kararlılık kazandığı görülmektedir. Bu durumun sebebinin organik bileşiğin metal ile etkileşimi sonucu bozunmanın geciktirmesinden kaynaklandığı düşünülmektedir. Ayrıca Cu(II) konsantrasyonun arttıkça 600 ºC'deki % atık miktarları da artmaktadır. Sıcaklığın artmasıyla birlikte moleküldeki zayıf etkileşimler ve kimyasal bağların kırılması ayrıca molekülde uçucu bileşenlerin ayrılması ile kütle kaybı olmuştur. Organik yapılarının bozunduğu son sıcaklık değerinde inorganik bileşenlerin daha kararlı olması sebebiyle bozunmadan kaldığı düşünülmektedir.

5   SONUÇLAR

Literatür çalışmaları incelendiğinde **DPCl-Kum** bileşiğinin ölçülen floresans özelliğine bağlı olarak Cu(II) iyonlarına karşı sensör özelliği gösterdiği tespit edilmiştir.

Bu sonuçlar yapılan bu çalışmanın da Cu(II) iyonuna karşı duyarlı olduğunu ve elektriksel özelliklerinde de değişime neden olduğunu açıkça gösteren ve ispatlayan parametrelerden olmuştur.

Bu tür malzemelerin yararlılığı bu maddelerin yapısal özelliklerinin yanında metal iyonları ile yapmış oldukları etkileşimde bağlı olduğunu göstermektedir. Kumarin bileşikleri metal iyonlarına karşı sensör özelliği göstermesinin [24] yanında aynı metal iyonlarına karşı elektriksel özelliklerinde değişimin olduğu yapılan bu çalışma ile ortaya koyulmuştur. Bu tür yapıların elektriksel aygıtlarda da kullanılabilme potansiyeline sahip olduğu belirlenmiştir.

Çıkar Çatışması

Yazarlar hiçbir rekabet eden finansal çıkar beyan etmemektedir.

Etik Onay: Bu çalışma için Etik Onayı gerekmemektedir.

KAYNAKLAR

[1]   D. Cao *et al.*, "Coumarin-Based Small-Molecule Fluorescent Chemosensors," *Chemical Reviews,* vol. 119, no. 18, pp. 10403-10519, 2019/09/25 2019.

[2]   E. A. Azzopardi *et al.*, "Chromophores in operative surgery: Current practice and rationalized development," *Journal of Controlled Release,* vol. 249, pp. 123-130, 2017/03/10/ 2017.

[3]   P. Chinna Ayya Swamy *et al.*, "Near Infrared (NIR) absorbing dyes as promising photosensitizer for photo dynamic therapy," *Coordination Chemistry Reviews,* vol. 411, p. 213233, 2020/05/31/ 2020.

[4]   Y. Jung, J. Jung, Y. Huh, and D. Kim, " Benzocoumarin-Based Fluorescent Probes for Bioimaging Applications," *Journal of Analytical Methods in Chemistry,* vol. 2018, p. 5249765, 2018/06/14 2018.

[5]   A. Vogel, "Darstellung von Benzoesäure aus der Tonka-Bohne und aus den Meliloten - oder Steinklee - Blumen," *Annalen der Physik,* vol. 64, no. 2, pp. 161-166, 1820.

[6]   W. H. Perkin, "On the artificial production of coumarin and formation of its homologues," *Journal of the Chemical Society,* vol. 21, pp. 53-63, 1868.

[7]   D. Yu, M. Suzuki, L. Xie, S. L. Morris-Natschke, and K.-H. Lee, "Recent progress in the development of coumarin derivatives as potent anti-HIV agents," *Medicinal Research Reviews,* vol. 23, no. 3, pp. 322-345, 2003.

[8]   S. Emami and S. Dadashpour, "Current developments of coumarin-based anti-cancer agents in medicinal chemistry," *European Journal of Medicinal Chemistry,* vol. 102, pp. 611-630, 2015/09/18/ 2015.

52

[9]   A. Stefanachi *et al.*, "Design, Synthesis, and Biological Evaluation of Imidazolyl Derivatives of 4,7-Disubstituted Coumarins as Aromatase Inhibitors Selective over 17-α-Hydroxylase/C17−20 Lyase," *Journal of Medicinal Chemistry,* vol. 54, no. 6, pp. 1613-1625, 2011/03/24 2011.

[10]   A. P. Dwivedi, S. Kumar, V. Varshney, A. B. Singh, A. K. Srivastava, and D. P. Sahu, "Synthesis and antihyperglycemic activity of novel N-acyl-2-arylethylamines and N-acyl-3-coumarylamines," *Bioorganic & Medicinal Chemistry Letters,* vol. 18, no. 7, pp. 2301-2305, 2008/04/01/ 2008.

[11]   C. A. Kontogiorgis and D. J. Hadjipavlou-Litina, "Synthesis and biological evaluation of novel coumarin derivatives with a 7-azomethine linkage," *Bioorganic & Medicinal Chemistry Letters,* vol. 14, no. 3, pp. 611-614, 2004/02/09/ 2004.

[12]   M. J. Matos *et al.*, "Structure-Based Optimization of Coumarin hA3 Adenosine Receptor Antagonists," *Journal of Medicinal Chemistry,* vol. 63, no. 5, pp. 2577-2587, 2020/03/12 2020.

[13]   J. Breidenbach, U. Bartz, and M. Gütschow, "Coumarin as a structural component of substrates and probes for serine and cysteine proteases," *Biochimica et Biophysica Acta (BBA) - Proteins and Proteomics,* vol. 1868, no. 9, p. 140445, 2020/09/01/ 2020.

[14]   S. Feng *et al.*, "Coumarin-Containing Light-Responsive Carboxymethyl Chitosan Micelles as Nanocarriers for Controlled Release of Pesticide," *Polymers,* vol. 12, no. 10, p. 2268, 2020.

[15]   Y.-H. Wang, B. Avula, N. P. D. Nanayakkara, J. Zhao, and I. A. Khan, "Cassia Cinnamon as a Source of Coumarin in Cinnamon-Flavored Food and Food Supplements in the United States," *Journal of Agricultural and Food Chemistry,* vol. 61, no. 18, pp. 4470-4476, 2013/05/08 2013.

[16]   F. Floc'h, F. Mauger, J. R. Desmurs, and A. Gard, "Coumarin in plants and fruits: implication in perfumery," *Perfum. Flavor.,* vol. 27, no. 2, pp. 32-36, 2002.

[17]   M. T. Baltazar *et al.*, "A Next-Generation Risk Assessment Case Study for Coumarin in Cosmetic Products," *Toxicological Sciences,* vol. 176, no. 1, pp. 236-252, 2020.

[18]   V. Decottignies, G. Filippi, and A. Bruchet, "Characterisation of odour masking agents often used in the solid waste industry for odour abatement," *Water Science and Technology,* vol. 55, no. 5, pp. 359-364, 2007.

[19]   F. A. Wan Mohd Nuzul Hakimi Wan Salleh, *Phytochemistry and Biological Activities of the Genus Ocotea (Lauraceae): A Review on Recent Research Results (2000-2016).* Issue: 5, 2017, pp. 204-218.

[20]   S. J. Sharma and N. Sekar, "Deep-red/NIR emitting coumarin derivatives - Synthesis, photophysical properties, and biological applications," *Dyes and Pigments,* vol. 202, p. 110306, 2022/06/01/ 2022.

[21]   R. H. Vekariya and H. D. Patel, "Recent Advances in the Synthesis of Coumarin Derivatives via Knoevenagel Condensation: A Review," *Synthetic Communications,* vol. 44, no. 19, pp. 2756-2788, 2014/10/02 2014.

[22]   M. M. Heravi, S. Khaghaninejad, and M. Mostofi, "Chapter One - Pechmann Reaction in the Synthesis of Coumarin Derivatives," in *Advances in Heterocyclic Chemistry*, vol. 112, A. R. Katritzky, Ed.: Academic Press, 2014, pp. 1-50.

[23]   B. Kahveci and E. Menteşe, "Microwave Assisted Synthesis of Coumarins: A Review From 2007 to 2018," *Current Microwave Chemistry,* vol. 5, no. 3, pp. 162-178, 2018.

[24]   Ş. N. Karuk Elmas, F. Ozen, K. Koran, I. Yilmaz, A. O. Gorgulu, and S. Erdemir, "Coumarin based highly selective "off-on-off" type novel fluorescent sensor for Cu2+ and S2− in aqueous solution," *Journal of fluorescence,* vol. 27, no. 2, pp. 463-471, 2017.

[25]   Priyanka, R. K. Sharma, and D. Katiyar, "Recent Advances in Transition-Metal-Catalyzed Synthesis of Coumarins," (in En), *Synthesis,* vol. 48, no. 15, pp. 2303-2322, 19.07.2016 2016.

[26]   F. Özen, S. Tekin, K. Koran, S. Sandal, and A. O. Görgülü, "Synthesis, structural characterization, and in vitro anti-cancer activities of new phenylacrylonitrile derivatives," *Applied Biological Chemistry,* vol. 59, no. 2, pp. 239-248, 2016/04/01 2016.

[27]   K. Koran, F. Özen, F. Biryan, K. Demirelli, and A. O. Görgülü, "Eu+ 3-doped chalcone substituted cyclotriphosphazenes: Synthesis, characterizations, thermal and dielectrical properties," *Inorganica Chimica Acta,* vol. 450, pp. 162-169, 2016.

[28]   F. Biryan and K. Demirelli, "Copolymerization of benzyl methacrylate and a methacrylate bearing benzophenoxy and hydroxyl side groups: Monomer reactivity ratios, thermal studies and dielectric measurements," *Fibers and polymers,* vol. 18, no. 9, pp. 1629-1637, 2017.

[29]   E. Çalışkan, F. Biryan, and K. Koran, "Dipeptit Kaplı Manyetik Fe3O4 Nanopartikülünün Termal ve Dielektrik Özelliklerinin İncelenmesi," *Türk Doğa ve Fen Dergisi,* vol. 10, no. 1, pp. 259-268.

[30]   K. Koran, "2, 2-(3-(Sübstitüe-florofenil)-1-(4-oksifenil) prop-2-en-1-one)-4, 4, 6, 6-bis [spiro (2', 2"-dioksi-1', 1"-bifenilil] SiklotrifosfazenlerinDielektrik ve Termal Özellikleri," *Afyon Kocatepe Üniversitesi Fen ve Mühendislik Bilimleri Dergisi,* vol. 18, no. 2, pp. 458-467.

[31]   F. Biryan and K. Demirelli, "Characterization, thermal behavior, and electrical measurements of poly[4-(2-bromoisobutyroyl methyl)styrene]," *Advances in Polymer Technology,* vol. 37, no. 6, pp. 1994-2012, 2018.